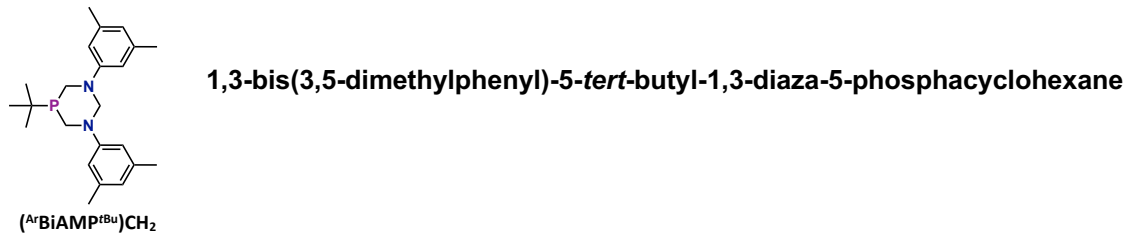
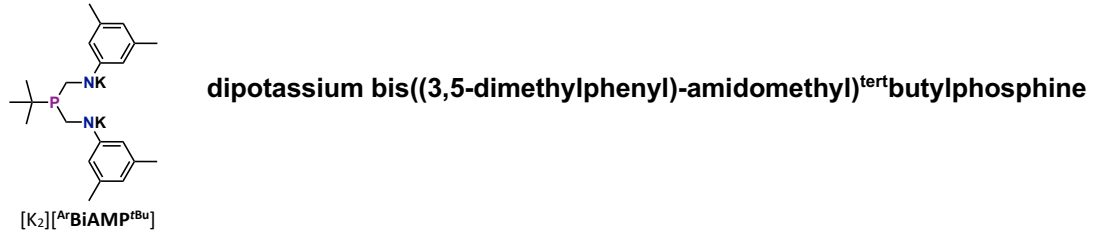
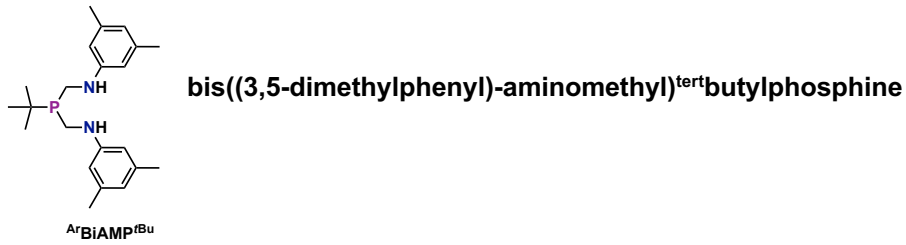


## **Flexible Interactions of the Rare-Earth Elements Y, La, and Lu with Phosphorus in Metallacyclohexane Rings**

## Table of Contents

<b>Glossary of Acronyms</b>	<b>S3</b>
<b>1. Experimental Details</b>	
<b>1.1 General Considerations</b>	<b>S4</b>
<b>1.2 Synthetic Considerations</b>	<b>S5-S9</b>
<b>1.3 Proposed Electronic Effects of M-P Bond</b>	<b>S9</b>
<b>2. Supplementary Data and Spectra</b>	
<b>2.1 NMR Spectra</b>	<b>S10-S29</b>
<b>2.2 IR (ATR) data</b>	<b>S30-S34</b>
<b>2.3 Supplemental Figures, Tables, and Graphs</b>	<b>S35-S38</b>
<b>3. Single Crystal X-ray Diffraction Data</b>	<b>S39</b>
<b>3.1 CCDC deposition numbers</b>	<b>S39</b>
<b>3.2 <math>^{Ar}BiAMP^{tBu}</math></b>	<b>S40-S41</b>
<b>3.3 <math>(^{Ar}BiAMP^{tBu})CH_2</math></b>	<b>S42-S43</b>
<b>3.4 YI(<math>^{Ar}BiAMP^{tBu}</math>)(thf)<sub>3</sub> (<b>1</b>)</b>	<b>S44-S46</b>
<b>3.5 Lal(<math>^{Ar}BiAMP^{tBu}</math>)(thf)<sub>3</sub> (<b>2</b>)</b>	<b>S47-S49</b>
<b>3.6 LuI(<math>^{Ar}BiAMP^{tBu}</math>)(thf)<sub>3</sub> (<b>3</b>)</b>	<b>S50-S52</b>
<b>3.7 Y(<math>\eta^5</math>-(1,3-diisopropyl-4,7-dimethylindenyl)(<math>^{Ar}BiAMP^{tBu}</math>)(thf) (<b>4</b>)</b>	<b>S53-S55</b>
<b>3.8 Y(<math>\eta^5</math>-(1,3-diisopropyl-4,7-dimethylindenyl)(<math>^{Ar}BiAMP^{tBu}</math>)(thf)(Et<sub>2</sub>O) (<b>4a</b>)</b>	<b>S56</b>
<b>3.9 La(<math>\eta^5</math>-(1,3-diisopropyl-4,7-dimethylindenyl)(<math>^{Ar}BiAMP^{tBu}</math>)(thf)<sub>2</sub> (<b>5</b>)</b>	<b>S57-S59</b>
<b>3.10 Lu(<math>\eta^5</math>-(1,3-diisopropyl-4,7-dimethylindenyl)(<math>^{Ar}BiAMP^{tBu}</math>)(thf) (<b>6</b>)</b>	<b>S60-S62</b>
<b>3.11 Connectivity of [La(<math>\eta^5</math>-(1,3-diisopropyl-4,7-dimethylindenyl)(<math>^{Ar}BiAMP^{tBu}</math>)]<sub>2</sub></b>	<b>S63</b>
<b>4. References</b>	<b>S64</b>

## Glossary of Ligand Acronyms



## 1. Additional Experimental Details

### 1.1 General Considerations

**Caution!** Na/K is a low-melting alloy of sodium and potassium with high reactivity and should be handled only by appropriately trained individuals. Here, we use a 1:1 (mol) ratio to generate the liquid alloy to dry the solvents.

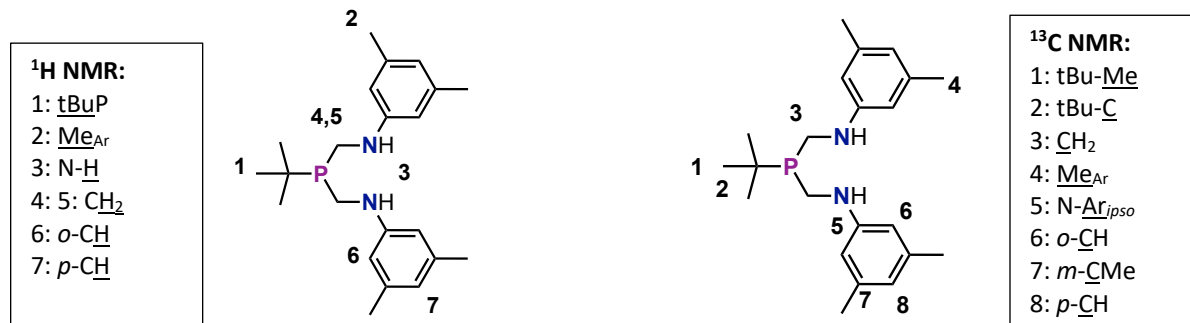
All air- and moisture-sensitive manipulations were carried out in an MBraun dry box containing a purified argon atmosphere. The solvents THF, diethyl ether, toluene, and pentane (Sigma) were dried on Na/K and filtered through dry, neutral alumina, stored on 4 Å molecular sieves and tested with Na-benzophenone ketyl radical before use. *Tert*butylphosphine (95 % or 95 % as 10 wt % solution in hexanes, Strem), 3,5-dimethylaniline (99 %, Sigma), paraformaldehyde (99 atom %, Sigma) was degassed and stored in an inert atmosphere drybox before use. Anhydrous LaI<sub>3</sub> (99.9 %, VWR), LuI<sub>3</sub> (99.9 %, Sigma) and YI<sub>3</sub> (99.9 %, VWR) were used as received and kept in an air- and moisture-free environment. THF-*d*<sub>8</sub> and benzene-*d*<sub>6</sub> were dried using Na/K alloy and filtered through dry, neutral alumina and stored under argon on 4Å molecular sieves. The reagents (trimethylsilyl)methyl potassium<sup>1</sup> and 1,3-diisopropyl-4,7-dimethyl-indene<sup>2</sup> were synthesized according to prior reports; potassium 1,3-diisopropyl-4,7-dimethyl-indenide was made by adding K-CH<sub>2</sub>SiMe<sub>3</sub> to the indene in THF prior to use. All NMR measurements for the metal complexes were conducted in J. Young valve NMR tubes sealed under an inert atmosphere of argon.

<sup>1</sup>H, <sup>13</sup>C{<sup>1</sup>H}, <sup>31</sup>P{<sup>1</sup>H}, and <sup>89</sup>Y NMR spectra were recorded on a Bruker Avance 400 MHz spectrometer operating at 400.132 MHz, 100.693 MHz, 161.978 MHz, and 19.61 MHz, respectively. The <sup>1</sup>H and <sup>13</sup>C chemical shifts are reported relative to SiMe<sub>4</sub> or via secondary standards based on residual solvent peaks relative to SiMe<sub>4</sub>; the <sup>31</sup>P chemical shifts are reported relative to the referenced <sup>1</sup>H NMR spectra; the <sup>89</sup>Y chemical shifts are reported relative to Y(NO<sub>3</sub>)<sub>3</sub> in H<sub>2</sub>O. CHN analyses were conducted by both Galbraith Laboratories and the University of Rochester CENTC Elemental Analysis Facility, B14 Hutchison Hall, 120 Trustee Road, Rochester, NY 14627. Note on Elemental Analysis: The metal complexes routinely failed elemental analysis, with analytical results low in carbon. The data obtained for each complex was consistent with loss of coordinating solvent. We note that the complexes are not stable at ambient temperature, discoloring within hours in an inert atmosphere, likely arising from the loss of THF. We have collected each complex at least three times, with differing degrees of crystallinity, and including additional experiments intended to minimize KI-THFx contamination. This includes partial precipitation of material at -35 °C by adding incremental amounts of hexane to the THF solutions, with little effect on the EA results.

UV-vis-NIR spectra were collected at RT on a Cary 5000 UV-Vis-NIR spectrophotometer from Agilent Technologies with different concentrations, which are noted. IR spectra were obtained using a Bruker Alpha II compact FT-IR spectrometer with an ATR attachment; 1-3 mg of material was used for the ATR-IR measurements.

Single crystals of complexes suitable for X-ray diffraction were coated with Krytox™ in a dry box, placed on a nylon loop and then transferred to a goniometer head of a Bruker D8 Quest equipped with a graphite-monochromatized molybdenum Kα X-ray tube ( $\lambda = 0.71073 \text{ \AA}$ ) and a CMOS detector, or the goniometer head of a Bruker D8 Quest using a Mo Kα ( $\alpha = 0.71073 \text{ \AA}$ ) IμS 3.0 Microfocus source X-ray generator.<sup>3</sup> A hemisphere routine was used for data collection and determination of lattice constants. The space group was identified, and the data were processed using the Bruker SAINT+ program and corrected for absorption using SADABS.<sup>4-8</sup> The structures were solved using direct methods (SHELXS) completed by subsequent Fourier synthesis and refined by full-matrix least-squares procedures.<sup>4</sup> Olex2 software was used as the graphical interface.<sup>9,10</sup> Crystallographic data for all structures are available from the Cambridge Structural Database.

**Graphical Key for the NMR Assignments: Correlating Shifts to Structure.** The resonances for the BiAMP fragment are related to their assignment in the NMR spectra through the shorthand notation given.



## 1.2. Synthetic Considerations

### Synthesis of bis((3,5-dimethylphenyl)-aminomethyl)<sup>tert</sup>butylphosphine (<sup>Ar</sup>**BiAMP**<sup>tBu</sup>)

In an inert atmosphere glove box, paraformaldehyde (0.636 g, 21.19 mmol; 2.01 equiv.) was placed in a 20 ml scintillation vial and suspended in 15 ml of toluene. To this suspension, <sup>tert</sup>butylphosphine (1.00 g, 10.54 mmol; 1.0 equiv.) was added at room temperature. The resulting mixture was stirred for 5 min followed by addition of 3,5-dimethylaniline (2.568 g, 21.19 mmol, 2.61 ml; 2.01 equiv.). The vial was sealed, and the reaction mixture was heated to 70 °C and stirred for 48 h. The initial pale-yellow opaque mixture turns nearly colorless, and a white precipitate formed over the course of the reaction. The mixture was allowed to cool to room temperature, and the precipitate was then removed using a glass filter frit and washed with 3 x 2 ml of toluene. The volatiles were then removed, and the pale-yellow, waxy solid residue was dissolved in a minimum amount (ca. 15 ml) of pentane with heating to 40 °C. Crystallization of the product from pentane at room temperature or at -35 °C resulted in the formation of crystalline blocks. <sup>Ar</sup>**BiAMP**<sup>tBu</sup> was isolated in 66% crystalline yield (2.479 g, 6.95 mmol).

<sup>1</sup>H NMR (400.13 MHz, C<sub>6</sub>D<sub>6</sub>) δ ppm 6.44 (s, 2H, *p*-CH), 6.26 (s, 4H, *o*-CH), 3.64 (brs, 2H, N-H), 3.25 (dt, *J*<sub>1</sub> = 12.8 Hz, *J*<sub>2</sub> = 5.2 Hz; 2H, CH<sub>2</sub>), 3.12 (dd, *J*<sub>1</sub> = 12.4 Hz, *J*<sub>2</sub> = 5.2 Hz; 2H, CH<sub>2</sub>), 2.21 (s, 12H, Me<sub>Ar</sub>), 0.95 (d, *J* = 11.6 Hz; 9H, tBuP). <sup>13</sup>C{<sup>1</sup>H} NMR (100.62 MHz, C<sub>6</sub>D<sub>6</sub>) δ ppm 149.2 (d, *J* = 8.0 Hz, N-Ar<sub>ipso</sub>), 138.7 (*m*-CMe), 120.3 (*p*-CH), 111.8 (*o*-CH), 40.5 (d, *J* = 13.1 Hz, CH<sub>2</sub>), 28.0 (d, *J* = 12.1 Hz, tBu-C), 27.7 (d, *J* = 12.1 Hz, tBu-Me), 21.8 (Me<sub>Ar</sub>). <sup>31</sup>P{<sup>1</sup>H} NMR (161.98 MHz, C<sub>6</sub>D<sub>6</sub>) δ ppm -6.25 (s, tBuP). Elemental Analysis for C<sub>22</sub>H<sub>33</sub>N<sub>2</sub>P: calcd. %C 74.12, %H 9.33, %N 7.86; Anal. %C 74.50, %H 9.49, %N 7.84.

### Isolation and characterization of 1,3-bis(3,5-dimethylphenyl)-5-*tert*-butyl-1,3-diaza-5-phosphacyclohexane ((<sup>Ar</sup>**BiAMP**<sup>tBu</sup>)CH<sub>2</sub>).

Following two crystallization cycles of <sup>Ar</sup>**BiAMP**<sup>tBu</sup> from pentane at room temperature from the initial (unoptimized) ligand synthesis, the remaining material was crystallized from pentane at -35 °C. This material contained roughly 85% of the cyclic biproduct (<sup>Ar</sup>**BiAMP**<sup>tBu</sup>)CH<sub>2</sub>. This mixture was recrystallized by dissolution into warm (~40 °C) pentane followed by cooling to -35 °C, resulting in fine needles of (<sup>Ar</sup>**BiAMP**<sup>tBu</sup>)CH<sub>2</sub> in a roughly 95% purity, with small resonances attributed to <sup>Ar</sup>**BiAMP**<sup>tBu</sup> present as minor peaks in the NMR spectra.

<sup>1</sup>H NMR (400.13 MHz, C<sub>6</sub>D<sub>6</sub>) δ ppm 6.73 (s, 2H, *p*-CH), 6.45 (s, 4H, *o*-CH), 5.08 (d, 1H, *J* = 12.8 Hz, N-CH<sub>2</sub>-N) 4.20 (dd, 2H, *J* = 12.8 Hz, 2.7 Hz, N-CH<sub>2</sub>-N), 3.84 (dd, *J*<sub>1</sub> = 17.7 Hz, *J*<sub>2</sub> = 13.5 Hz; 2H, CH<sub>2</sub>), 3.36 (dd, *J*<sub>1</sub> = 13.5 Hz, *J*<sub>2</sub> = 5.3 Hz; 2H, CH<sub>2</sub>), 2.00 (s, 12H, Me<sub>Ar</sub>), 0.93 (d, *J* = 11.3 Hz; 9H, tBuP). <sup>13</sup>C{<sup>1</sup>H} NMR (100.62 MHz, C<sub>6</sub>D<sub>6</sub>) δ ppm 150.4 (s, N-Ar<sub>ipso</sub>), 138.7 (*m*-CMe), 121.9 (*p*-CH), 115.2 (*o*-CH), 70.4 (d, *J* = 22.0 Hz, N-CH<sub>2</sub>-N), 40.5 (d, *J* = 13.1 Hz, CH<sub>2</sub>), 27.7 (d, *J* = 13.8 Hz, tBu-Me), 27.6 (d, *J* = 16.8 Hz, tBu-C), 21.8 (Me<sub>Ar</sub>). <sup>31</sup>P{<sup>1</sup>H} NMR (161.98 MHz, C<sub>6</sub>D<sub>6</sub>) δ ppm -41.2 (tBuP). Elemental Analysis for C<sub>23</sub>H<sub>33</sub>N<sub>2</sub>P: calcd. %C 74.76, %H 9.03, %N 7.60; Anal. %C 74.75, %H 8.96, %N 7.62.

### NMR Characterization of [K]<sub>2</sub>[<sup>Ar</sup>**BiAMP**<sup>tBu</sup>].

<sup>1</sup>H NMR (400.13 MHz, C<sub>6</sub>D<sub>6</sub>) δ ppm 5.79 (s, 2H, *p*-CH), 5.43 (s, 4H, *o*-CH), 3.47 (dd, *J*<sub>1</sub> = 12.6 Hz, *J*<sub>2</sub> = 8.6 Hz; 2H, CH<sub>2</sub>), 3.28 (dd, *J*<sub>1</sub> = 12.6 Hz, *J*<sub>2</sub> = 8.6 Hz; 2H, CH<sub>2</sub>), 2.01 (s, 12H, Me<sub>Ar</sub>), 1.21 (d, *J* = 9.5 Hz; 9H, tBuP). <sup>13</sup>C{<sup>1</sup>H} NMR (100.62 MHz, C<sub>6</sub>D<sub>6</sub>) δ ppm 162.7 (d, *J* = 13.8 Hz, N-Ar<sub>ipso</sub>), 138.2 (*m*-CMe), 110.0 (*p*-CH), 108.6 (*o*-CH), 51.6 (s, CH<sub>2</sub>), 29.1 (d, *J* = 10.8 Hz, tBu-Me), 28.7 (d, *J* = 12.7 Hz, tBu-C), 22.6 (Me<sub>Ar</sub>). <sup>31</sup>P{<sup>1</sup>H} NMR (161.98 MHz, C<sub>6</sub>D<sub>6</sub>) δ ppm -18.4 (tBuP).

### General Procedure I: synthesis of (<sup>Ar</sup>**BiAMP**<sup>tBu</sup>)M<sub>1</sub>(thf)<sub>3</sub> (M = Y, La, Lu)

In a glove box under inert Ar atmosphere, M<sub>1</sub> starting material (1.0 equiv.) was placed in a 20 ml scintillation vial, suspended in THF and stirred at ambient temperature for 1 h until a white slurry of M<sub>1</sub>-thf adduct formed. The resulting mixture was cooled to -35 °C. In a separate reaction vial, <sup>Ar</sup>**BiAMP**<sup>tBu</sup> ligand (1.01 equiv.) was dissolved in THF and cooled to -35 °C. A freshly prepared solution of (trimethylsilyl)methyl potassium (2.02 equiv.) in cold THF was then added dropwise to the pre-cooled solution of <sup>Ar</sup>**BiAMP**<sup>tBu</sup>. This reaction mixture was then cooled at -35 °C for 20 min, and the resulting clear light-green homogeneous solution of the <sup>Ar</sup>**BiAMP**<sup>tBu</sup> bis(potassium) salt was added dropwise to the cold stirring slurry of the M<sub>1</sub>-thf adduct. The reaction mixture was then allowed to warm to room temperature and was stirred for 3 h. White precipitated KI was separated from the reaction mixture using centrifugation (10 min @5,000 rpm) and filtration through a glass fiber filter. Homogeneous filtrate was then concentrated under reduced pressure, and the residue was recrystallized using either vapor diffusion of pentane into concentrated THF solution of the crude material or by layering technique using the same solvents at -35 °C. During <sup>1</sup>H NMR analysis of coordination complexes, the observed multiplet resonances at δ 3.64-3.59 ppm and δ 1.78-1.73 ppm, attributed to the

coordinated THF ligand, were observed to have variable integration values attributed exchange with THF-*d*<sub>8</sub> used as a solvent for NMR samples of the title compound.

**tert-Butyl(bis(methyleneamido3,5-dimethylphenyl))phosphine-yttrium(III)iodide tris(tetrahydrofuran) complex (1)**

The title compound was prepared according to General Procedure I using YI<sub>3</sub> (319.3 mg; 0.68 mmol) suspended in 4.0 ml of THF. Bis(potassium) salt of <sup>Ar</sup>BiAMP<sup>tBu</sup> ligand was prepared in 6.0 ml of THF using <sup>Ar</sup>BiAMP<sup>tBu</sup> (244 mg; 0.69 mmol) and (trimethylsilyl)methylpotassium (173.3 mg; 1.37 mmol). The title compound was isolated as crystalline off-white solid (483 mg; 0.61 mmol) in 90% crystalline yield. Single crystals suitable for SC-XRD analysis were obtained by slow vapor diffusion at -35 °C (48-72 h) using pentane and concentrated THF solution of the title compound.

<sup>1</sup>H NMR (400.13 MHz, THF-*d*<sub>8</sub>) δ ppm 6.22 (s, 4H, *o*-CH), 5.98 (s, 2H, *p*-CH), 3.64-3.59 (m, 6H, (thf-OCH<sub>2</sub>-), 3.47 (dd, 2H, *J*<sub>1</sub> = 11.6 Hz, *J*<sub>2</sub> = 7.6 Hz, CH<sub>2</sub>), 3.34 (d, 2H, *J* = 11.6 Hz, CH<sub>2</sub>), 2.14 (s, 12H, Me<sub>Ar</sub>), 1.78-1.73 (m, 6H, thf-CH<sub>2</sub>-), 1.25 (d, 9H, *J* = 11.6 Hz, tBuP). <sup>13</sup>C{<sup>1</sup>H} NMR (100.62 MHz, THF-*d*<sub>8</sub>) δ ppm 157.9 (d, *J* = 19.9 Hz, N-Ar<sub>ipso</sub>), 137.8 (*m*-CMe), 115.4 (*p*-CH), 110.1 (*o*-CH), 68.0 (thf-OCH<sub>2</sub>-), 48.2 (d, *J* = 4.7 Hz, CH<sub>2</sub>), 28.2 (d, *J* = 10.6 Hz, tBu-C), 28.1 (d, *J* = 7.2 Hz, tBu-C), 25.6 (thf-CH<sub>2</sub>-), 21.6 (Me<sub>Ar</sub>). <sup>31</sup>P{<sup>1</sup>H} NMR (161.98 MHz, THF-*d*<sub>8</sub>) δ ppm -15.7 (d, *J* = 2.8 Hz). <sup>89</sup>Y NMR (19.62 MHz, THF-*d*<sub>8</sub>) δ ppm 422.4 (d, *J* = 2.7 Hz, tBuP). Elemental Analysis (see note above) for: C<sub>34</sub>H<sub>55</sub>IN<sub>2</sub>O<sub>3</sub>PY calcd. %C, 51.92, %H, 7.05, %N 3.56; Anal. %C, 50.82, %H, 6.86, %N, 3.36.

**tert-Butyl(bis(methyleneamido3,5-dimethylphenyl))phosphine-lanthanum(III)iodide tris(tetrahydrofuran) complex (2)**

The title compound was prepared according to General Procedure I using LaI<sub>3</sub> (358.5 mg; 0.69 mmol) suspended in 4.0 ml of THF. Bis(potassium) salt of <sup>Ar</sup>BiAMP<sup>tBu</sup> ligand was prepared in 6.0 ml of THF using <sup>Ar</sup>BiAMP<sup>tBu</sup> (250 mg; 0.70 mmol) and (trimethylsilyl)methylpotassium (178.1 mg; 1.41 mmol). The title compound was isolated as crystalline off-white solid (525 mg; 0.63 mmol) in 91.3% crystalline yield. Single crystals suitable for SC-XRD analysis were obtained by slow vapor diffusion at -35 °C (48-72 h) using pentane and concentrated THF solution of the title compound.

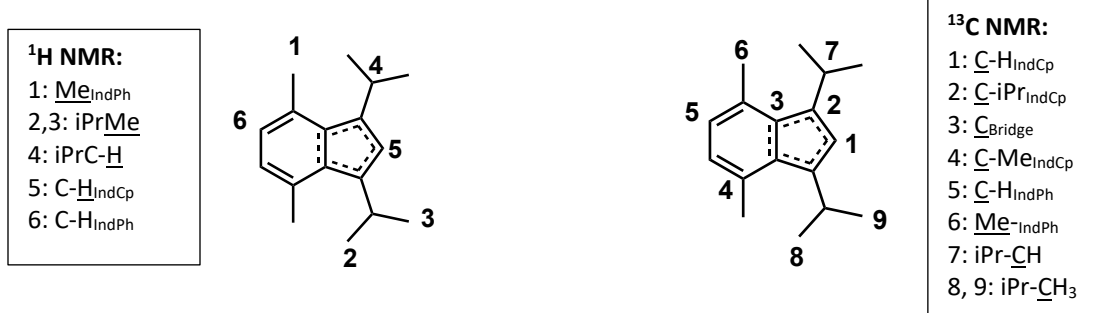
<sup>1</sup>H NMR (400.13 MHz, THF-*d*<sub>8</sub>) δ ppm 6.11 (s, 4H, *o*-CH), 6.00 (s, 2H, *p*-CH), 3.63-3.59 (m, 10H, thf-OCH<sub>2</sub>- & CH<sub>2</sub>), 3.45 (d, 2H, *J* = 12 Hz, CH<sub>2</sub>), 2.15 (s, 12H, Me<sub>Ar</sub>), 1.80-1.73 (m, 8H, thf-CH<sub>2</sub>-), 1.25 (d, 9H, *J* = 11.6 Hz, tBuP). Note: a multiplet resonance at δ 3.63-3.59 (THF) is partially overlapped with one of the methylene (-CH<sub>2</sub>-) group signals of the <sup>Ar</sup>BiAMP<sup>tBu</sup> ligand. <sup>13</sup>C{<sup>1</sup>H} NMR (100.62 MHz, THF-*d*<sub>8</sub>) δ ppm 157.3 (d, *J* = 18.3 Hz, N-Ar<sub>ipso</sub>), 138.6 (*m*-CMe), 115.5 (*p*-CH), 108.4 (*o*-CH), 68.0 (thf-OCH<sub>2</sub>-), 48.1 (CH<sub>2</sub>), 28.0 (d, *J* = 10.4 Hz, tBu-C), 26.1 (thf-CH<sub>2</sub>-), 21.7 (Me<sub>Ar</sub>). <sup>31</sup>P{<sup>1</sup>H} NMR (161.98 MHz, THF-*d*<sub>8</sub>) δ ppm -16.3 (tBuP). Elemental Analysis (see note above) for: C<sub>34</sub>H<sub>55</sub>ILaN<sub>2</sub>O<sub>3</sub>P calcd. %C, 48.81, %H, 6.63, %N, 3.35; Anal. %C, 47.65, %H, 6.61, %N, 3.07.

**tert-Butyl(bis(methyleneamido3,5-dimethylphenyl))phosphine-lutetium(III)iodide tris(tetrahydrofuran) complex (3)**

The title compound was prepared according to General Procedure I using LuI<sub>3</sub> (377.9 mg; 0.68 mmol) suspended in 4.0 ml of THF. Bis(potassium) salt of <sup>Ar</sup>BiAMP<sup>tBu</sup> ligand was prepared in 6.0 ml of THF using <sup>Ar</sup>BiAMP<sup>tBu</sup> (244 mg; 0.69 mmol) and (trimethylsilyl)methylpotassium (173.3 mg; 1.37 mmol). The title compound was isolated as crystalline off-white solid (417.8 mg; 0.48 mmol) in 70.6% crystalline yield. Single crystals suitable for SC-XRD analysis were obtained by slow vapor diffusion at -35 °C (48-72 h) using pentane and concentrated THF solution of the title compound.

<sup>1</sup>H NMR (400.13 MHz, THF-*d*<sub>8</sub>) δ ppm 6.34 (s, 4H, *o*-CH), 6.00 (s, 2H, *p*-CH), 3.64-3.59 (m, 10H, thf-OCH<sub>2</sub>-), 3.54 (dd, 2H, *J*<sub>1</sub> = 11.6 Hz, *J*<sub>2</sub> = 7.6 Hz, CH<sub>2</sub>), 3.35 (dd, 2H, *J*<sub>1</sub> = 12 Hz, *J*<sub>2</sub> = 1.6 Hz, CH<sub>2</sub>), 2.15 (s, 12H, Me<sub>Ar</sub>), 1.80-1.73 (m, 10H, thf-CH<sub>2</sub>-), 1.25 (d, 9H, *J* = 11.6 Hz, tBuP). <sup>13</sup>C NMR (100.62 MHz, THF-*d*<sub>8</sub>) δ ppm 157.9 (d, *J* = 18.3 Hz, N-Ar<sub>ipso</sub>), 137.6 (*m*-CMe), 115.5 (*p*-CH), 110.5 (*o*-CH), 68.0 (thf-OCH<sub>2</sub>-), 48.3 (CH<sub>2</sub>), 28.2 (d, *J* = , tBu-C), 27.9 (d, *J* = tBu-Me), 26.0 (thf-CH<sub>2</sub>-), 21.5 (Me<sub>Ar</sub>). <sup>31</sup>P NMR (161.98 MHz, THF-*d*<sub>8</sub>) δ ppm -18.2 (s, tBuP). Elemental Analysis (see note above) for: C<sub>34</sub>H<sub>55</sub>ILuN<sub>2</sub>O<sub>3</sub>P calcd. %C, 46.80, %H, 6.35, %N, 3.21; Anal. %C, 45.05, %H, 6.20, %N, 2.93.

**Graphical Key for the NMR Assignments: Correlating Shifts to Structure.** Additional resonances for the Indenide fragment are related to their assignment in the NMR spectra through the shorthand notation given.



**General Procedure II: synthesis of M(<sup>Ar</sup>BiAMP<sup>tBu</sup>)(η<sup>5</sup>-1,3-Diisopropyl-4,7-dimethyl-indenide)(thf)<sub>n</sub> (M = La (n = 2), Lu, Y (n = 1))**

In a glove box under inert Ar atmosphere, (<sup>Ar</sup>BiAMP<sup>tBu</sup>)MI(thf)<sub>3</sub> (1.0 equiv.) was placed in a 20 ml scintillation vial, dissolved in THF, and cooled down to -35 °C. In a separate vial 1,3-diisopropyl-4,7-dimethylindenyl potassium salt (1.01 equiv.) was dissolved in cold THF. This freshly prepared solution was then added dropwise to the pre-cooled solution of the (<sup>Ar</sup>BiAMP<sup>tBu</sup>)MI(thf)<sub>3</sub> complex and the reaction mixture was then allowed to warm up to room temperature and was stirred for 3 h. White precipitate of KI was separated from the reaction mixture using centrifugation (10 min @5,000 rpm) and filtration through a glass fiber filter. Homogeneous filtrate was then concentrated under reduced pressure, and the residue was recrystallized using either vapor diffusion of pentane into concentrated THF solution of the crude material or by layering technique using the same solvents at -35 °C. During <sup>1</sup>H NMR analysis of coordination complexes, the observed multiplet resonances at δ 3.64-3.59 and δ 1.78-1.73 ppm, attributed to the coordinated THF ligand, were observed to have variable integration values attributed exchange with THF-*d*<sub>8</sub> used as a solvent for NMR samples of the title compound.

**η<sup>5</sup>-(1,3-diisopropyl-4,7-dimethylindenyl)tert-Butyl(bis(methyleneamido3,5-dimethylphenyl))phosphine-yttrium(III)-tetrahydrofuran, (4)**

The title compound was prepared according to the General Procedure II using complex **1** (167.3 mg; 0.20 mmol) as a starting material and 1,3-diisopropyl-4,7-dimethylindenyl potassium salt (53.8 mg, 0.202 mmol) in 4.0 ml of THF. The title compound was isolated as crystalline pale-yellow solid (109.1 mg; 0.147 mmol) in 73.5 % crystalline yield. Single crystals suitable for SC-XRD analysis were obtained by slow vapor diffusion at -35 °C (48-72 h) using pentane and concentrated THF solution of the title compound.

<sup>1</sup>H NMR (400.13 MHz, THF-*d*<sub>8</sub>) δ ppm 7.16 (d, *J* = 4.4 Hz; 1H, C-H<sub>IndCp</sub>), 6.67 (s, 2H, C-H<sub>IndPh</sub>), 5.95 (s, 2H, *p*-CH), 5.69 (s, 4H, *o*-CH), 3.62 (sep, *J* = 6.8 Hz; 2H, iPrC-H), 3.56-3.52 (m, 1H, thf-OCH<sub>2</sub>), 3.44 (dd, *J*<sub>1</sub> = 11.6 Hz, *J*<sub>2</sub> = 8.0 Hz; 2H, CH<sub>2</sub>), 3.34 (d, *J* = 11.6 Hz; 2H, CH<sub>2</sub>), 2.81 (s, 6H, Me<sub>IndPh</sub>), 2.08 (s, 12H, Me<sub>Ar</sub>), 1.80-1.76 (m, 1H, thf-CH<sub>2</sub>), 1.47 (d, *J* = 6.8 Hz; 6H, iPrMe), 1.31 (d, *J* = 12.8 Hz; 9H, tBuP), 1.08 (d, *J* = 6.8 Hz; 6H, iPrMe). <sup>13</sup>C{<sup>1</sup>H} NMR (100.62 MHz, THF-*d*<sub>8</sub>) δ ppm 158.0 (dd, *J* = 21.9, 1.7 Hz, N-Ar<sub>ipso</sub>), 138.1 (m-CMe), 130.5 (C-Me<sub>IndCp</sub>), 127.5 (C<sub>Bridge</sub>), 123.9 (C-H<sub>IndPh</sub>), 123.1 (d, *J* = 1.4 Hz, C-iPr<sub>IndCp</sub>), 117.5 (d, *J* = 4.3 Hz, C-H<sub>IndCp</sub>), 116.7 (*p*-CH), 112.3 (*o*-CH), 47.5 (d, *J* = 9.1 Hz, CH<sub>2</sub>), 29.4 (iPr-CH<sub>3</sub>), 29.1 (d, *J* = 2.8 Hz, tBu-C), 28.7 (iPr-CH<sub>3</sub>), 28.4 (d, *J* = 9.5 Hz, tBu-Me), 23.5 (d, *J* = 3.3 Hz, iPr-CH), 22.8 (Me-<sub>IndPh</sub>), 22.1 (Me<sub>Ar</sub>). <sup>31</sup>P{<sup>1</sup>H} NMR (161.98 MHz, THF-*d*<sub>8</sub>) δ ppm -13.6 (d, *J* = 17.5 Hz). <sup>89</sup>Y NMR (19.62 MHz, THF-*d*<sub>8</sub>) δ ppm 176.0 (d, *J* = 17.4 Hz). Elemental Analysis (see note above) for: C<sub>43</sub>H<sub>62</sub>N<sub>2</sub>OPY calcd. %C, 69.52, %H, 8.41, %N, 3.77; Anal. %C, 68.18, %H, 8.42, %N, 3.62.

**η<sup>5</sup>-(1,3-diisopropyl-4,7-dimethylindenyl)tert-Butyl(bis(methyleneamido3,5-dimethylphenyl))phosphine-lanthanum(III)-bis(tetrahydrofuran), (5)**

The title compound was prepared according to the General Procedure II using complex **2** (167.3 mg; 0.200 mmol) as a starting material and 1,3-diisopropyl-4,7-dimethylindenyl potassium salt (53.8 mg, 0.202 mmol) in 4.0 ml of THF. The title compound was isolated as crystalline pale-yellow solid (124.4 mg; 0.143 mmol) in 71.5 % crystalline yield. Single crystals suitable for SC-XRD analysis were obtained by slow vapor diffusion technique at -35 °C (48-72 h) using pentane and concentrated THF solution of the title compound.

<sup>1</sup>H NMR (400.13 MHz, THF-*d*<sub>8</sub>) δ ppm 7.03 (s, 1H, C-H<sub>IndCp</sub>), 6.59 (s, 2H, C-H<sub>IndPh</sub>), 5.93 (s, 2H, *p*-CH), 5.76 (s, 4H, *o*-CH), 3.68 (sep, 2H, *J* = 6.1 Hz, iPrC-H), 3.63-3.58 (m, 7H, thf-OCH<sub>2</sub>), 3.46 (d, 2H, *J* = 12.2 Hz, CH<sub>2</sub>), 3.30 (dd, 2H, *J*<sub>1</sub> = 12.3 Hz, *J*<sub>2</sub> = 2.5 Hz, CH<sub>2</sub>), 2.81 (s, 6H, Me<sub>IndPh</sub>), 2.09 (s, 12H, Me<sub>Ar</sub>), 1.81-1.74 (m, 8H, thf-CH<sub>2</sub>), 1.54 (d, *J* = 6.8 Hz, 6H, iPrMe), 1.23 (d, *J* = 11.6 Hz, 9H, tBuP), 1.10 (d, *J* = 6.6 Hz, 6H, iPrMe). Note: multiplet signals at δ 3.61 and δ 1.76 ppm assigned to the coordinated THF ligand exhibited variable integration values due to partial

exchange with THF-*d*<sub>8</sub> used as a solvent for NMR samples of the title compound. <sup>13</sup>C{<sup>1</sup>H} NMR (100.62 MHz, THF-*d*<sub>8</sub>) δ ppm 156.5 (d, *J* = 16.2 Hz, N-Ar<sub>ipso</sub>), 138.9 (*m*-CMe), 129.8 (C-Me<sub>IndCp</sub>), 128.6 (C<sub>Bridge</sub>), 124.5 (C-H<sub>IndPh</sub>), 122.5 (C-iPr<sub>IndCp</sub>), 117.2 (d, *J* = 6.0 Hz, C-H<sub>IndCp</sub>), 116.0 (*p*-CH), 109.35 (*o*-CH), 48.4 (CH<sub>2</sub>), 29.8 (iPr-CH<sub>3</sub>), 29.1 (iPr-CH<sub>3</sub>), 28.8 (d, *J* = 8.3 Hz, tBu-C), 28.4 (d, *J* = 10.3 Hz, tBu-Me), 23.5 (d, *J* = 2.6 Hz, iPr-CH), 22.7 (Me-<sub>IndPh</sub>), 22.1 (Me<sub>Ar</sub>). <sup>31</sup>P{<sup>1</sup>H} NMR (161.98 MHz, THF-*d*<sub>8</sub>) δ ppm -18.1 (s). Elemental Analysis (see note above) for: C<sub>47</sub>H<sub>70</sub>LaN<sub>2</sub>O<sub>2</sub>P calcd. %C, 65.26, %H, 8.16, %N, 3.24; Anal. %C, 62.02, %H, 7.80, %N, 3.12.

### **η<sup>5</sup>-(1,3-diisopropyl-4,7-dimethylindenyl)tert-Butyl(bis(methyleneamido3,5-dimethylphenyl))phosphine-lutetium(III)-tetrahydrofuran, (6)**

The title compound was prepared according to the General Procedure II using complex **3** (174.5 mg; 0.200 mmol) as a starting material and 1,3-diisopropyl-4,7-dimethylindenyl potassium salt (53.8 mg, 0.202 mmol) in 4.0 ml of THF. The title compound was isolated as crystalline colorless solid (108.2 mg; 0.130 mmol) in 65% crystalline yield. Single crystals suitable for SC-XRD analysis were obtained by slow vapor diffusion technique at -35 °C (48-72 h) using pentane and concentrated THF solution of the title compound.

<sup>1</sup>H NMR (400.13 MHz, THF-*d*<sub>8</sub>) δ ppm 7.09 (d, *J* = 5.6 Hz; 1H, C-H<sub>IndCp</sub>), 6.65 (s, 2H, C-H<sub>IndPh</sub>), 5.95 (s, 2H, *p*-CH), 5.73 (s, 4H, *o*-CH), 3.58-3.55 (m, 3H, thf-OCH<sub>2</sub>), 3.47 (dd, *J*<sub>1</sub> = 11.6 Hz, *J*<sub>2</sub> = 7.2 Hz; 2H, CH<sub>2</sub>), 3.29 (d, *J* = 10.8 Hz; 2H, CH<sub>2</sub>), 2.80 (s, 6H, Me<sub>IndPh</sub>), 2.07 (s, 12H, Me<sub>Ar</sub>), 1.74-1.70 (m, 2H, thf-CH<sub>2</sub>), 1.43 (d, *J* = 6.8 Hz; 6H, iPrMe), 1.29 (d, *J* = 12.8 Hz; 9H, tBuP), 1.05 (d, *J* = 6.4 Hz; 6H, iPrMe). Note: the isopropyl methine overlaps with the THF / THF-*d*<sub>8</sub> resonances. <sup>13</sup>C{<sup>1</sup>H} NMR (100.62 MHz, THF-*d*<sub>8</sub>) δ ppm 158.0 (d, *J* = 22.5 Hz, N-Ar<sub>ipso</sub>), 137.8 (*m*-CMe), 130.7 (C-Me<sub>IndCp</sub>), 127.3 (C<sub>Bridge</sub>), 123.9 (C-H<sub>IndPh</sub>), 121.6 (C-iPr<sub>IndCp</sub>), 117.9 (d, *J* = 6.0 Hz, C-H<sub>IndCp</sub>), 116.7 (*p*-CH), 111.6 (*o*-CH), 47.2 (d, *J* = 9.2 Hz, CH<sub>2</sub>), 29.3 (iPr-CH<sub>3</sub>), 29.1 (d, *J* = 3.5 Hz, tBu-C), 28.6 (iPr-CH<sub>3</sub>), 28.3 (d, *J* = 8.7 Hz, tBu-Me), 23.2 (d, *J* = 3.3 Hz, iPr-CH), 22.8 (Me-<sub>IndPh</sub>), 22.0 (Me<sub>Ar</sub>). <sup>31</sup>P{<sup>1</sup>H} NMR (161.98 MHz, THF-*d*<sub>8</sub>) δ ppm -14.5. Elemental Analysis (see note above) for: C<sub>43</sub>H<sub>62</sub>LuN<sub>2</sub>OP calcd. %C, 62.31, %H, 7.54, %N, 3.38; Anal. %C, 61.28, %H, 7.52, %N, 3.52.

### **Procedure for NMR scale addition of TEPO (P(O)Et<sub>3</sub>) to form 7, 8, and 9**

In an inert atmosphere Argon filled glovebox, Y(<sup>Ar</sup>BiAMP<sup>tBu</sup>)(η<sup>5</sup>-iPrMeInd)(thf) (**4**, 46.5 mg, 0.062 mmol) was added to an oven-dried *J*-Young NMR tube and dissolved in approximately 0.750 g of THF-*d*<sub>8</sub>. To this solution, triethylphosphine oxide (8.5 mg, 1.0 equiv.) was added at rt. The reaction was sealed. The reaction remained homogenous and nearly colorless. The reaction mixture was then analyzed by NMR spectroscopy. **NMR analysis of 7:** <sup>1</sup>H NMR (400.13 MHz, THF-*d*<sub>8</sub>) δ ppm 6.94 (d, 1H, *J* = 2.5 Hz, C-H<sub>IndCp</sub>), 6.48 (s, 2H, C-H<sub>IndPh</sub>), 5.90 (s, 2H, *p*-CH), 5.77 (s, 4H, *o*-CH), 3.77 (sep, 2H, *J* = 6.7 Hz, iPrC-H), 3.33 (dd, 2H, *J*<sub>1</sub> = 11.5 Hz, *J*<sub>2</sub> = 6.9 Hz, CH<sub>2</sub>), 3.19 (d, 2H, *J*<sub>1</sub> = 11.3 Hz, CH<sub>2</sub>), 2.80 (s, 6H, Me<sub>IndPh</sub>), 2.09 (s, 12H, Me<sub>Ar</sub>), 1.50 (d, 6H, *J* = 6.6 Hz, iPrMe), 1.23 (d, 9H, *J* = 12.2 Hz, tBuP), 1.17 (m, 6H, TEPO-CH<sub>2</sub>), 1.10 (d, 6H, *J* = 6.5 Hz, iPrMe), 0.71 (dt, 9H, *J*<sub>1</sub> = 17.7 Hz, *J*<sub>2</sub> = 7.7 Hz, TEPO-CH<sub>3</sub>). <sup>13</sup>C{<sup>1</sup>H} NMR (100.62 MHz, THF-*d*<sub>8</sub>) δ ppm 159.1 (dd, *J* = 21.9, 1.7 Hz, N-Ar<sub>ipso</sub>), 137.4 (*m*-CMe), 129.3 (C-Me<sub>IndCp</sub>), 126.6 (C<sub>Bridge</sub>), 122.9 (C-H<sub>IndPh</sub>), 121.7 (d, *J* = 1.3 Hz, C-iPr<sub>IndCp</sub>), 115.7 (*p*-CH), 114.5 (d, *J* = 2.7 Hz, C-H<sub>IndCp</sub>), 112.2 (*o*-CH), 48.8 (d, *J* = 7.2 Hz, CH<sub>2</sub>), 29.2 (iPr-CH<sub>3</sub>), 28.7 (iPr-CH<sub>3</sub>), 28.5 (d, *J* = 5.8 Hz, tBu-C), 28.0 (d, *J* = 9.5 Hz, tBu-Me), 23.1 (Me-<sub>IndPh</sub>), 22.8 (iPr-CH), 21.7 (Me<sub>Ar</sub>), 17.3 (d, *J* = 66.2 Hz, TEPO-CH<sub>2</sub>), 5.0 (d, *J* = 4.4 Hz, TEPO-CH<sub>3</sub>). <sup>31</sup>P{<sup>1</sup>H} NMR (161.98 MHz, THF-*d*<sub>8</sub>) δ ppm 70.6 (dd, *J* = 10.0 Hz, 3.0 Hz, TEPO), -13.9 (dd, *J* = 10.2 Hz, 2.7 Hz, BiAMP).

In an inert atmosphere Argon filled glovebox, La(<sup>Ar</sup>BiAMP<sup>tBu</sup>)(η<sup>5</sup>-iPrMeInd)(thf)<sub>2</sub> (**5**, 44.0 mg, 0.051 mmol) was added to an oven-dried *J*-Young NMR tube and dissolved in approximately 0.750 g of THF-*d*<sub>8</sub>. To this solution, triethylphosphine oxide (6.8 mg, 1.0 equiv.) was added at rt. The reaction was sealed. The reaction remained homogenous and nearly colorless. The reaction mixture was then analyzed by NMR spectroscopy. **NMR analysis of 8:** <sup>1</sup>H NMR (400.13 MHz, THF-*d*<sub>8</sub>) δ ppm 6.83 (s, 1H, C-H<sub>IndCp</sub>), 6.51 (s, 2H, C-H<sub>IndPh</sub>), 5.88 (s, 2H, *p*-CH), 5.72 (s, 4H, *o*-CH), 3.87 (sep, 2H, *J* = 6.6 Hz, iPrC-H), 3.39 (dd, 2H, *J*<sub>1</sub> = 11.6 Hz, *J*<sub>2</sub> = 7.6 Hz, CH<sub>2</sub>), 3.19 (dd, 2H, *J*<sub>1</sub> = 12 Hz, *J*<sub>2</sub> = 1.6 Hz, CH<sub>2</sub>), 2.80 (s, 6H, Me<sub>IndPh</sub>), 2.08 (s, 12H, Me<sub>Ar</sub>), 1.56 (d, 6H, *J* = 6.6 Hz, iPrMe), 1.23 (d, 9H, *J* = 11.6 Hz, tBuP), 1.16 (d, 6H, *J* = 6.6 Hz, iPrMe), 0.73 (dt, 9H, *J*<sub>1</sub> = 17.7 Hz, 7.7 Hz, TEPO-CH<sub>3</sub>). Note: the TEPO CH<sub>2</sub> overlaps with the tBu-Me and one of the iPr-Me resonances, which is supported by the broad base of those resonances and integration. <sup>13</sup>C{<sup>1</sup>H} NMR (100.62 MHz, THF-*d*<sub>8</sub>) δ ppm 157.8 (d, *J* = 21.9, N-Ar<sub>ipso</sub>), 137.4 (*m*-CMe), 128.5 (C-Me<sub>IndCp</sub>), 127.7 (C<sub>Bridge</sub>), 123.6 (C-H<sub>IndPh</sub>), 122.1 (C-iPr<sub>IndCp</sub>), 114.8 (*p*-CH), 114.5 (d, *J* = 2.7 Hz, C-H<sub>IndCp</sub>), 110.4 (*o*-CH), 47.8 (d, *J* = 7.2 Hz, CH<sub>2</sub>), 29.2 (iPr-CH<sub>3</sub>), 28.7 (iPr-CH<sub>3</sub>), 28.5 (d, *J* = 5.8 Hz, tBu-C), 28.0 (d, *J* = 9.5 Hz, tBu-Me), 23.1 (Me-<sub>IndPh</sub>), 22.8 (iPr-CH), 21.4 (Me<sub>Ar</sub>), 17.7 (d, *J* = 66.2 Hz, TEPO-CH<sub>2</sub>), 4.6 (d, *J* = 4.4 Hz, TEPO-CH<sub>3</sub>).

$^{31}\text{P}\{\text{H}\}$  NMR (161.98 MHz, THF-*d*<sub>8</sub>, Room Temp.)  $\delta$  ppm 68.8 (s, TEPO-P), -13.7 (s, BiAMP).  $^{31}\text{P}\{\text{H}\}$  NMR (161.98 MHz, THF-*d*<sub>8</sub>, -50 °C)  $\delta$  ppm 70.3 (*d*, *J* = 3.2 Hz, TEPO), -14.9 (*d*, *J* = 2.7 Hz, BiAMP)

In an inert atmosphere Argon filled glovebox, Lu(<sup>Ar</sup>**BiAMP**<sup>tBu</sup>)(η<sup>5</sup>-iPrMeInd)(thf) (**6**, 21.0 mg, 0.025 mmol) was added to an oven-dried *J*-Young NMR tube and dissolved in approximately 0.750 g of THF-*d*<sub>8</sub>. To this solution, triethylphosphine oxide (3.4 mg, 1.0 equiv.) was added at rt. The reaction was sealed. The reaction remained homogenous and nearly colorless. The reaction mixture was then analyzed by NMR spectroscopy. **NMR analysis of 9:**  $^1\text{H}$  NMR (400.13 MHz, THF-*d*<sub>8</sub>)  $\delta$  ppm 6.93 (d, 1H, *J* = 3.6 Hz, C-H<sub>IndCp</sub>), 6.47 (s, 2H, C-H<sub>IndPh</sub>), 5.92 (s, 2H, *p*-CH), 5.84 (s, 4H, *o*-CH), 3.71 (sep, 2H, *J* = 6.6 Hz, iPrC-H), 3.39 (dd, 2H, *J*<sub>1</sub> = 11.6 Hz, *J*<sub>2</sub> = 7.6 Hz, CH<sub>2</sub>), 3.11 (d, 2H, *J* = 12.0 Hz, CH<sub>2</sub>), 2.80 (s, 6H, Me<sub>IndPh</sub>), 2.10 (s, 12H, Me<sub>Ar</sub>), 1.47 (d, 6H, *J* = 6.6 Hz, iPrMe), 1.24 (d, 9H, *J* = 12.0 Hz, tBuP), 1.17 (td, 6H, *J* = 13.1 Hz, 7.7 Hz, TEPO-CH<sub>2</sub>), 1.08 (d, 6H, *J* = 6.6 Hz, iPrMe), 0.70 (dt, 9H, *J* = 17.7 Hz, 7.7 Hz, TEPO-CH<sub>3</sub>).  $^{13}\text{C}\{\text{H}\}$  NMR (100.62 MHz, THF-*d*<sub>8</sub>)  $\delta$  ppm 159.7 (d, *J* = 21.9, N-Ar<sub>ipso</sub>), 137.5 (*m*-CMe), 129.9 (C-Me<sub>IndCp</sub>), 126.8 (C-Bridge), 123.0 (C-H<sub>IndPh</sub>), 120.7 (C-iPr<sub>IndCp</sub>), 116.2 (*p*-CH), 115.5 (d, *J* = 4.4 Hz, C-H<sub>IndCp</sub>), 112.9 (*o*-CH), 49.3 (d, *J* = 6.5 Hz, CH<sub>2</sub>), 29.5 (iPr-CH<sub>3</sub>), 29.0 (d, *J* = 1.8 Hz, iPr-CH<sub>3</sub>), 28.9 (d, *J* = 7.1 Hz, tBu-C), 28.3 (d, *J* = 9.8 Hz, tBu-Me), 23.2-23.0, (m, Me<sub>IndPh</sub>, iPr-CH), 22.0 (Me<sub>Ar</sub>), 18.1 (d, *J* = 66.2 Hz, TEPO-CH<sub>2</sub>), 5.3 (d, *J* = 4.4 Hz, TEPO-CH<sub>3</sub>).  $^{31}\text{P}\{\text{H}\}$  NMR (161.98 MHz, THF-*d*<sub>8</sub>)  $\delta$  ppm 72.6 (d, *J* = 3.2 Hz, TEPO), -17.2 (d, *J* = 2.9 Hz, BiAMP).

The collected NMR spectra for the in-situ generated TEPO adducts **7**, **8** and **9** are shown on pages S24 through S29.

### 1.3. Proposed Electronic Effects of M-P Bond

Given the small *J*-value observed for the P-Y interaction, and the nature of the REEs as hard, electropositive metals, we hypothesize that the *J*-value depends mainly on the electron rich/deficient nature of the metal. As the ligand coordination sphere of the metal becomes increasingly electron donating, the electrostatic interaction between the phosphorus lone pair and the metal center will decrease, inducing a decrease in the *J* value.

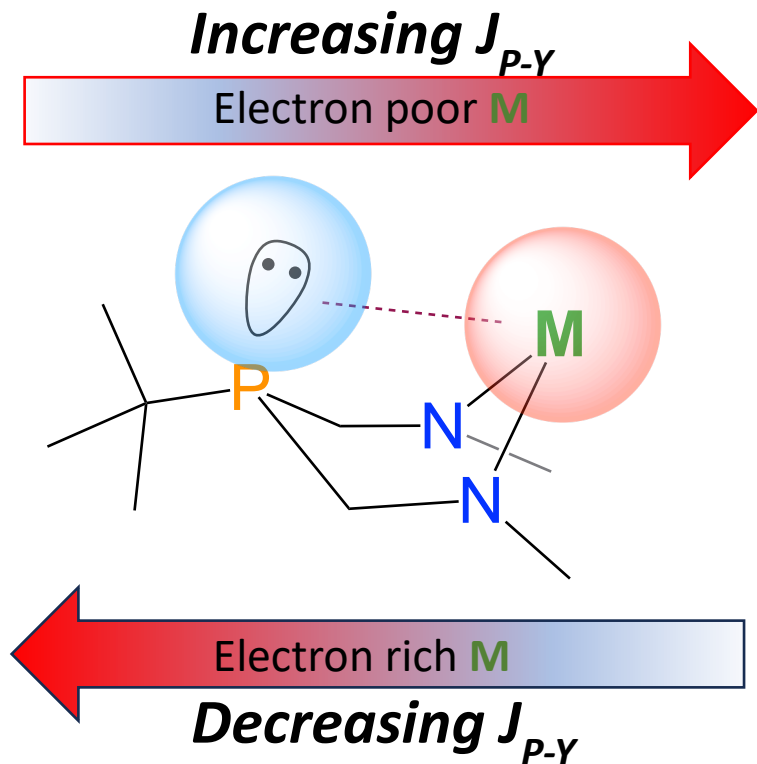


**Figure S1.** Proposed effect of metal coordination sphere on the M-Y interaction; the more electron rich metal centers will poorly interact with the lone-pair of the phosphorus, while the more electron poor metal centers will display an increased M-P interaction.

## 2. Supplementary Data and Experimental Details

### 2.1. NMR spectra

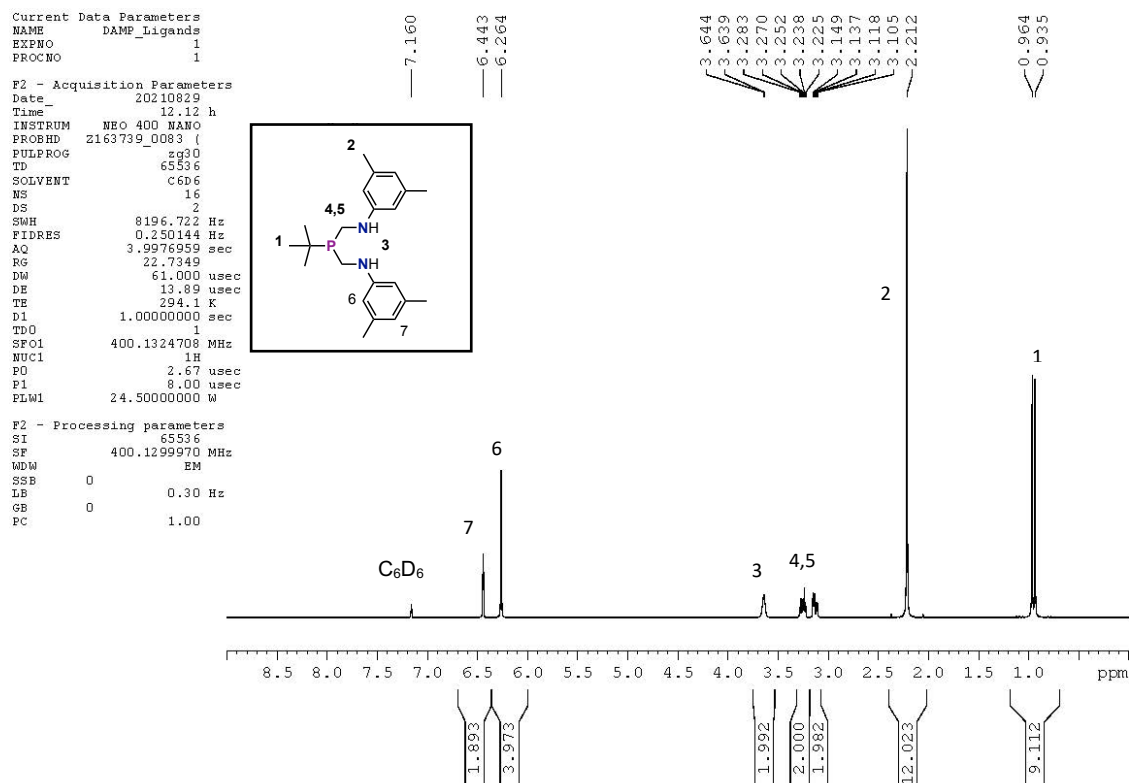


Figure S2.  $^1\text{H}$  NMR spectrum of  $^{\text{Ar}}\text{BiAMP}^{\text{tBu}}$  acquired in  $\text{C}_6\text{D}_6$  at room temperature.

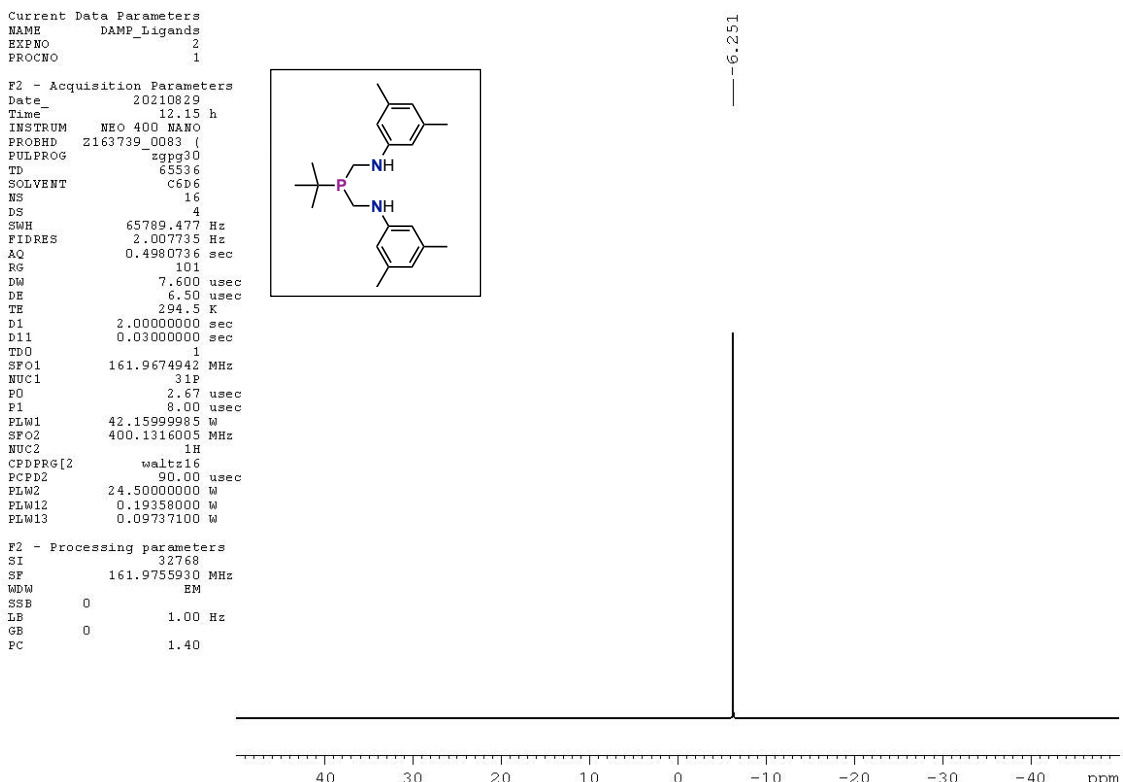
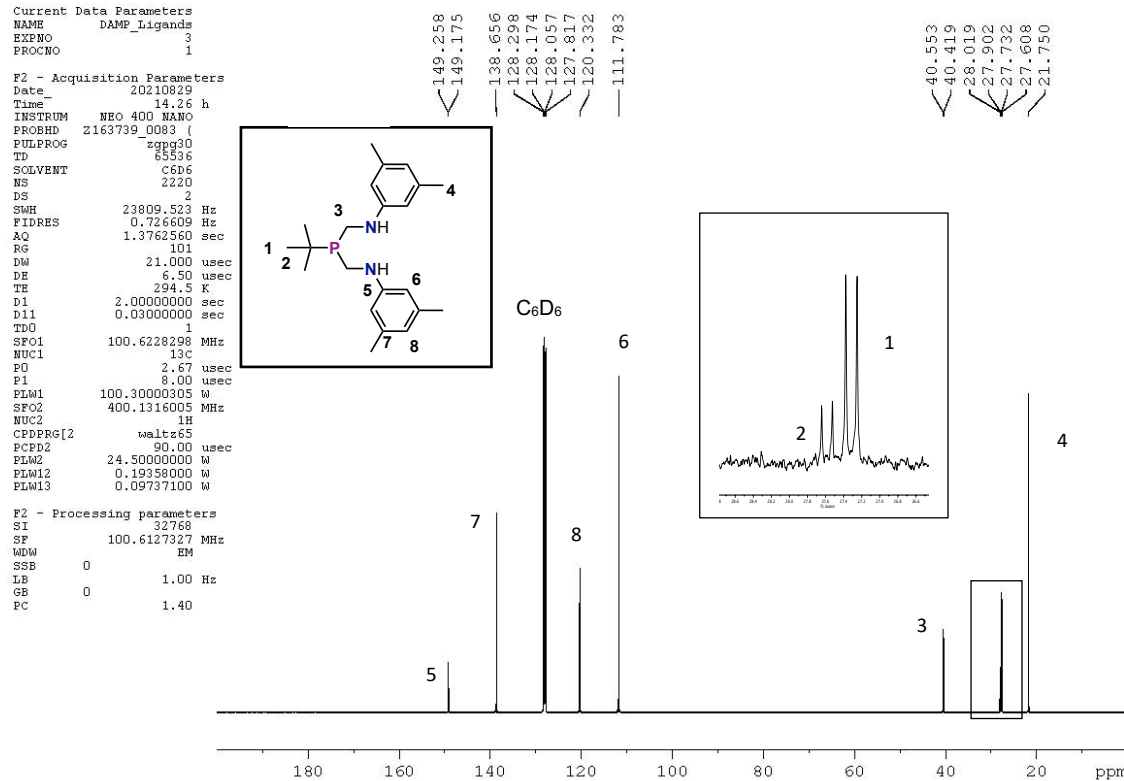
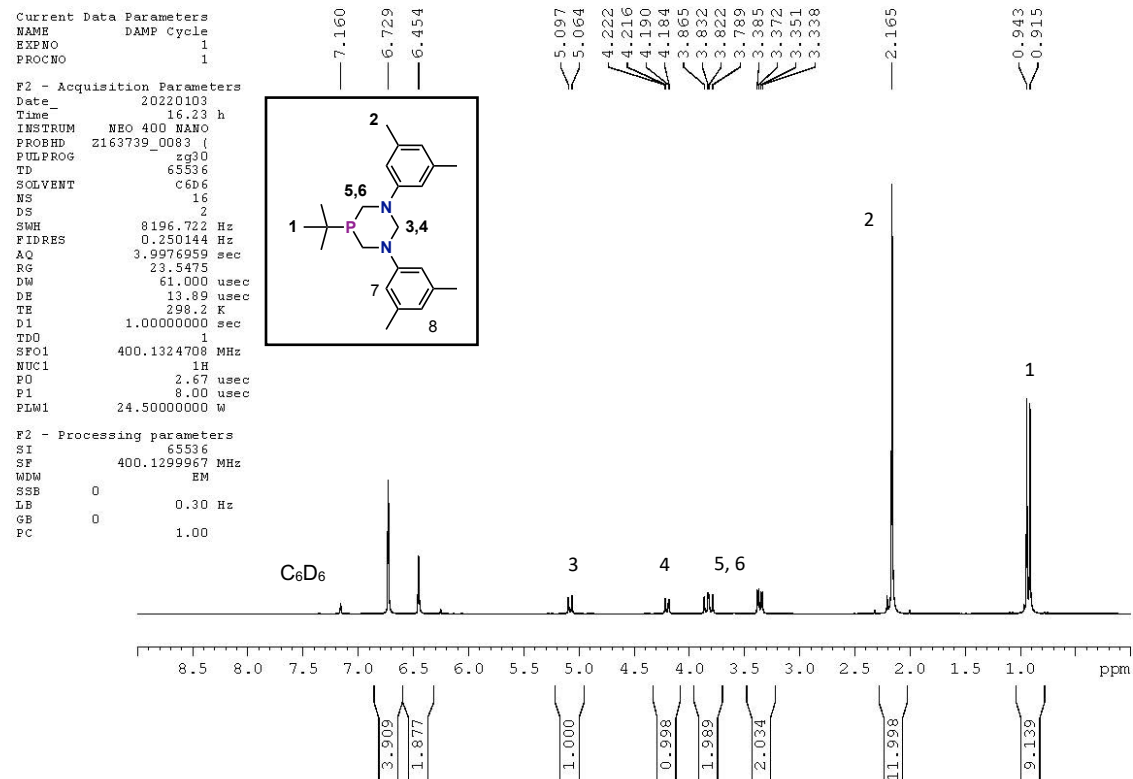


Figure S3.  $^{31}\text{P}\{^1\text{H}\}$  NMR spectrum of  $^{\text{Ar}}\text{BiAMP}^{\text{tBu}}$  acquired in  $\text{C}_6\text{D}_6$  at room temperature.



**Figure S4.**  $^{13}\text{C}\{^1\text{H}\}$  NMR spectrum of  $^{Ar}\text{BiAMP}^{\text{tBu}}$  acquired in  $\text{C}_6\text{D}_6$  at room temperature with an expansion of the 26 ppm to 29 ppm region to show the doublet resonances attributed to the tBu-carbon atoms of the phosphine.



**Figure S5.**  $^1\text{H}$  NMR spectrum of  $(^{Ar}\text{BiAMP}^{\text{tBu}})\text{CH}_2$  acquired in  $\text{C}_6\text{D}_6$  at room temperature.

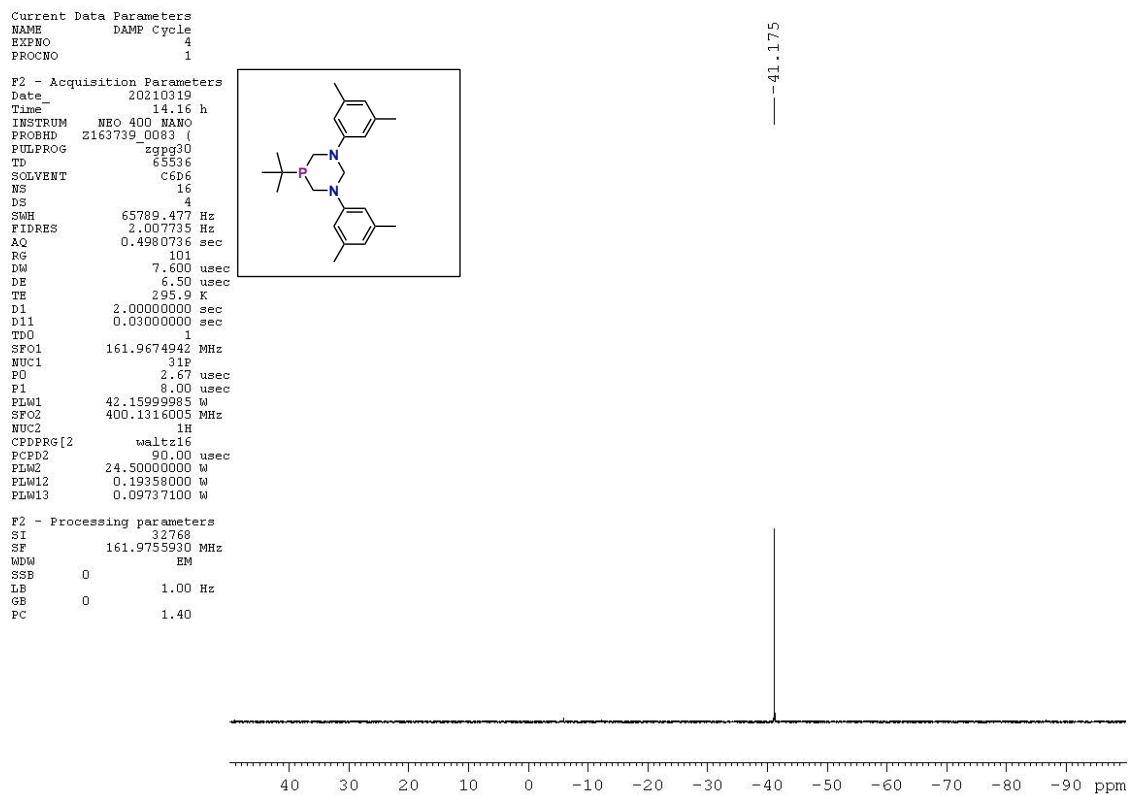


Figure S6.  $^{31}\text{P}\{\text{H}\}$  NMR spectrum of  $(^4\text{BiAMP}^{\text{tBu}})\text{CH}_2$  acquired in  $\text{C}_6\text{D}_6$  at room temperature.

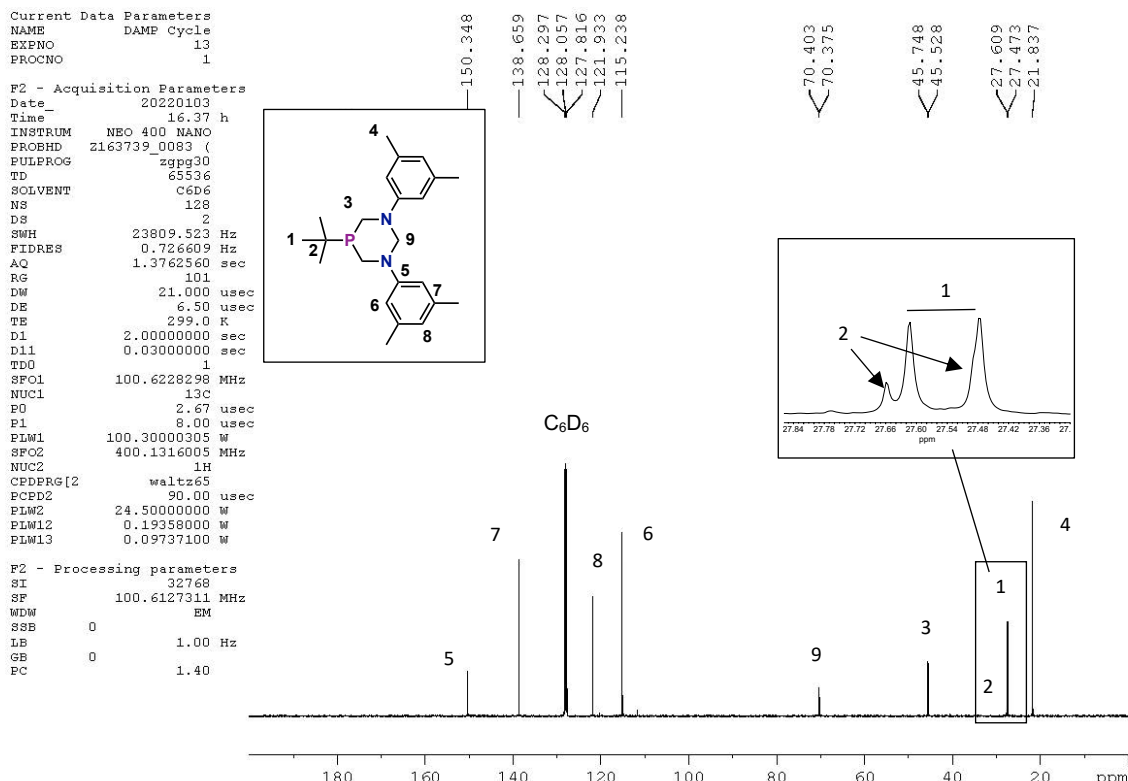


Figure S7.  $^{13}\text{C}\{\text{H}\}$  NMR spectrum of  $(^4\text{BiAMP}^{\text{tBu}})\text{CH}_2$  acquired in  $\text{C}_6\text{D}_6$  at room temperature. An expansion is provided to show the 4° carbon of the tert-butyl group; it is partially overlapping with the tBu-methyl peaks, and only one peak of the expected doublet is observed while the other appears as a shoulder of the tBu-methyl resonance.

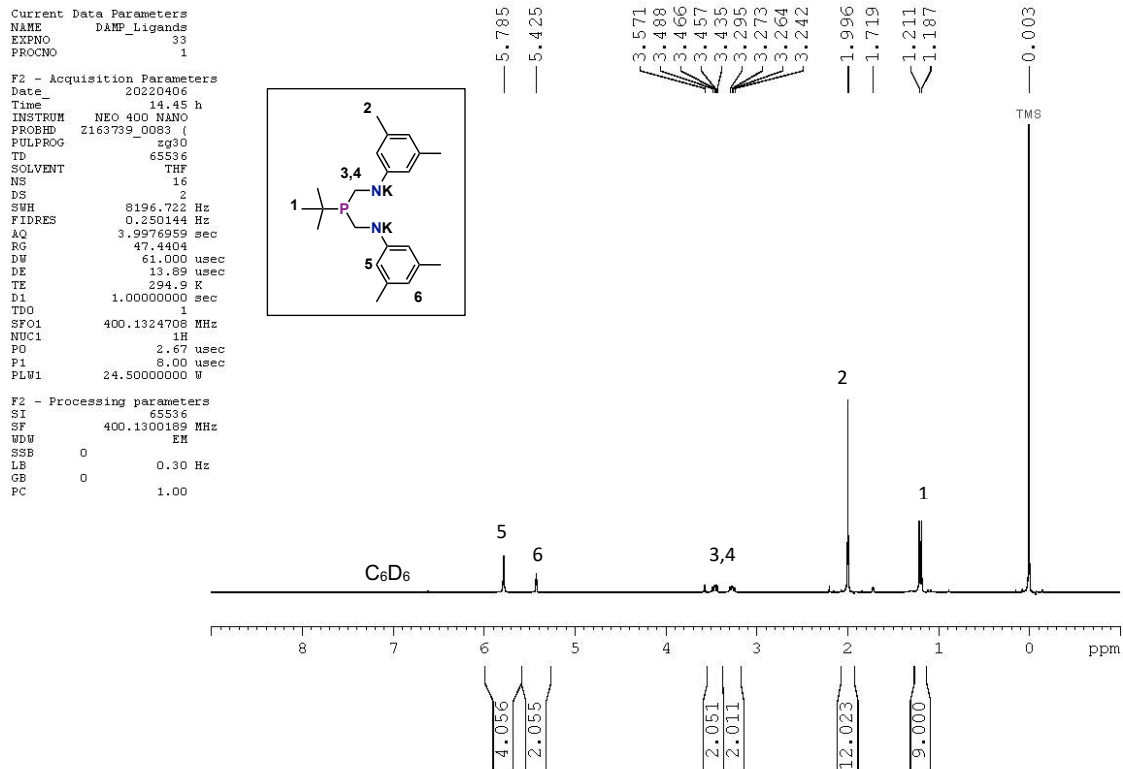


Figure S8.  $^1\text{H}$  NMR spectrum of a freshly prepared ( $^{Ar}\text{BiAMP}^{Bu}_2\text{K}_2$ ) acquired in THF- $d_8$  at room temperature.

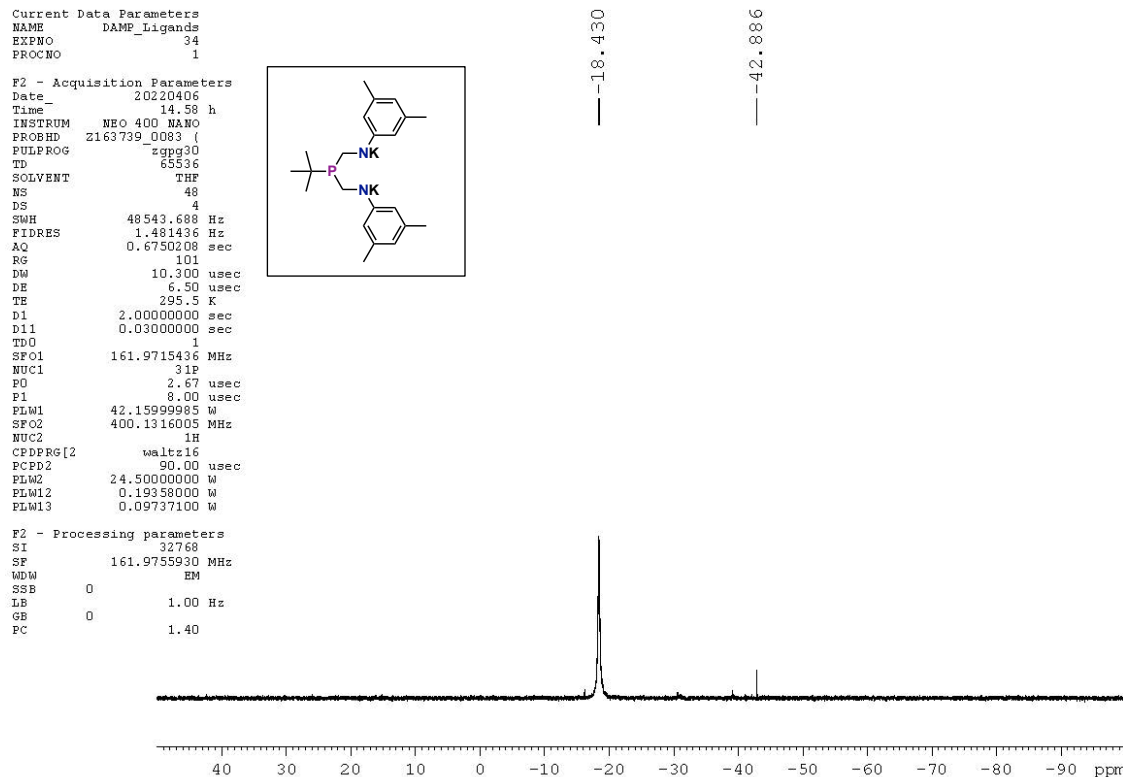


Figure S9.  $^{31}\text{P}\{^1\text{H}\}$  NMR spectrum of a freshly prepared ( $^{Ar}\text{BiAMP}^{Bu}_2\text{K}_2$ ) acquired in THF- $d_8$  at room temperature.

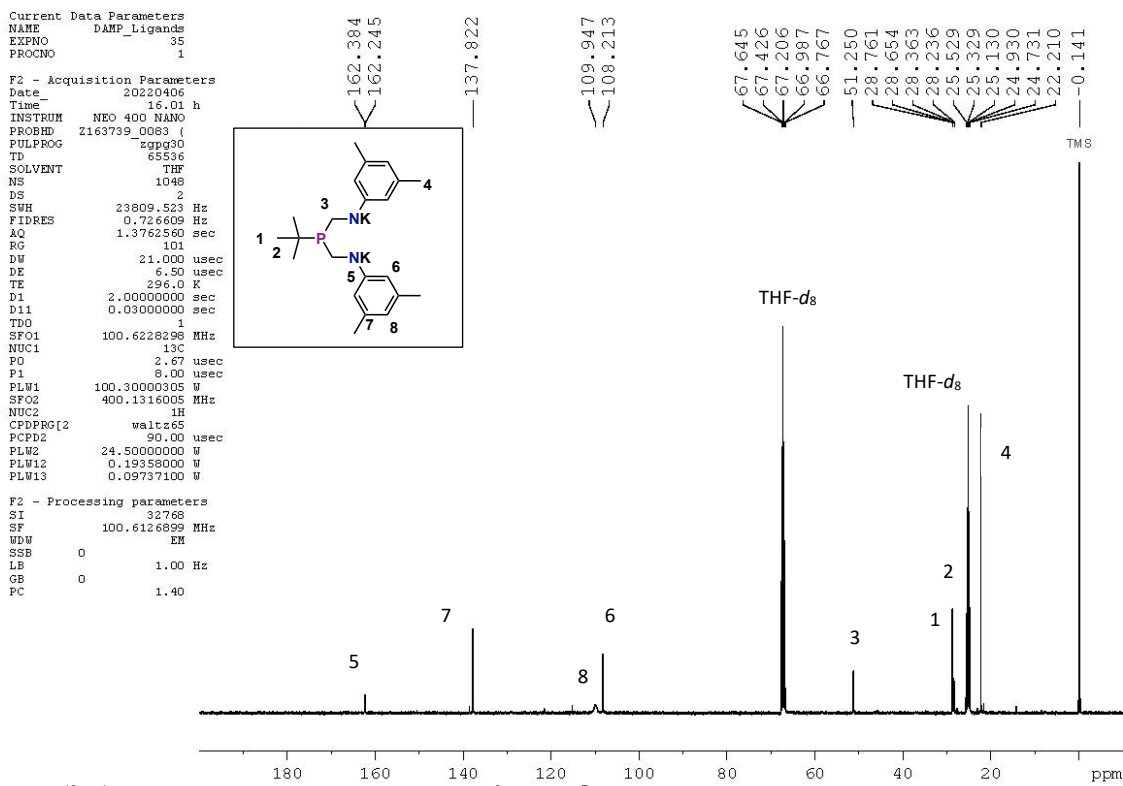
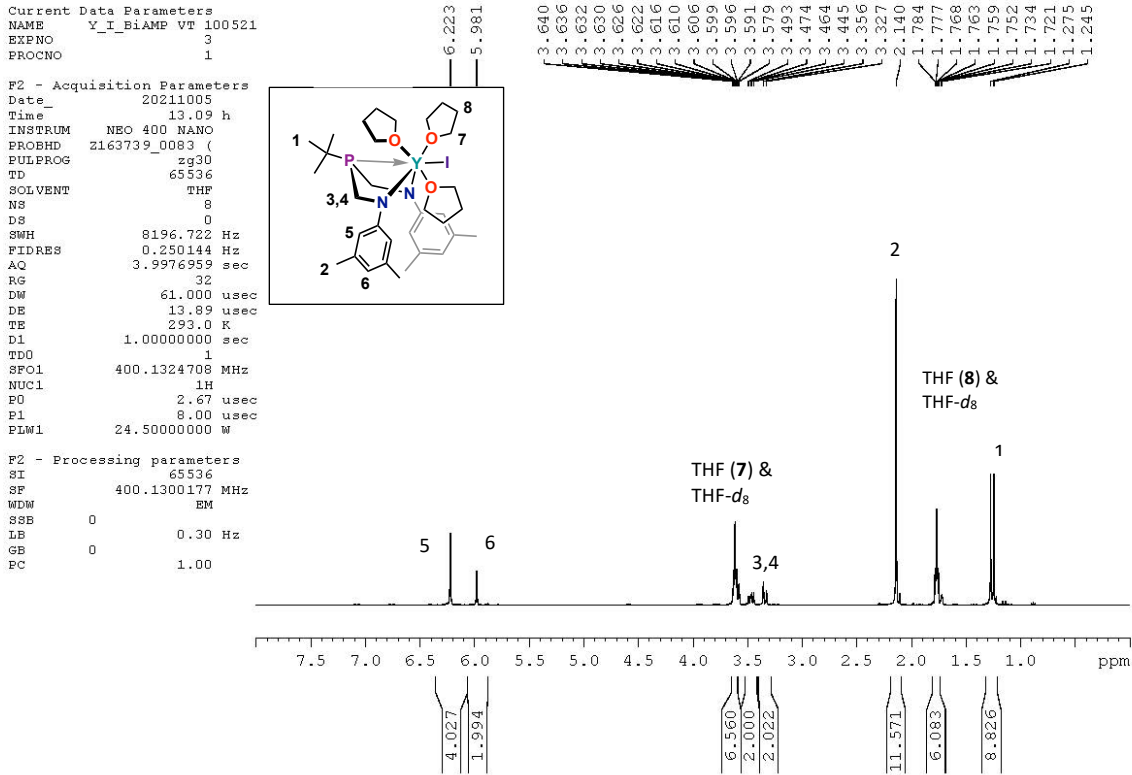


Figure S10.  $^{13}\text{C}\{\text{H}\}$  NMR spectrum of a freshly prepared ( $^{\text{Ar}}\text{BiAMP}^{\text{tBu}}\text{K}_2$ )<sub>2</sub> acquired in THF- $d_8$  at room temperature.



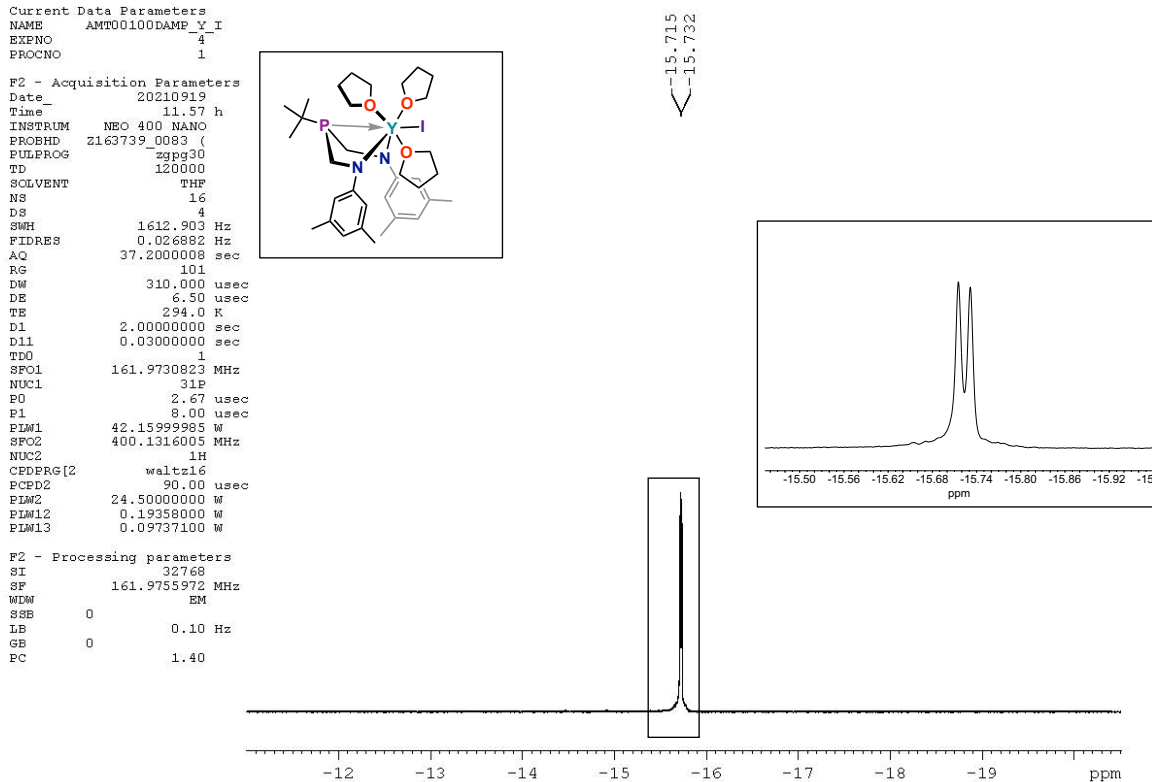


Figure S12.  ${}^3\text{P}\{{}^1\text{H}\}$  NMR spectrum of  $\text{YI}({}^{\text{Ar}}\text{BiAMP}^{\text{Bu}})(\text{THF})_3$  (1) recrystallized from THF:pentane acquired in THF- $d_8$  at room temperature.

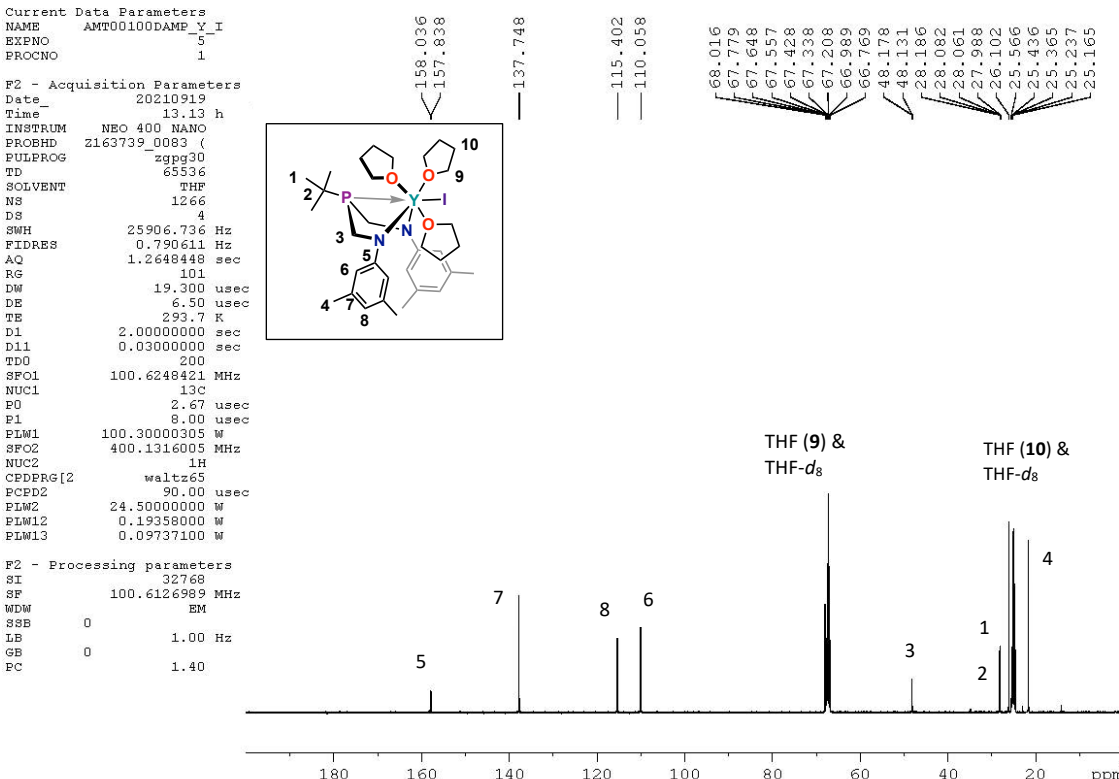
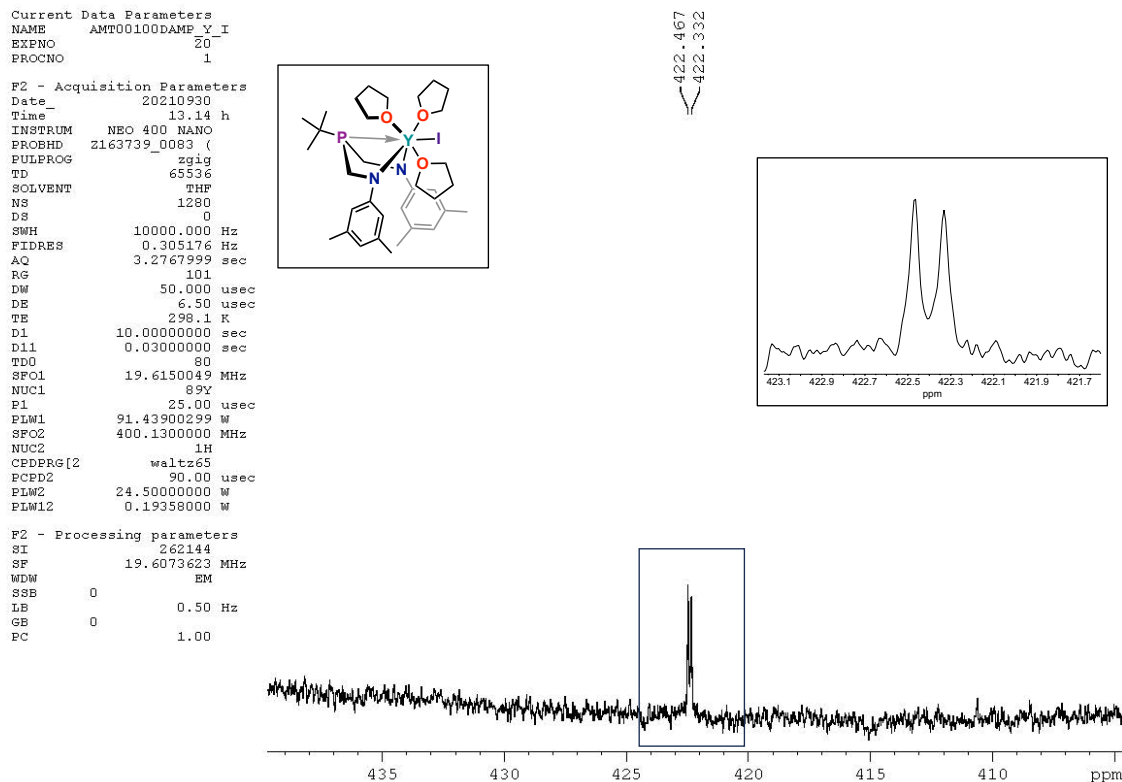
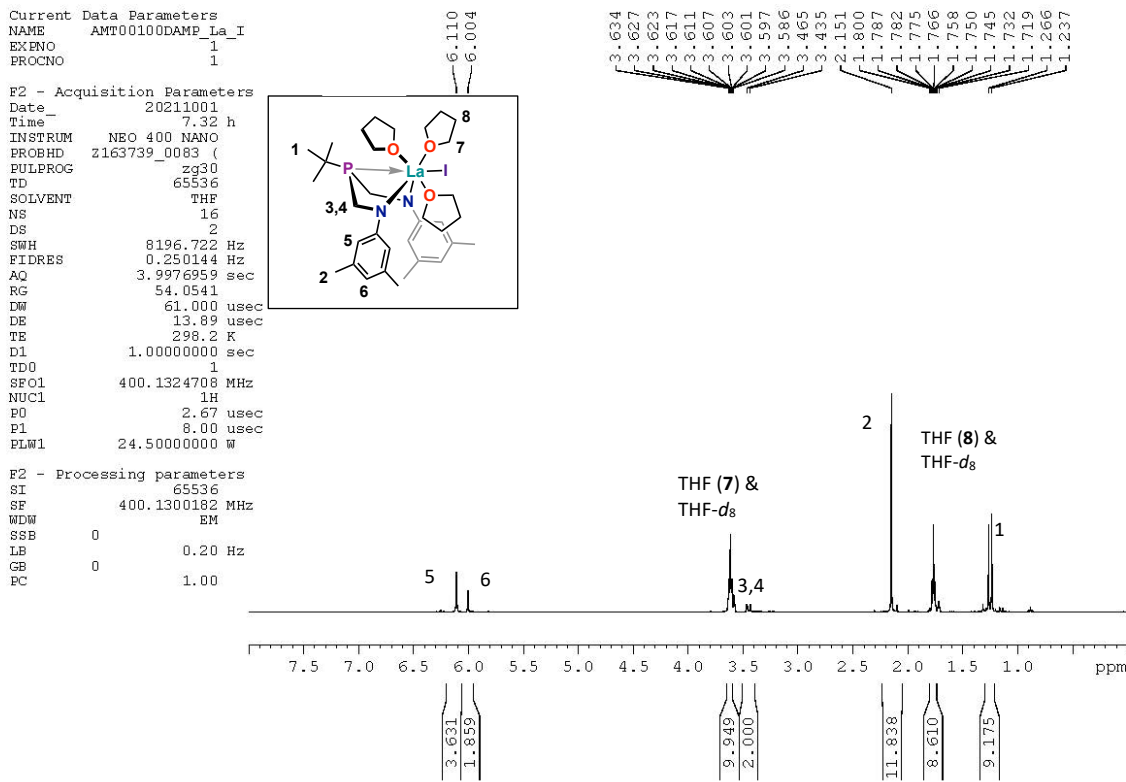


Figure S13.  ${}^{13}\text{C}\{{}^1\text{H}\}$  NMR spectrum of  $\text{YI}({}^{\text{Ar}}\text{BiAMP}^{\text{Bu}})(\text{THF})_3$  (1) recrystallized from THF:pentane acquired in THF- $d_8$  at room temperature.



**Figure S14.**  $^{89}\text{Y}\{\text{H}\}$  NMR spectrum of  $\text{Yl}(^{\text{Ar}}\text{BiAMP}^{\text{Bu}})(\text{THF})_3$  (**1**) recrystallized from THF:pentane acquired in  $\text{THF-d}_8$  at room temperature.



**Figure S15.**  $^1\text{H}$  NMR spectrum of  $\text{LaI}(^{\text{Ar}}\text{BiAMP}^{\text{Bu}})(\text{THF})_3$  (**2**) recrystallized from THF:pentane acquired in  $\text{THF-d}_8$  at room temperature.

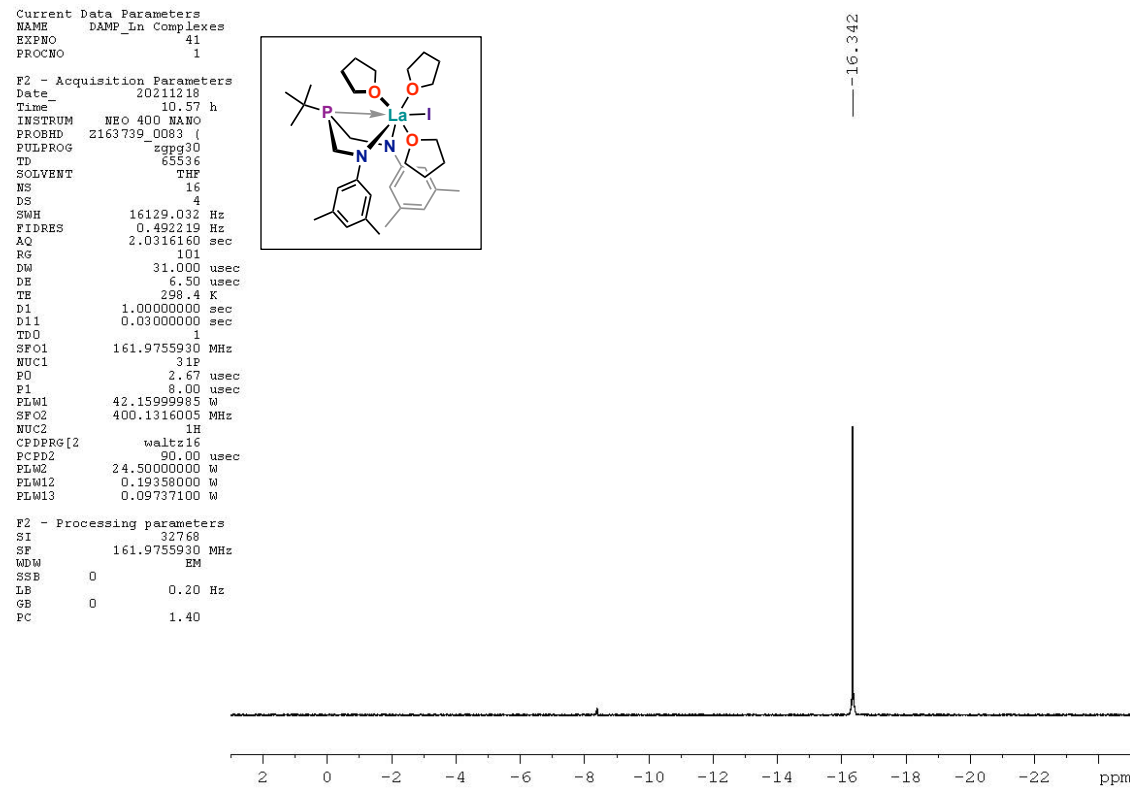


**Figure S16.**  $^{31}\text{P}\{\text{H}\}$  NMR spectrum of  $\text{La}(\text{ArBiAMP}^{\text{tBu}})(\text{THF})_3$  (**2**) recrystallized from THF:pentane acquired in  $\text{THF-d}_8$  at room temperature.

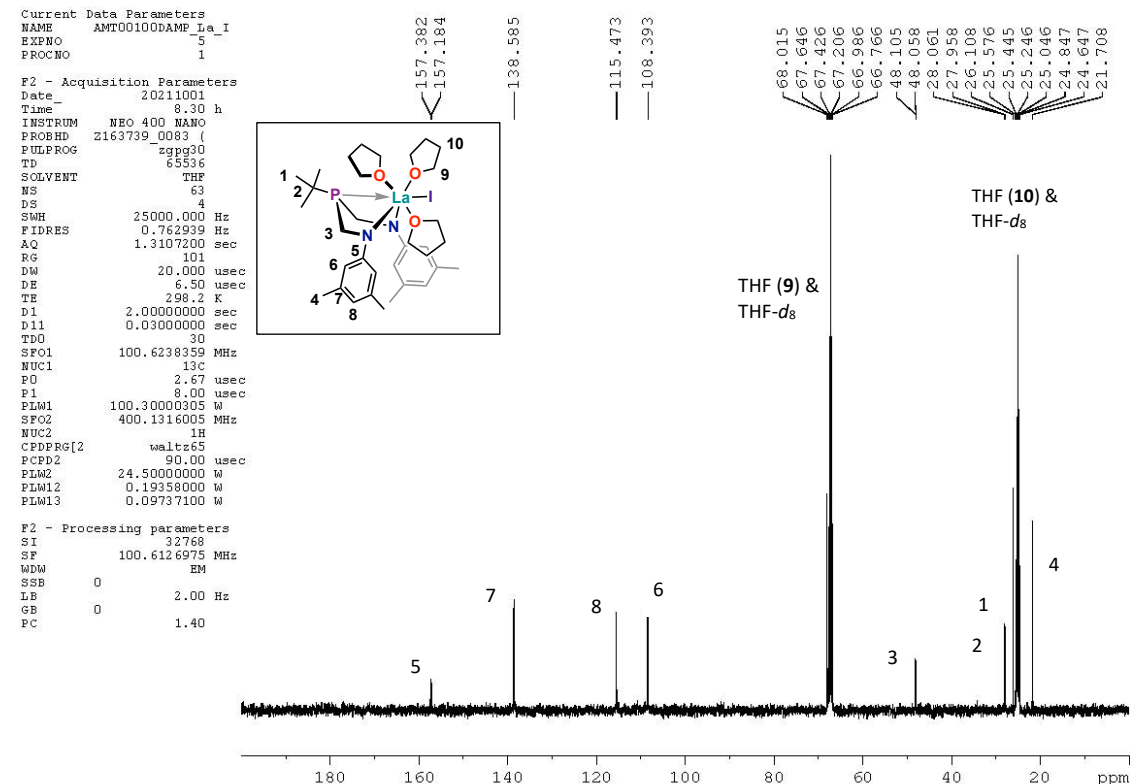


**Figure S17.**  $^{13}\text{C}\{\text{H}\}$  NMR spectrum of  $\text{La}(\text{ArBiAMP}^{\text{tBu}})(\text{THF})_3$  (**2**) recrystallized from THF:pentane acquired in  $\text{THF-d}_8$  at room temperature.

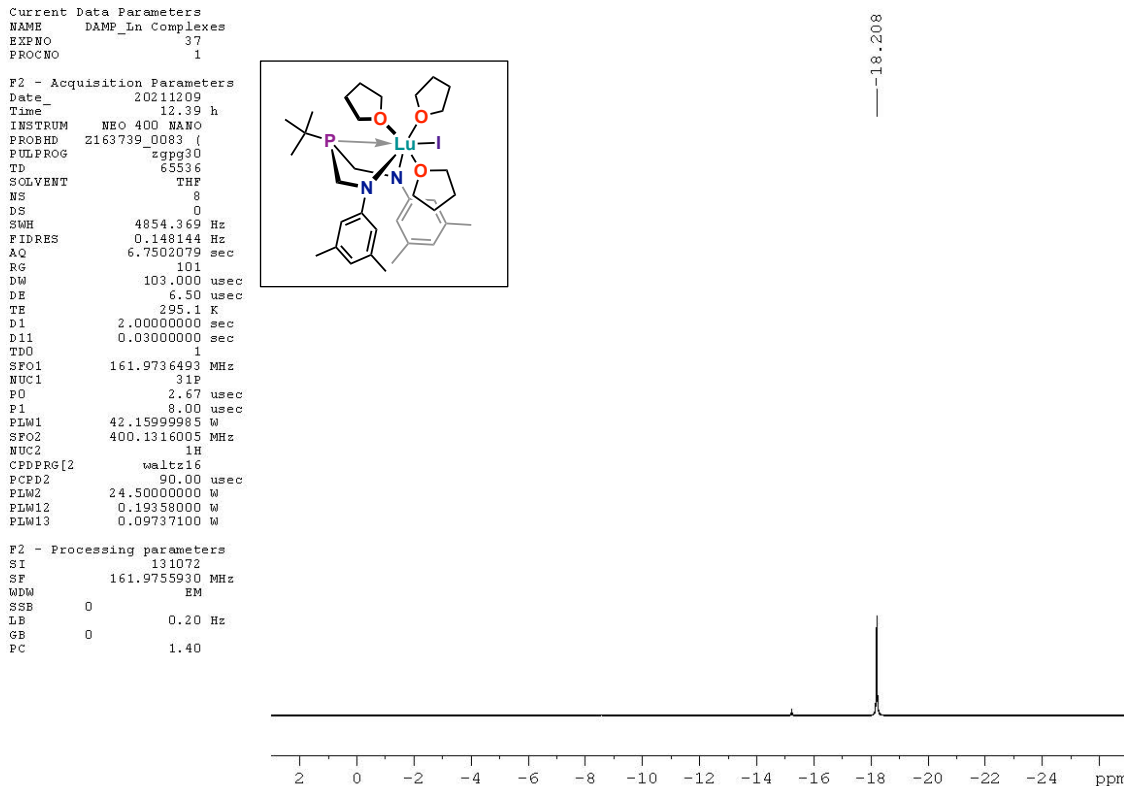
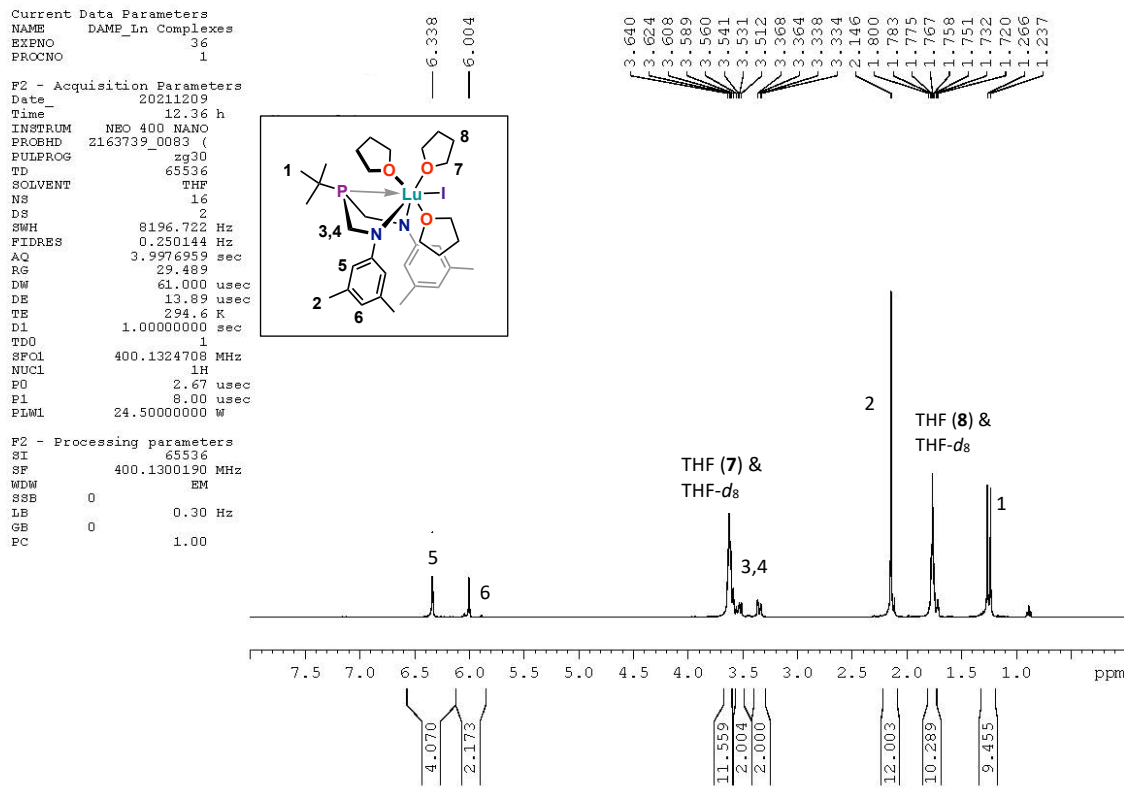


**Figure S19.**  $^{31}\text{P}\{\text{H}\}$  NMR spectrum of  $\text{Lu}(\text{I}^r\text{BiAMP}^{t\text{Bu}})(\text{THF})_3$  (3) recrystallized from THF:pentane acquired in  $\text{THF}-d_8$  at room temperature.

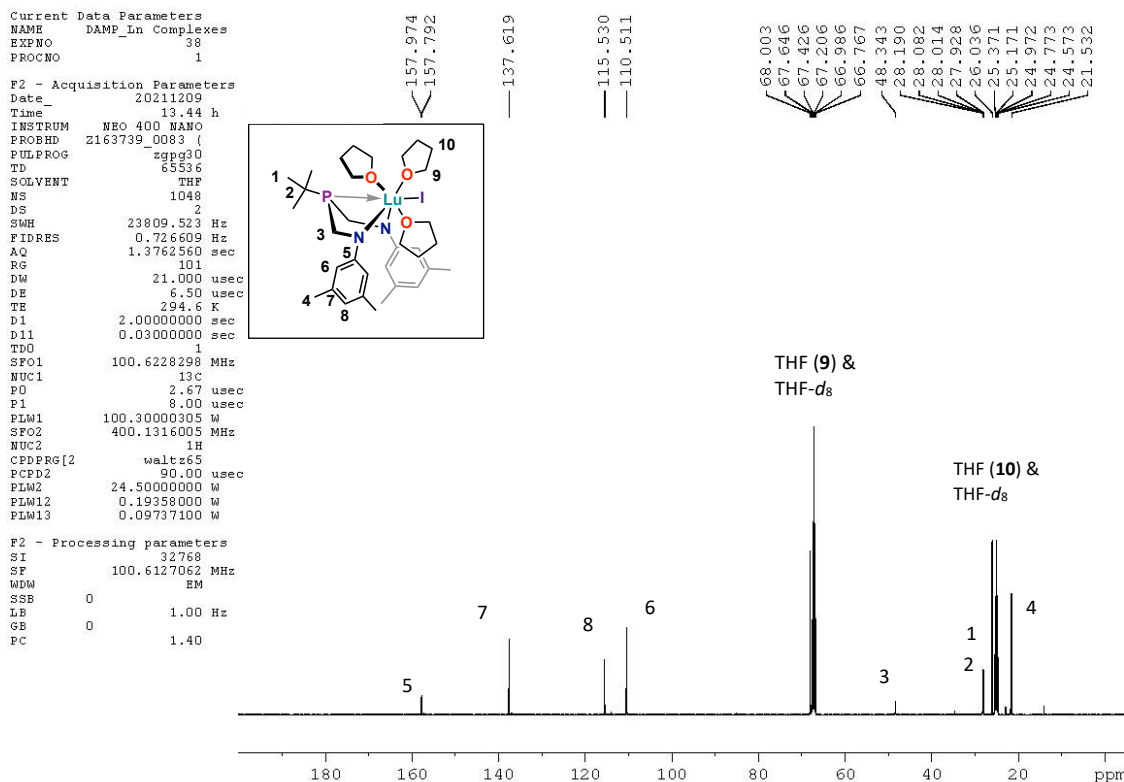


**Figure S20.**  $^{13}\text{C}\{\text{H}\}$  NMR spectrum of  $\text{LuI}(\text{^ArBiAMP}^{\text{Bu}})(\text{THF})_3$  (3) recrystallized from THF:pentane acquired in  $\text{THF-d}_8$  at room temperature.

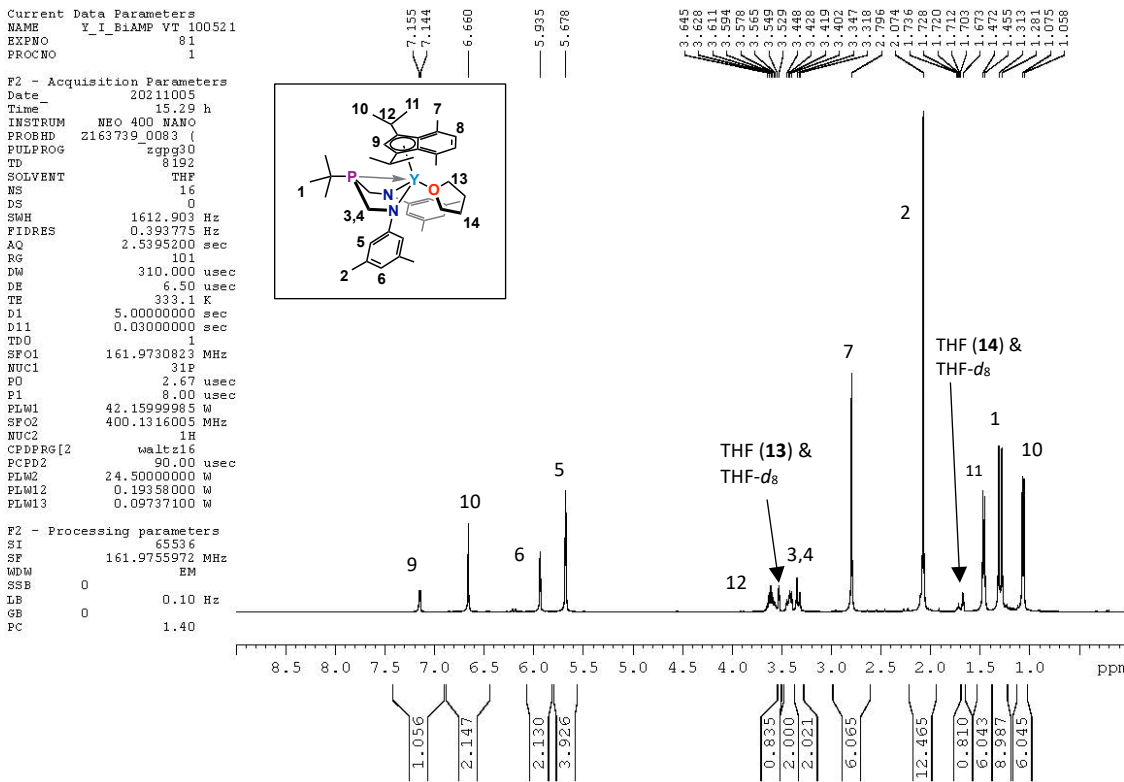


**Figure S21.**  $^1\text{H}$  NMR spectrum of  $\text{Y}(\eta^5\text{-}(1,3\text{-diisopropyl-4,7-dimethylindenyl})(\text{^ArBiAMP}^{\text{Bu}})(\text{THF})$  (4) recrystallized from THF:pentane acquired in  $\text{THF-d}_8$  at room temperature.

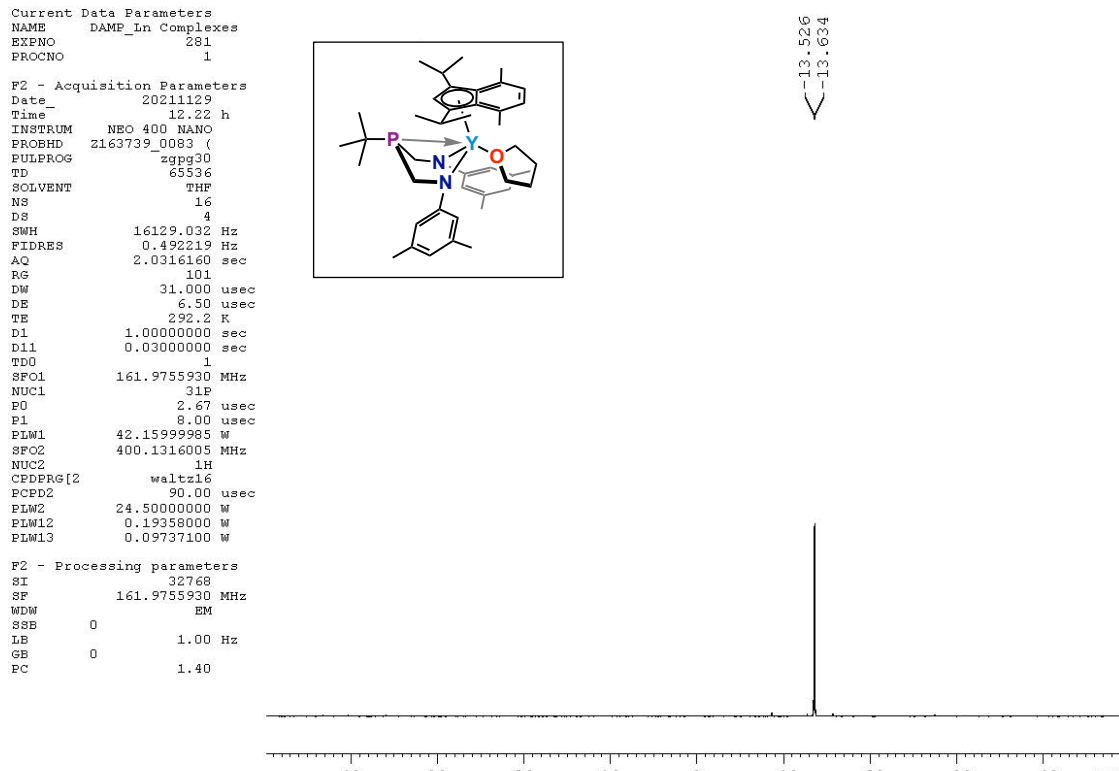


**Figure S22.**  $^{31}\text{P}\{\text{H}\}$  NMR spectrum of  $\text{Y}(\eta^5\text{-}(1,3\text{-diisopropyl-4,7-dimethylindenyl})^{4+}\text{BiAMP}^{6+}\text{Bu})(\text{THF})$  (**4**) recrystallized from THF:pentane acquired in  $\text{THF-d}_8$  at room temperature.

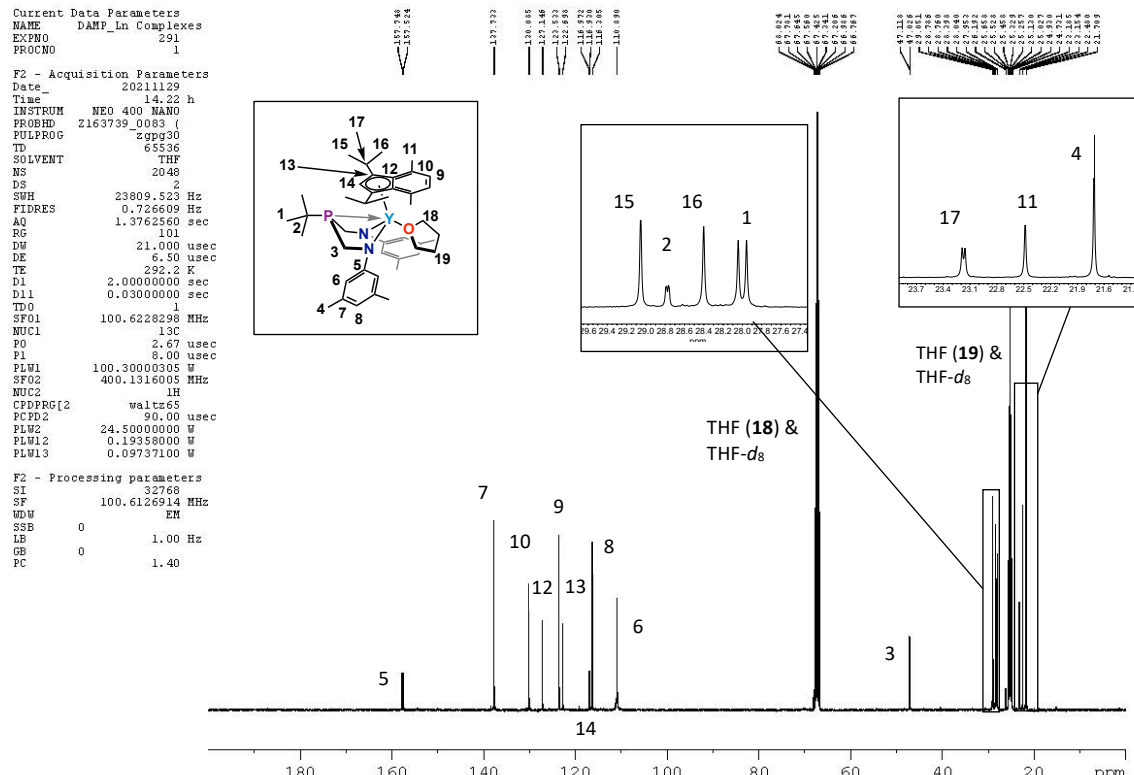


**Figure S23.**  $^{13}\text{C}\{\text{H}\}$  NMR spectrum of  $\text{Y}(\eta^5\text{-}(1,3\text{-diisopropyl-4,7-dimethylindenyl})^{4+}\text{BiAMP}^{6+}\text{Bu})(\text{THF})$  (**4**) recrystallized from THF:pentane acquired in  $\text{THF-d}_8$  at room temperature.

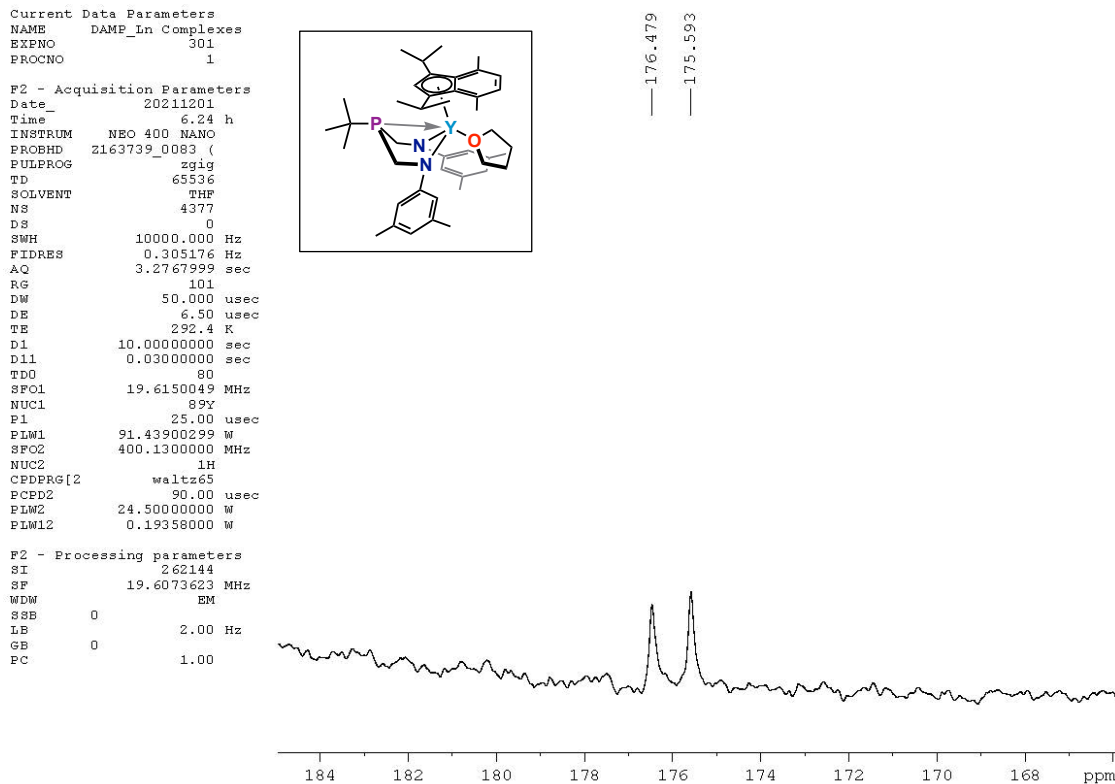


**Figure S24.**  $^{89}\text{Y}\{^1\text{H}\}$  NMR spectrum of  $\text{Y}(\eta^5\text{-}(1,3\text{-diisopropyl-4,7-dimethylindenyl})(^{47}\text{BiAMP}^{4\text{Bu}})(\text{THF})$  (4) recrystallized from THF:pentane in acquired in  $\text{THF-}d_8$  at room temperature.

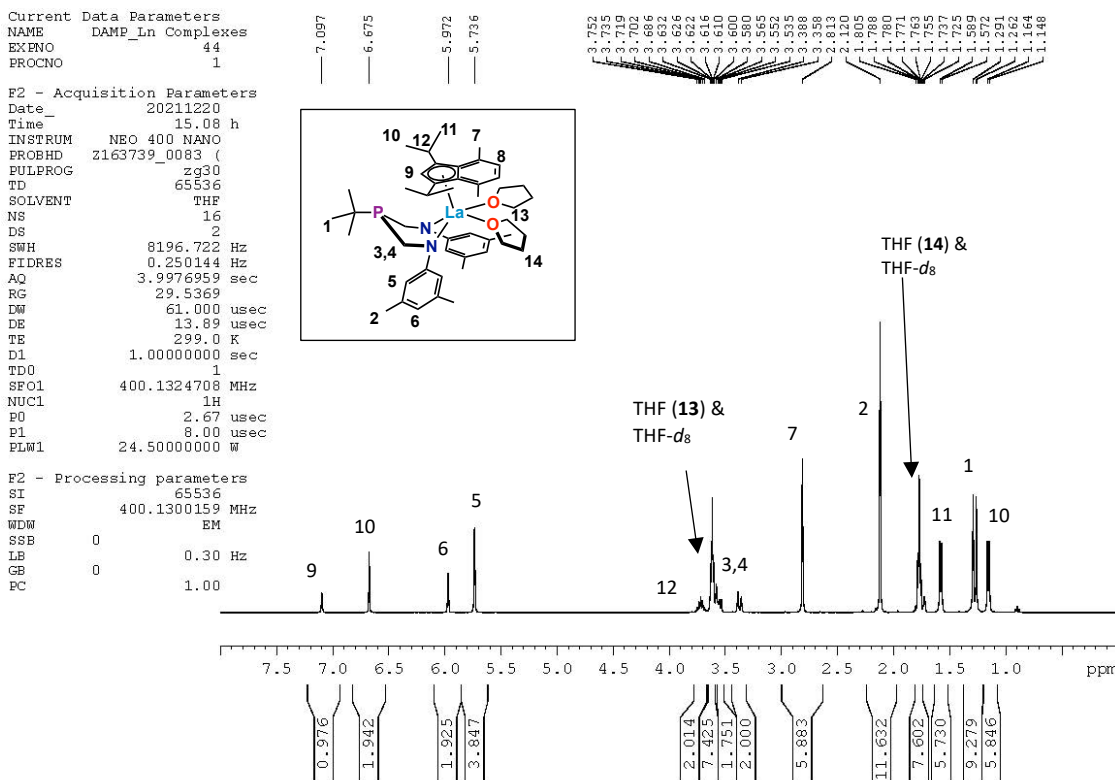


**Figure S25.**  $^1\text{H}$  NMR spectrum of  $\text{La}(\eta^5\text{-}(1,3\text{-diisopropyl-4,7-dimethylindenyl})(^{47}\text{BiAMP}^{4\text{Bu}})(\text{THF})_2$  (5) recrystallized from THF:pentane in acquired in  $\text{THF-}d_8$  at room temperature.

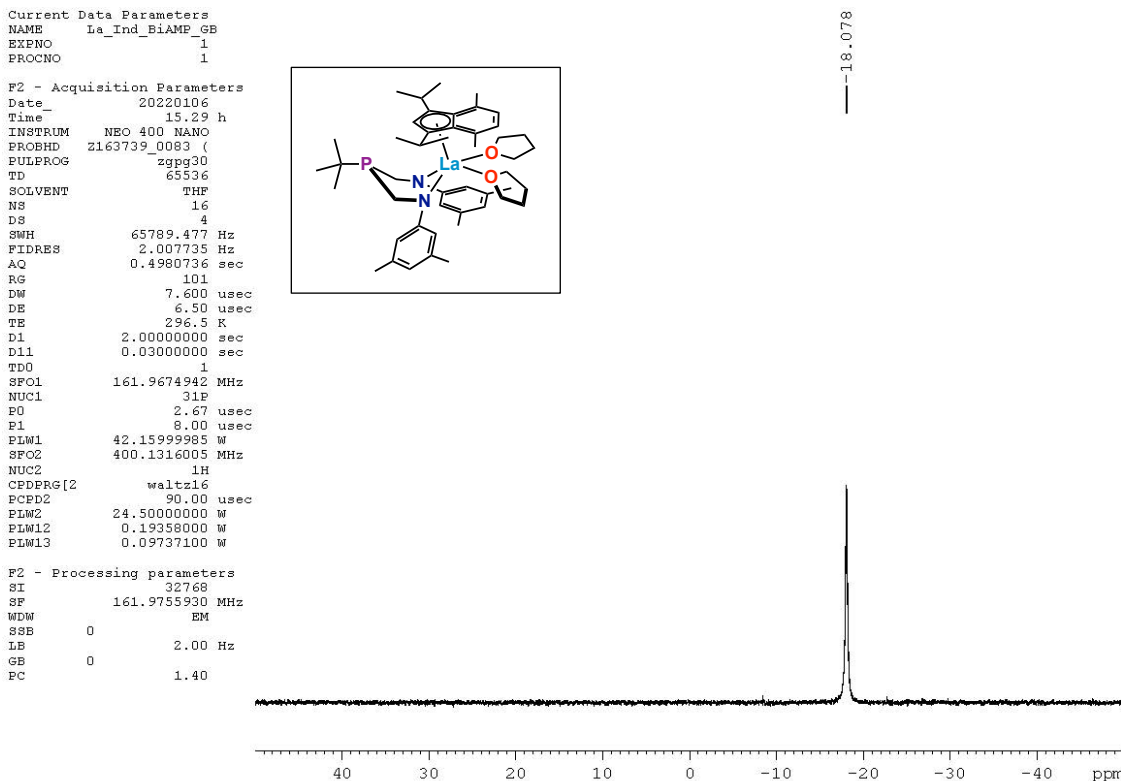


**Figure S26.**  $^{31}\text{P}\{\text{H}\}$  NMR spectrum of  $\text{La}(\eta^5\text{-}(1,3\text{-diisopropyl-4,7-dimethylindenyl})(\text{⁴⁺BiAMP}^{\text{Bu}})\text{(THF)}_2$  (5) recrystallized from THF:pentane acquired in THF- $d_8$  at room temperature.

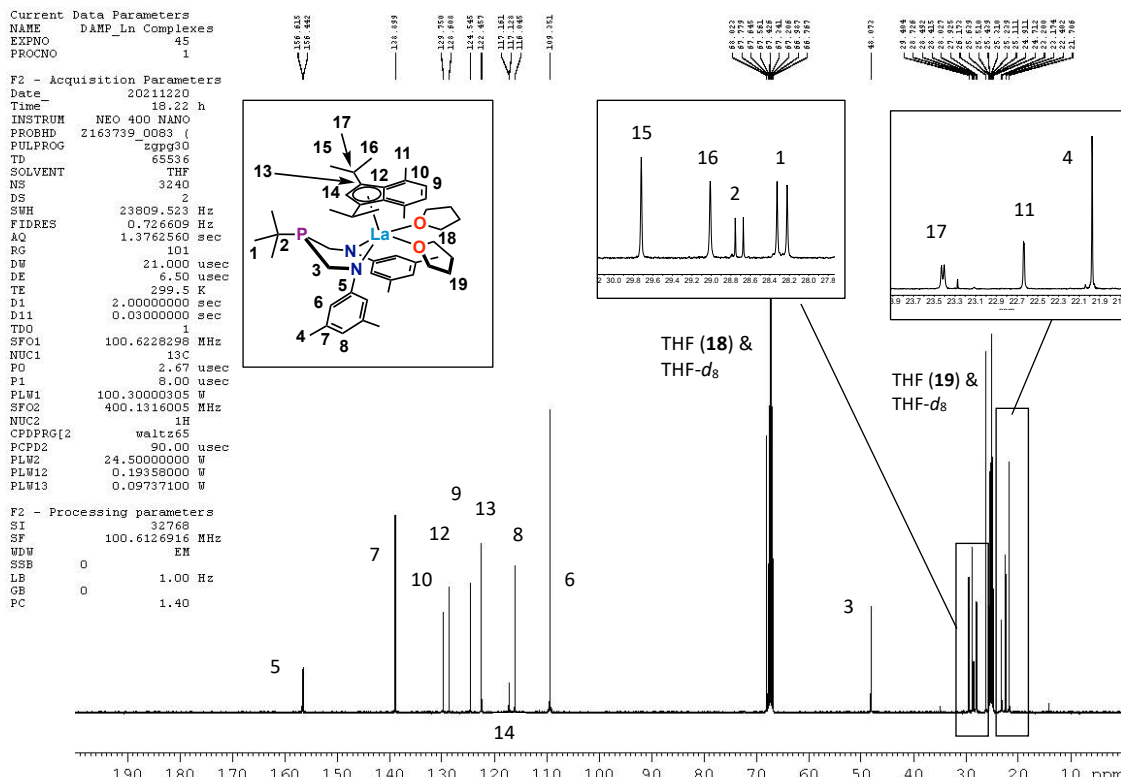


**Figure S27.**  $^{13}\text{C}\{\text{H}\}$  NMR spectrum of  $\text{La}(\eta^5\text{-}(1,3\text{-diisopropyl-4,7-dimethylindenyl})(\text{⁴⁺BiAMP}^{\text{Bu}})\text{(THF)}_2$  (5) recrystallized from THF:pentane acquired in THF- $d_8$  at room temperature. Expansions are provided for two aliphatic regions to assist with visualization of the assigned resonances.

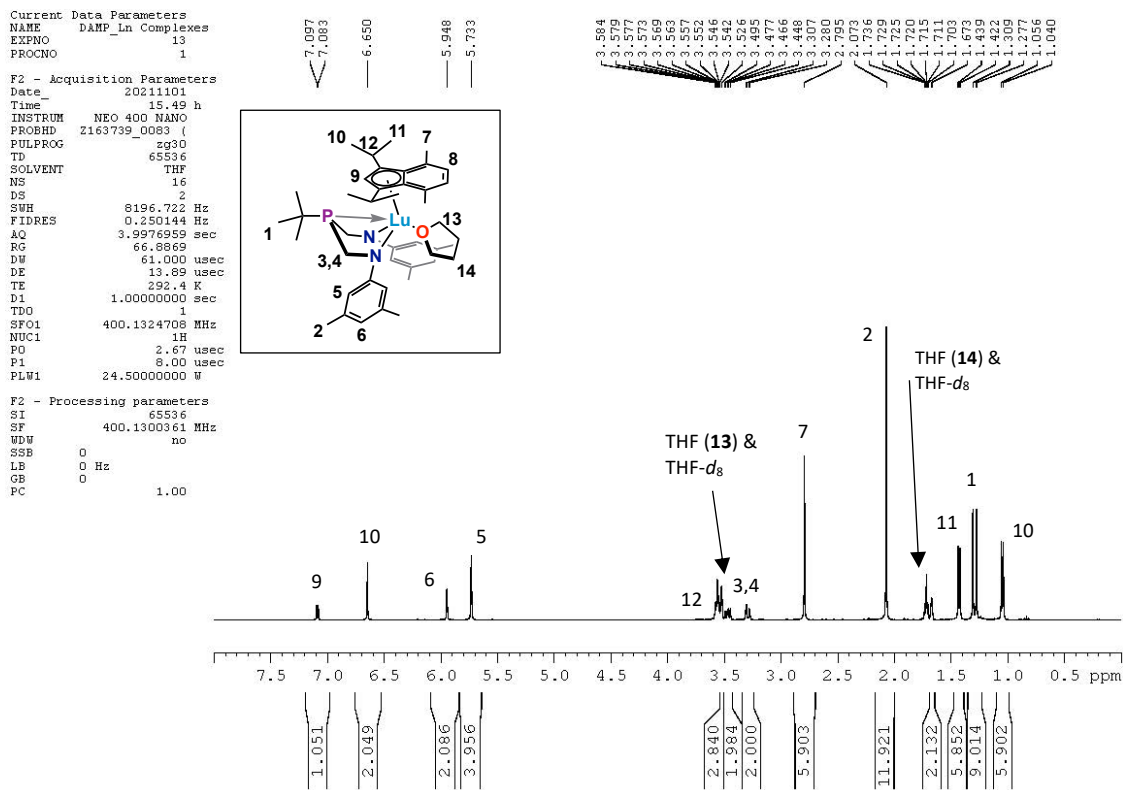


**Figure S28.** <sup>1</sup>H NMR spectrum of Lu(η⁵-(1,3-diisopropyl-4,7-dimethylindenyl)(⁴⁷BiAMP⁴Bu)(THF) (6) recrystallized from THF:pentane acquired in THF-d<sub>8</sub> at room temperature.

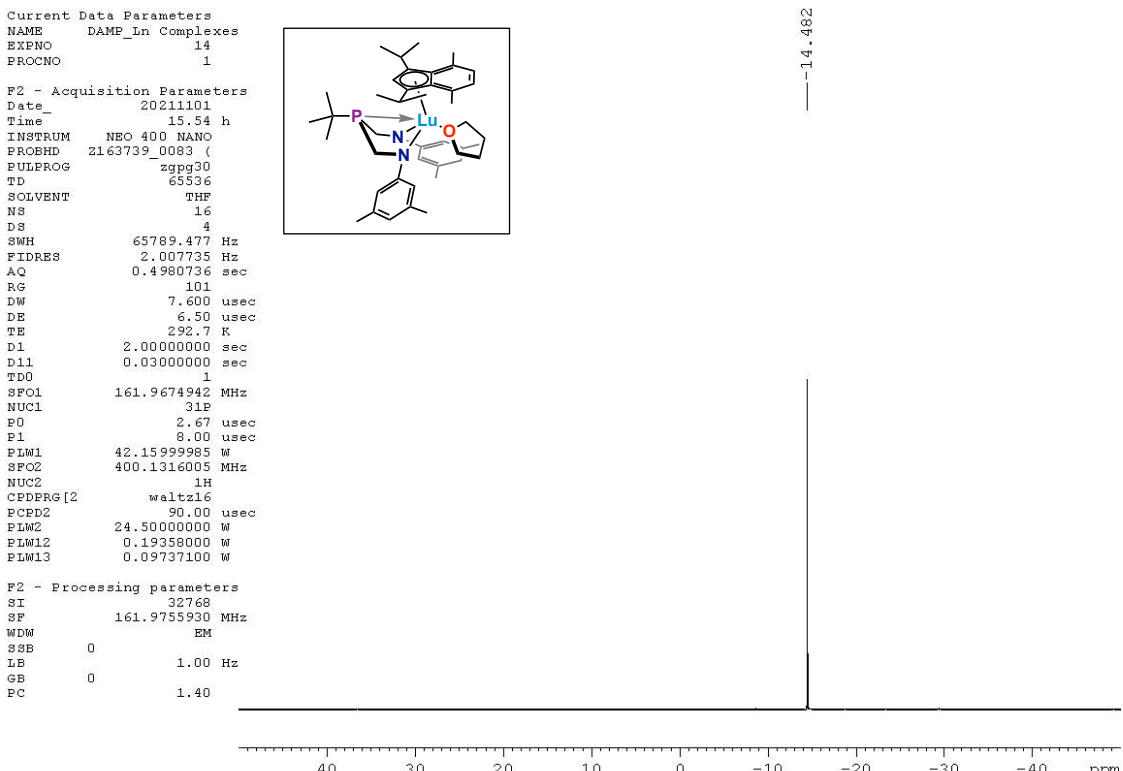


**Figure S29.** <sup>31</sup>P{<sup>1</sup>H} NMR spectrum of Lu(η⁵-(1,3-diisopropyl-4,7-dimethylindenyl)(⁴⁷BiAMP⁴Bu)(THF) (6) recrystallized from THF:pentane acquired in THF-d<sub>8</sub> at room temperature.

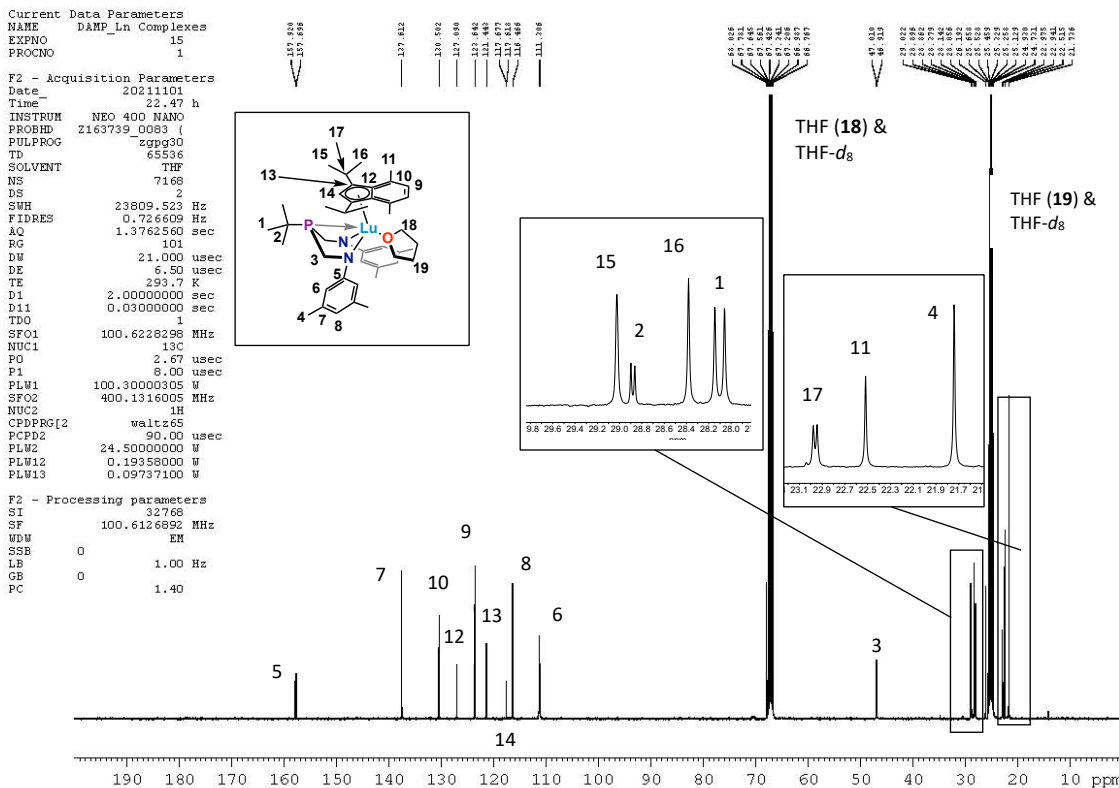


**Figure S30.**  $^{13}\text{C}\{\text{H}\}$  NMR spectrum of  $\text{Lu}(\eta^5\text{-}(1,3\text{-diisopropyl-4,7-dimethylindenyl})(^{49}\text{BiAMP}^{89}\text{O})(\text{THF})$  (6) recrystallized from THF:pentane acquired in THF- $d_8$  at room temperature. Expansions are provided for two aliphatic regions to assist with visualization of the assigned resonances.

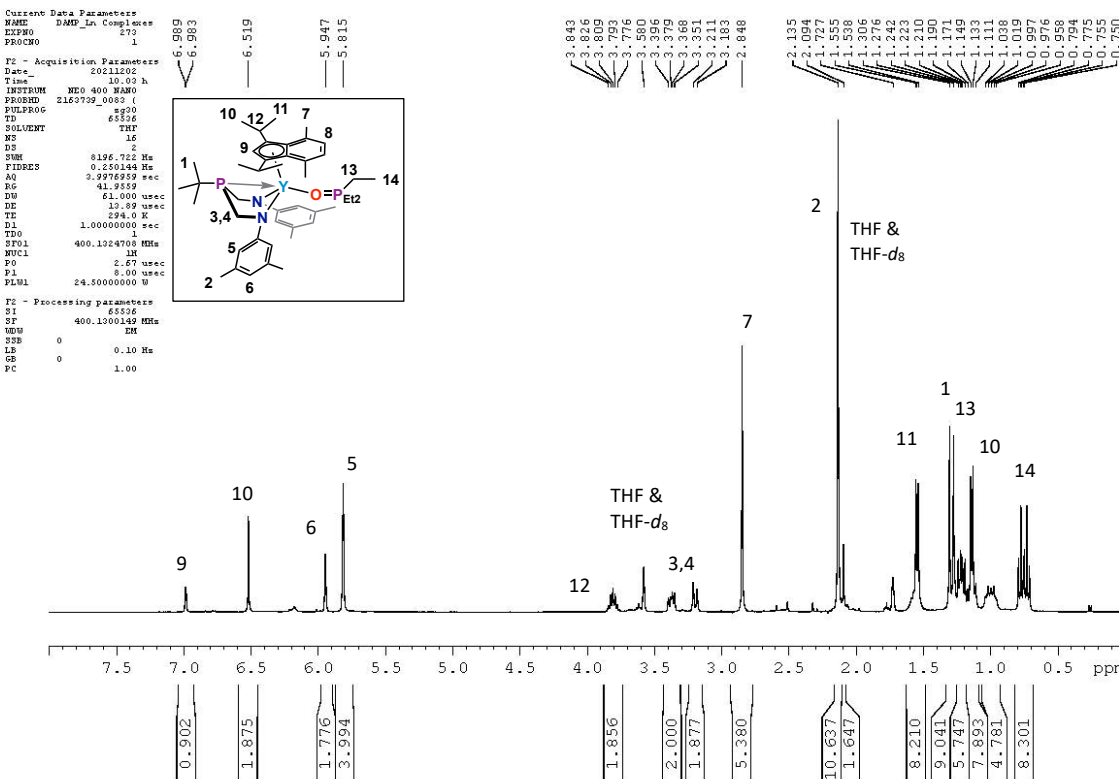


**Figure S31.**  $^1\text{H}$  NMR spectrum of the in-situ formed  $\text{Y}(\eta^5\text{-}(1,3\text{-diisopropyl-4,7-dimethylindenyl})(^{49}\text{BiAMP}^{89}\text{O})(\text{O=PEt}_3)$  (7) acquired in THF- $d_8$  at room temperature.

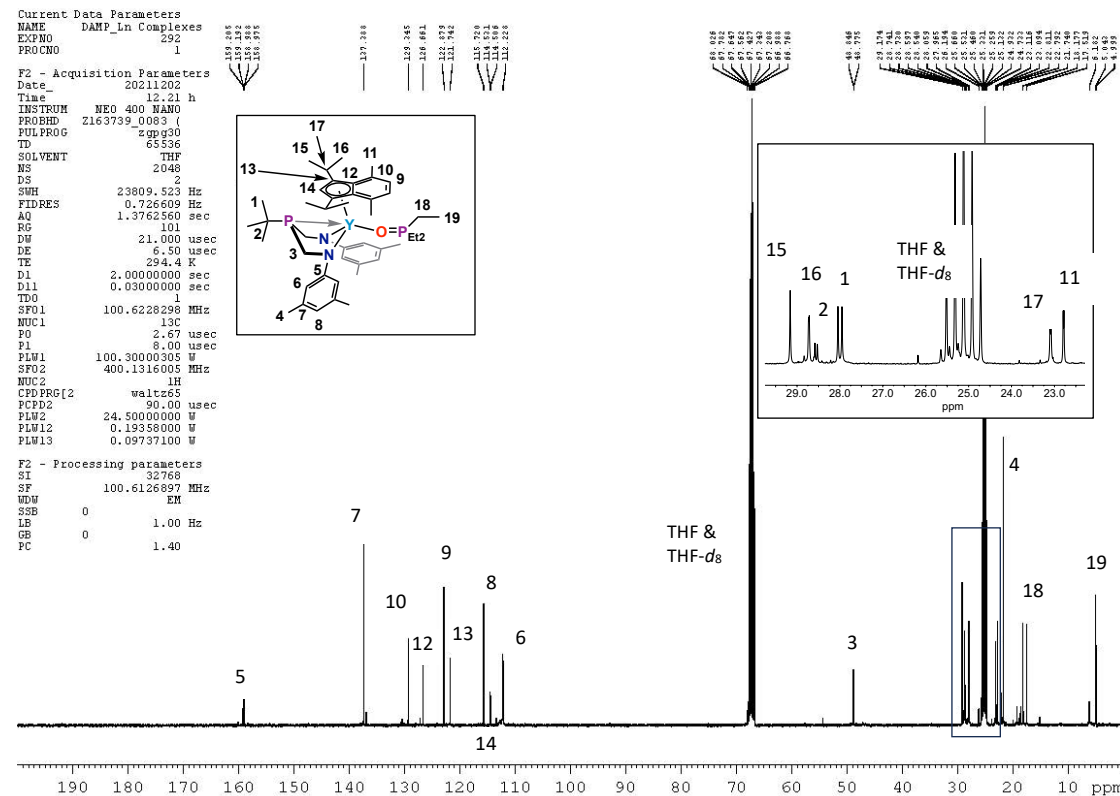


**Figure S32.**  $^{13}\text{C}\{\text{H}\}$  NMR spectrum of the in-situ formed  $\text{Y}(\eta^5\text{-}(1,3\text{-diisopropyl-4,7-dimethylindenyl})(^{4r}\text{BiAMP}^{t\text{Bu}})(\text{O}=\text{PEt}_3)$  (7) acquired in  $\text{THF-d}_8$  at room temperature. An expansion is provided for two aliphatic regions to assist with visualization of the assigned resonances.

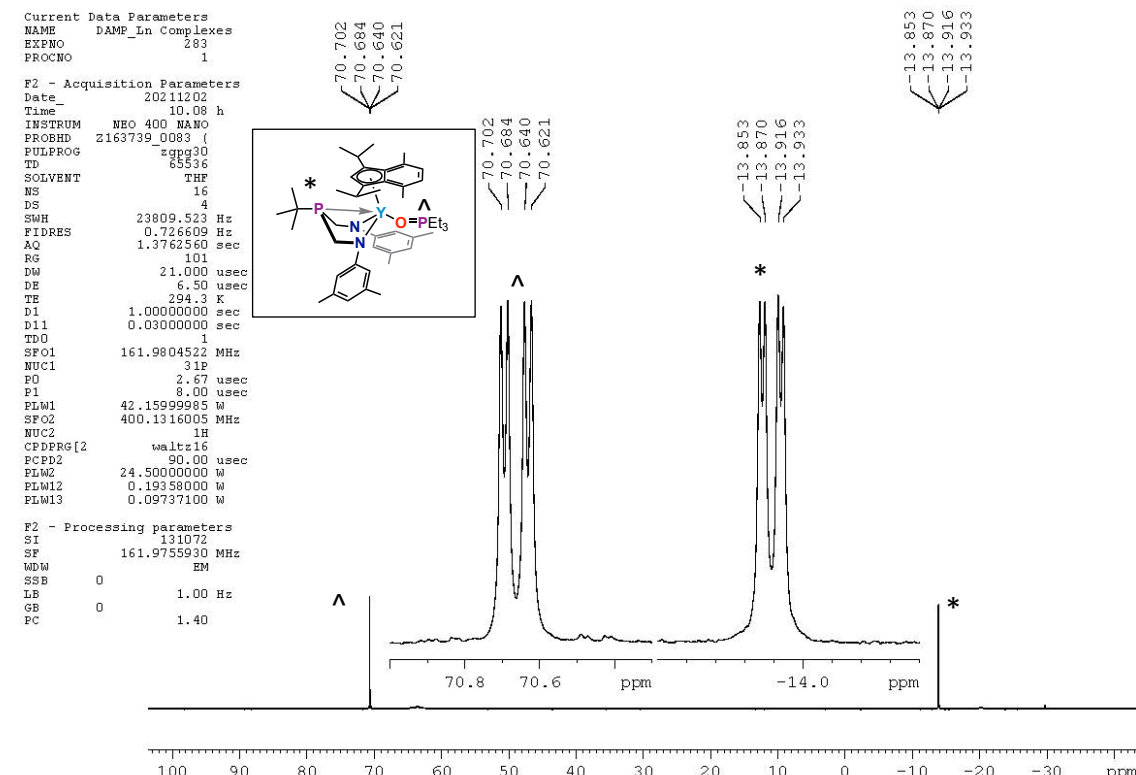


**Figure S33.**  $^{31}\text{P}\{\text{H}\}$  NMR spectrum of the in-situ formed  $\text{Y}(\eta^5\text{-}(1,3\text{-diisopropyl-4,7-dimethylindenyl})(^{4r}\text{BiAMP}^{t\text{Bu}})(\text{O}=\text{PEt}_3)$  (7) acquired in  $\text{THF-d}_8$  recorded at 25 °C (298 K).

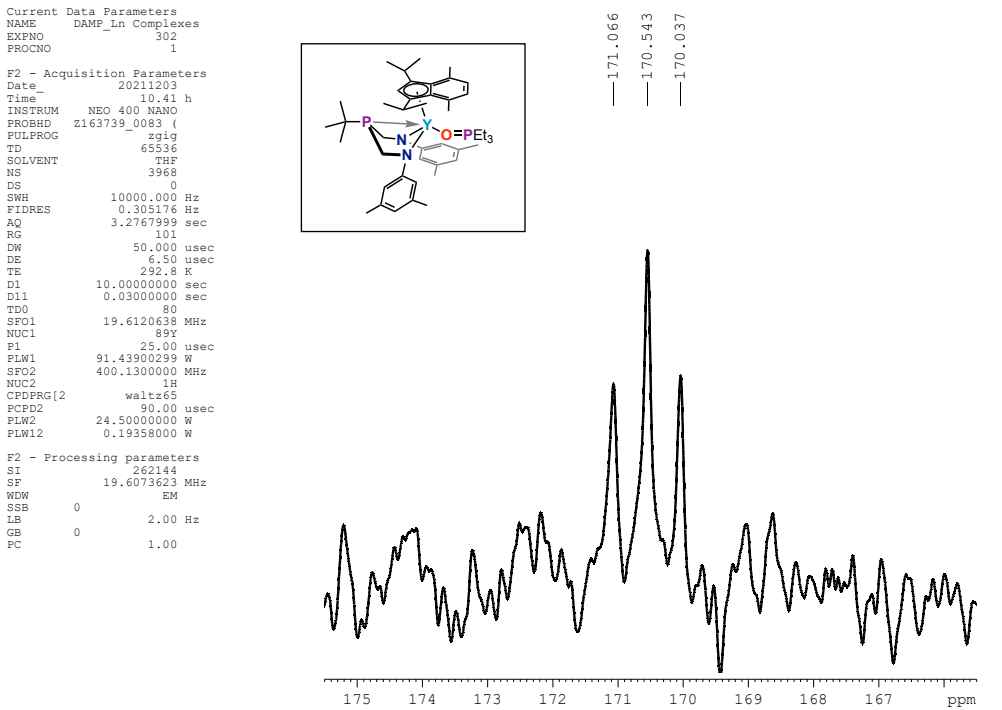


**Figure S34.**  $^{18}\text{Y}$  NMR spectrum of the in-situ formed  $\text{Y}(\eta^5\text{-}(1,3\text{-diisopropyl-4,7-dimethylindenyl})(^{4+}\text{BiAMP}^{8+})(\text{O=PEt}_3)$  (8) acquired in  $\text{THF-d}_8$ .

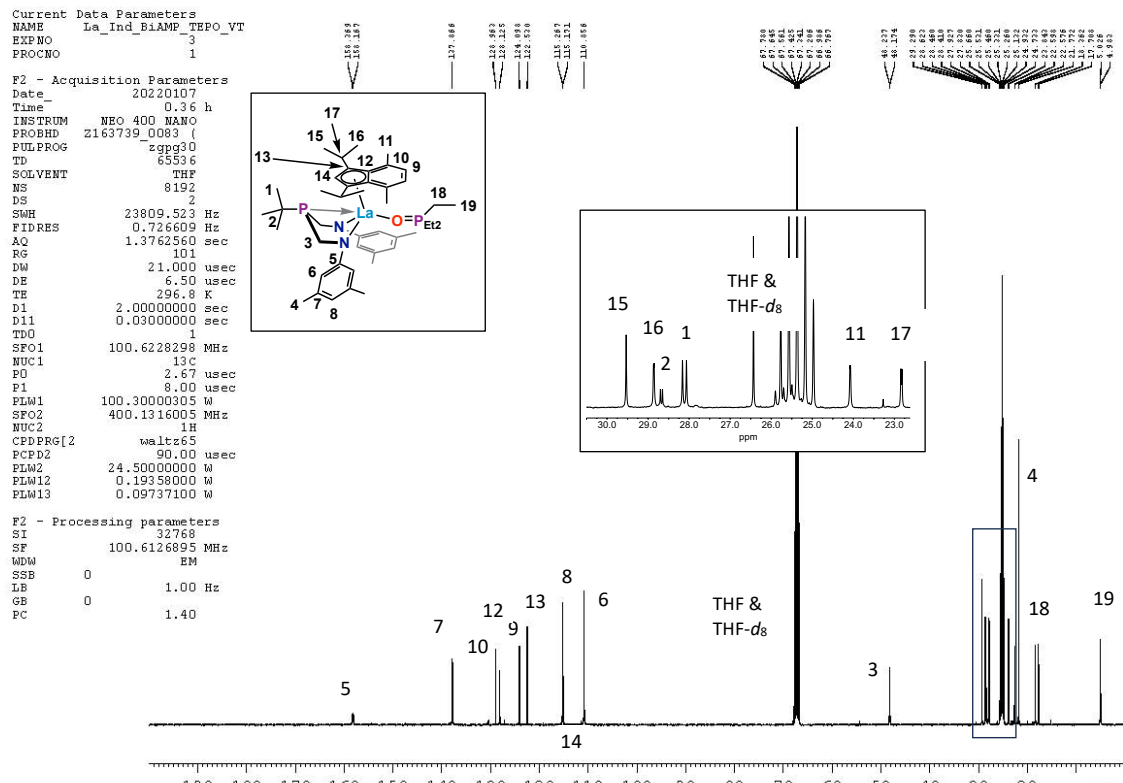


**Figure S35.**  $^{13}\text{C}\{^1\text{H}\}$  NMR spectrum of the in-situ formed  $\text{La}(\eta^5\text{-}(1,3\text{-diisopropyl-4,7-dimethylindenyl})(^{4+}\text{BiAMP}^{8+})(\text{O=PEt}_3)$  (8) acquired in  $\text{THF-d}_8$  at room temperature. An expansion is provided for two aliphatic regions to assist with visualization of the assigned resonances. Pentane can be observed in the spectrum.

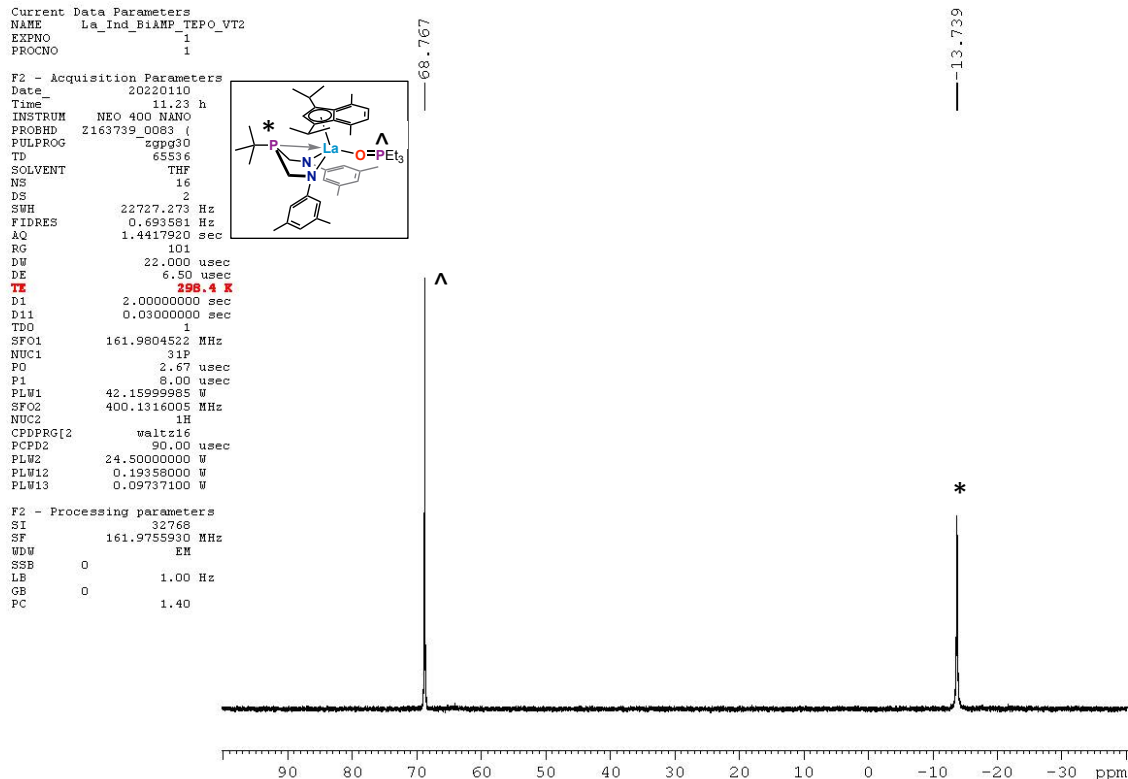


**Figure S36.**  $^{31}P\{^1H\}$  NMR spectrum of the in-situ formed  $\text{La}(\eta^5\text{-}(1,3\text{-diisopropyl-4,7-dimethylindenyl})\text{BiAMP}^{t\text{Bu}})(\text{O=PEt}_3)$  (8) acquired in  $\text{THF}-d_8$  recorded at 25 °C (298 K).

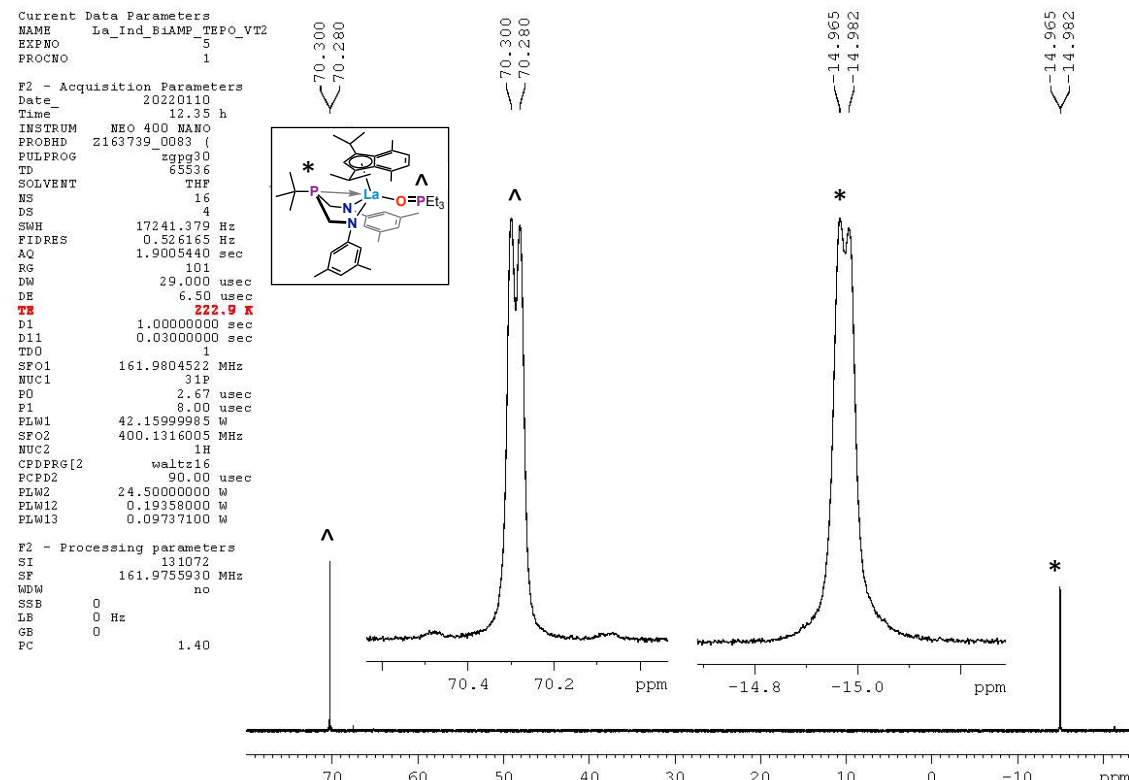


**Figure S37.** Expansion of the phosphorus resonances of the  $^{31}P\{^1H\}$  NMR spectrum of the in-situ formed  $\text{La}(\eta^5\text{-}(1,3\text{-diisopropyl-4,7-dimethylindenyl})\text{BiAMP}^{t\text{Bu}})(\text{O=PEt}_3)$  (8) acquired in  $\text{THF}-d_8$  recorded at -50 °C (223 K).

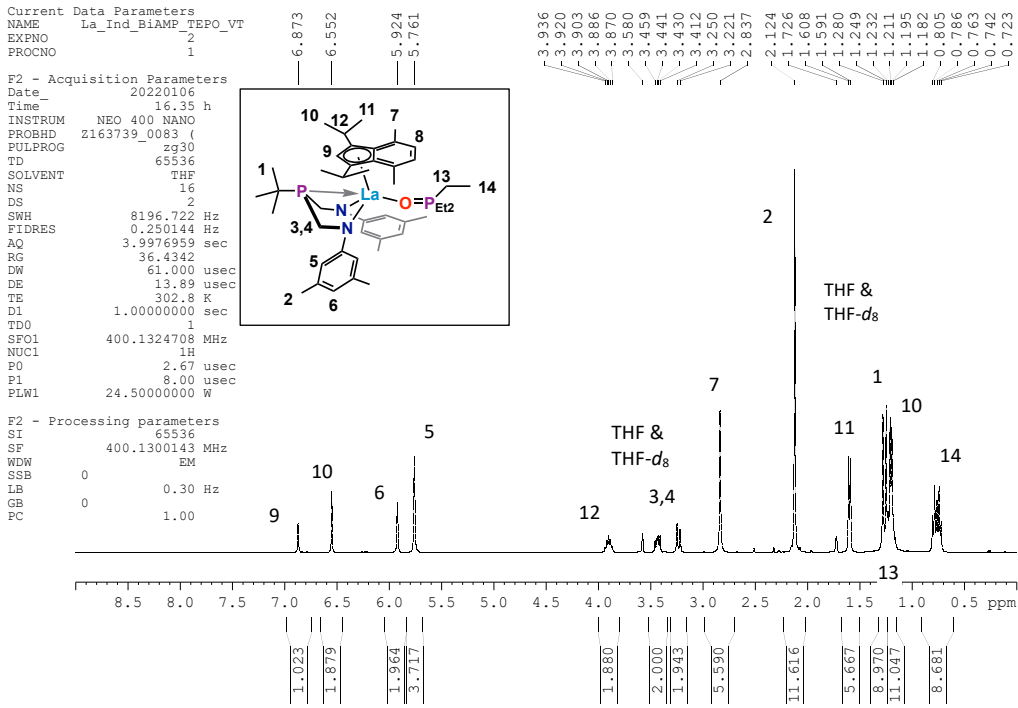


**Figure S38.**  $^1\text{H}$  NMR spectrum of the in-situ formed  $\text{La}(\eta^5\text{-}(1,3\text{-diisopropyl-4,7-dimethylindenyl})(\text{ArBiAMP}^{\text{tBu}})(\text{O=PEt}_3))$  (9) acquired in  $\text{THF-d}_6$  at room temperature.

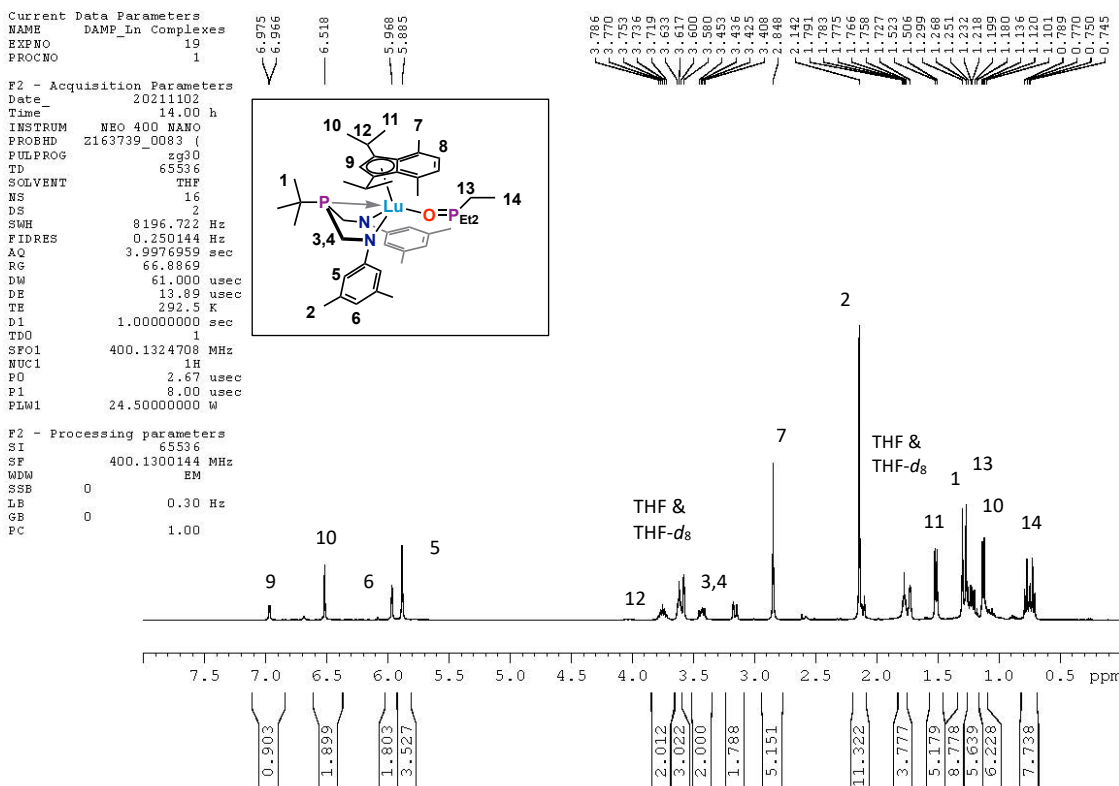


**Figure S39.**  $^1\text{H}$  NMR spectrum of the in-situ formed  $\text{Lu}(\eta^5\text{-}(1,3\text{-diisopropyl-4,7-dimethylindenyl})(\text{ArBiAMP}^{\text{tBu}})(\text{O=PEt}_3))$  (9) acquired in  $\text{THF-d}_6$  at room temperature.

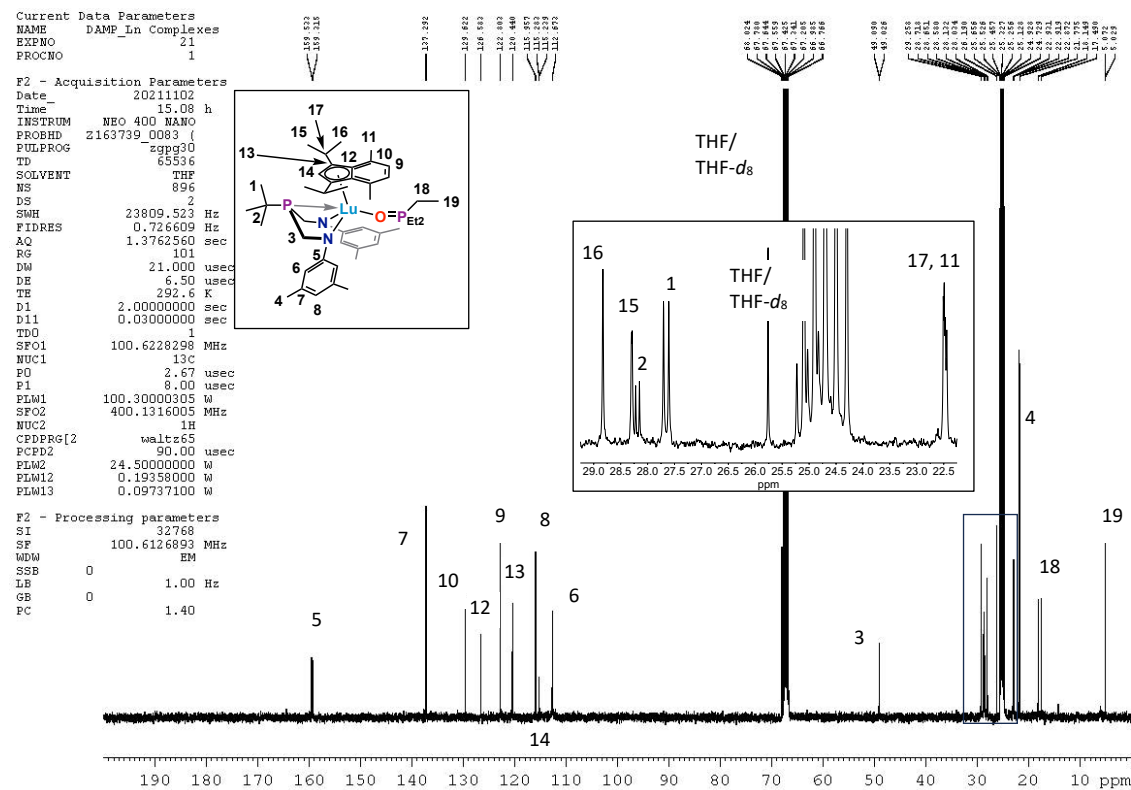


**Figure S40.**  $^{13}\text{C}\{^1\text{H}\}$  NMR spectrum of the *in-situ* formed  $\text{Lu}(\eta^5\text{-}(1,3\text{-diisopropyl-4,7-dimethylindenyl})(\text{ArBiAMP}^1\text{Bu})(\text{O=PEt}_3))$  (9) acquired in  $\text{THF-d}_6$  at room temperature. An expansion is provided for two aliphatic regions to assist with visualization of the assigned resonances.

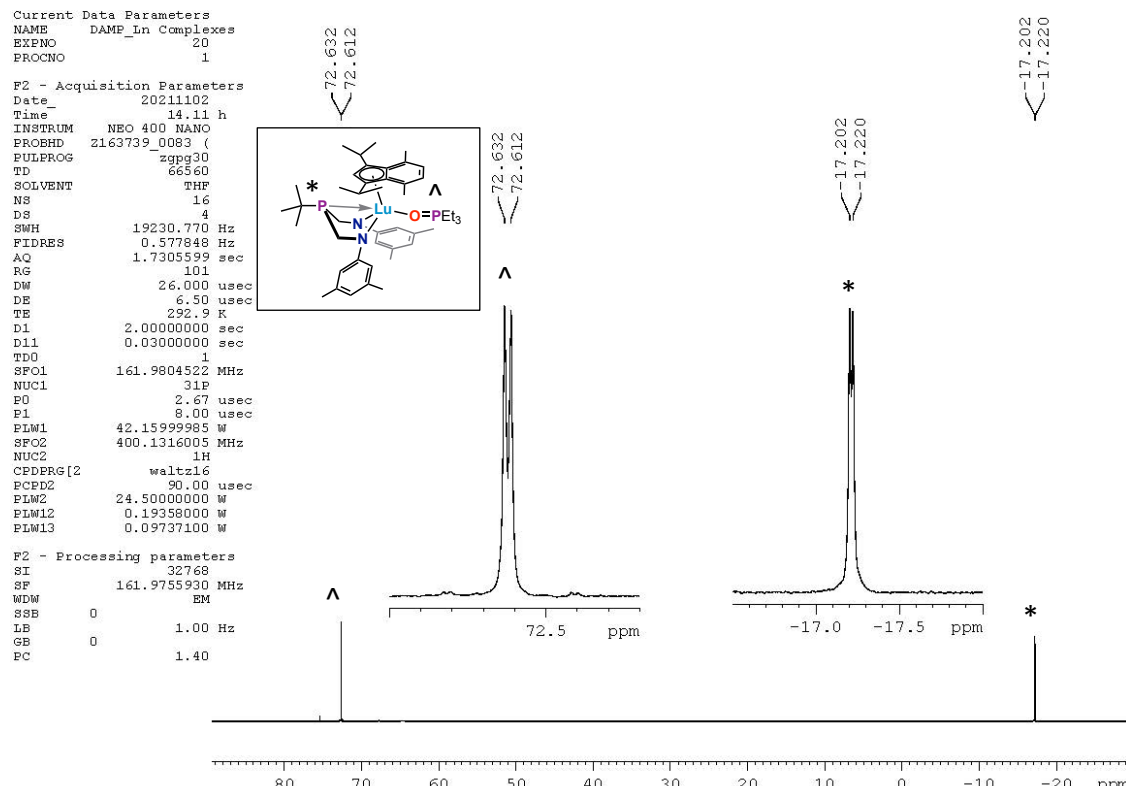


**Figure S41.**  $^{31}\text{P}\{^1\text{H}\}$  NMR spectrum of the *in-situ* formed  $\text{Lu}(\eta^5\text{-}(1,3\text{-diisopropyl-4,7-dimethylindenyl})(\text{ArBiAMP}^1\text{Bu})(\text{O=PEt}_3))$  (9) acquired in  $\text{THF-d}_6$  at 25 °C (298 K).

## 2.2. IR (ATR) data

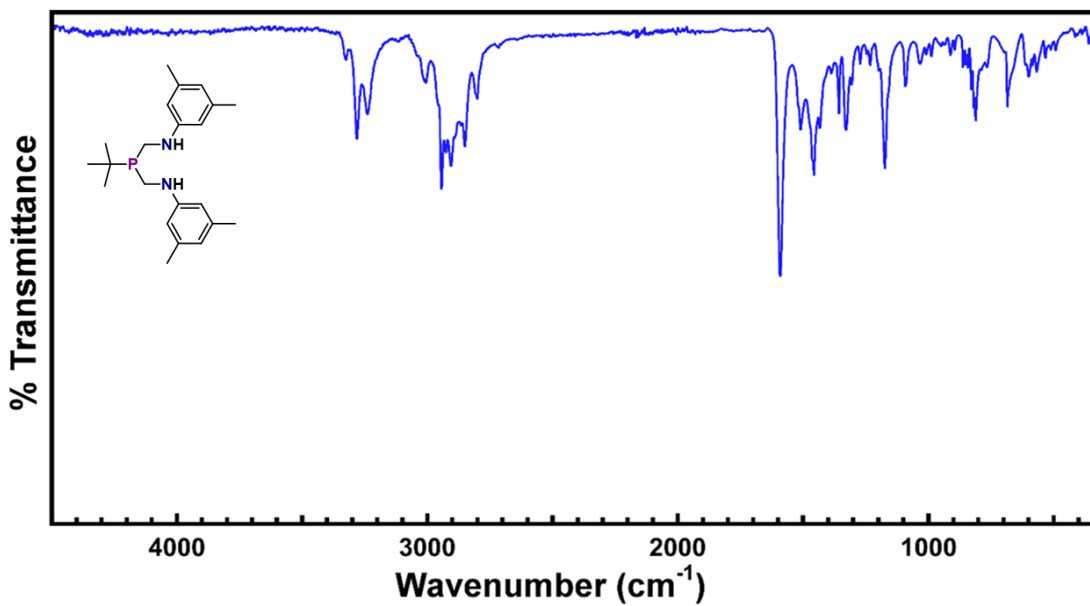


**Figure S42.** FT-IR (ATR) spectrum of  $^{Ar}BiAMP^{tBu}$ .  $\nu$  ( $\text{cm}^{-1}$ ): 359 (w), 413 (w), 491 (w), 533 (w), 568 (m), 599 (m), 684 (s), 765 (m), 811 (s), 842 (m), 911 (m), 988 (m), 1032 (m), 1092 (m), 1173 (s), 1232 (m), 1272 (m), 1328 (s), 1357 (s), 1456 (s), 1509 (s), 1591 (s), 2801 (m), 2850 (s), 2905 (s), 2926 (s), 2944 (s), 3005 (m), 3237 (s), 3281 (s), 3324 (m).

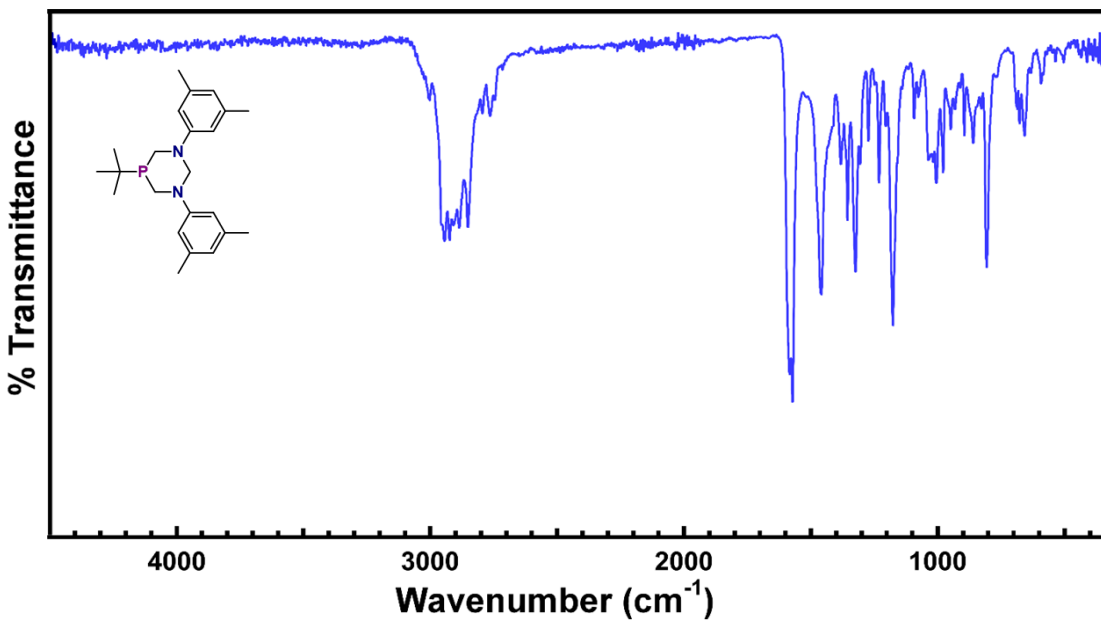


**Figure S43.** FT-IR (ATR) spectrum of  $(^{Ar}BiAMP^{tBu})\text{CH}_2$ .  $\nu$  ( $\text{cm}^{-1}$ ): 501 (w), 535 (w), 592 (m), 657 (m), 677 (m), 807 (s), 859 (m), 894 (m), 931 (m), 948 (m), 978 (s), 1004 (s), 1017 (s), 1075 (m), 1176 (s), 1230 (s), 1272 (s), 1324 (s), 1355 (s), 1380 (m), 1458 (s), 1572 (s), 2746 (m), 2765 (m), 2794 (m), 2851 (s), 2886 (s), 2924 (s), 2943 (s), 3002 (m).

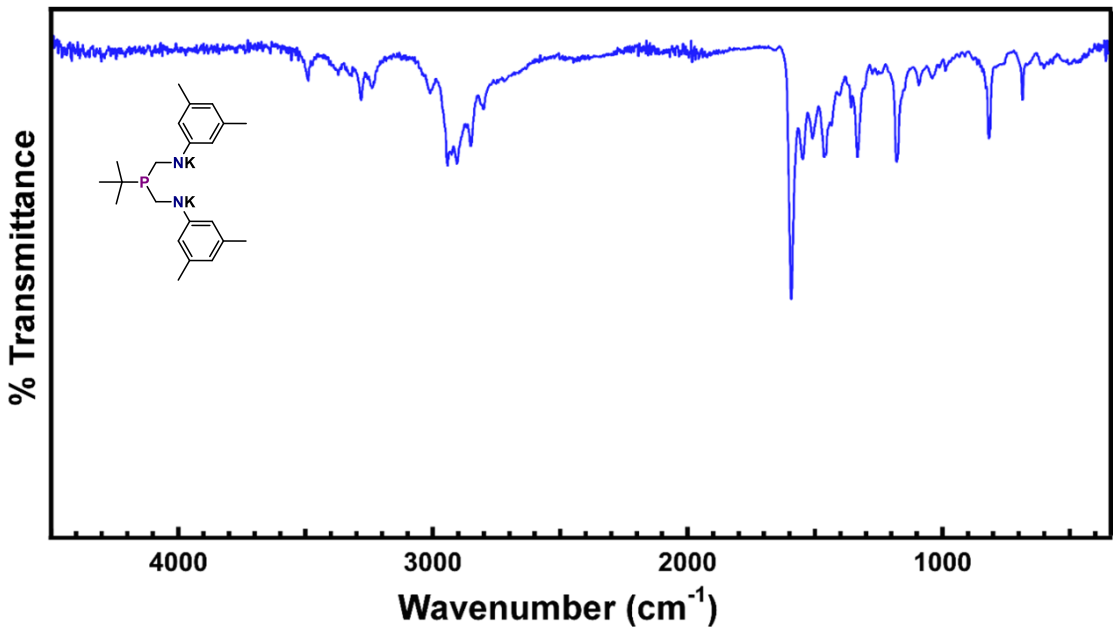


**Figure S44.** FT-IR (ATR) spectrum of (<sup>Ar</sup>**BiAMP<sup>tBu</sup>**)K<sub>2</sub>.  $\nu$  (cm<sup>-1</sup>): 358 (w), 458 (w), 504 (w), 601 (w), 685 (m), 816 (s) 987 (w), 1038 (w), 1092 (w), 1179 (s), 1333 (s), 1464 (s), 1509 (m), 1548 (s), 1593 (s), 2801 (m), 2850 (s), 2904 (s), 2942 (s), 3010 (m), 3238 (m), 3281 (m), 3318 (w), 3371 (w), 3489 (m).

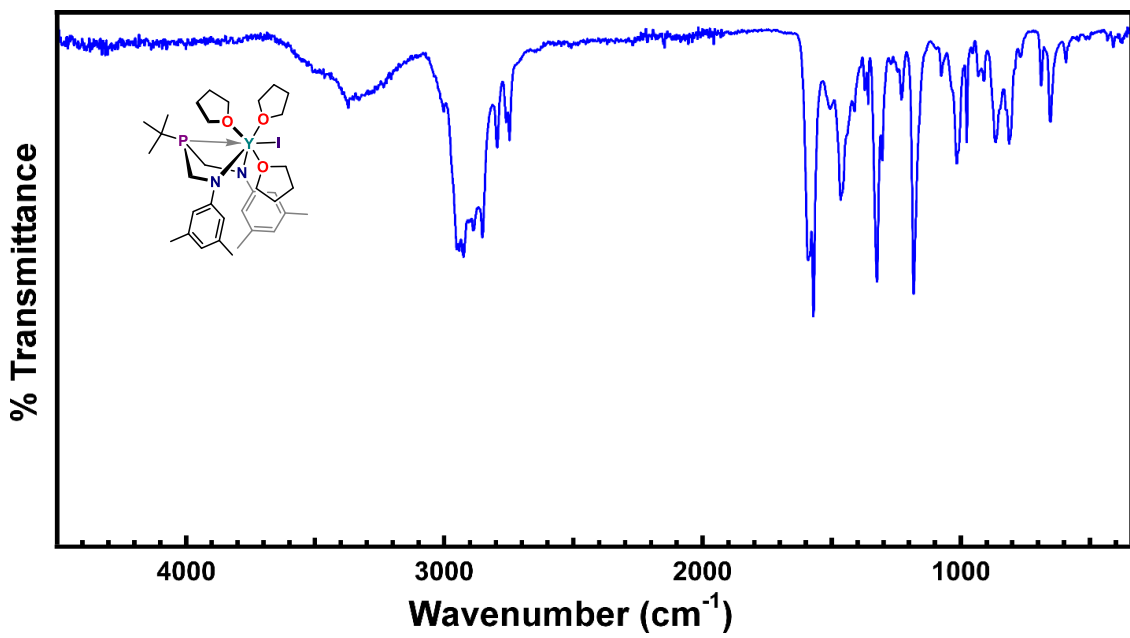


**Figure S45.** FT-IR (ATR) spectrum of YI(<sup>Ar</sup>**BiAMP<sup>tBu</sup>**)(THF)<sub>3</sub> (1).  $\nu$  (cm<sup>-1</sup>): 375 (w), 409 (w), 592 (w), 652 (s), 688 (m), 767 (w), 812 (s), 865 (s), 909 (w), 932 (w), 976 (s), 1015 (s), 1075 (w), 1182 (s), 1229 (s), 1324 (s), 1464 (s), 1570 (s), 1566 (s), 2747 (s), 2765 (s), 2852 (s), 2886 (s), 2924 (s), 2928 (s), 3368 (m, br).

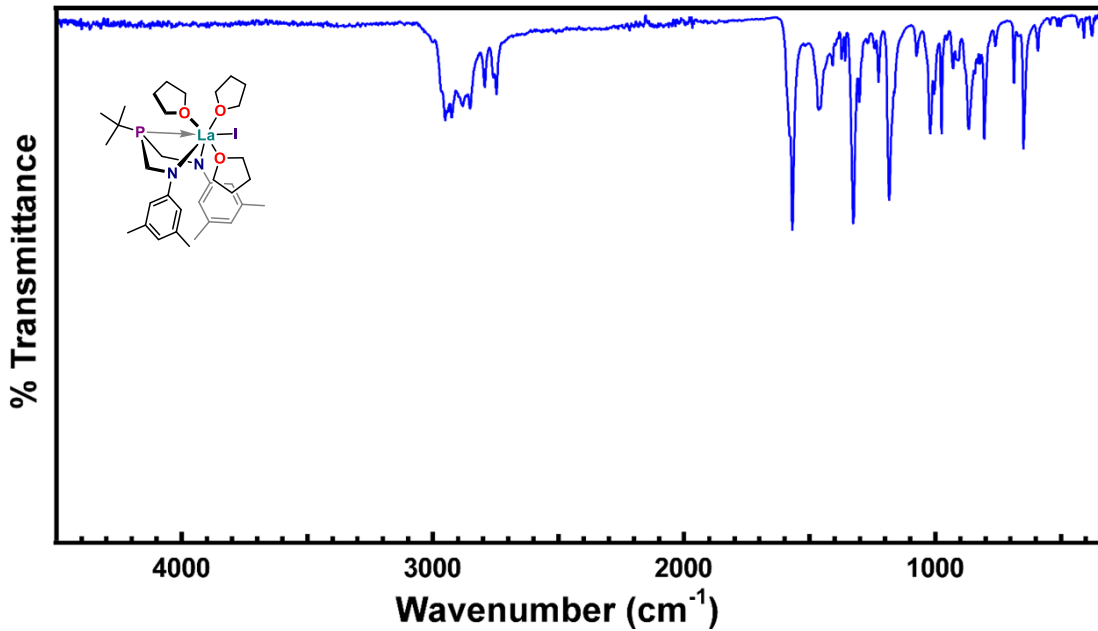


**Figure S46.** FT-IR (ATR) spectrum of  $\text{LaI}(\text{⁴⁹BiAMP}^{\text{⁶Bu}})(\text{THF})_3$  (2).  $\nu$  ( $\text{cm}^{-1}$ ): 373 (w), 409 (w), 500 (w), 503 (w), 542 (w), 592 (m), 648 (s), 686 (m), 758 (w), 804 (s), 869 (s), 917 (w), 931 (w), 976 (s), 1019 (s), 1072 (m), 1182 (s), 1225 (m), 1315 (m), 1325 (s), 1341 (m), 1359 (m), 1410 (m), 1459 (s), 1568 (s), 2749 (m), 2793 (m), 2850 (m), 2878 (m), 2924 (m), 2950 (m).

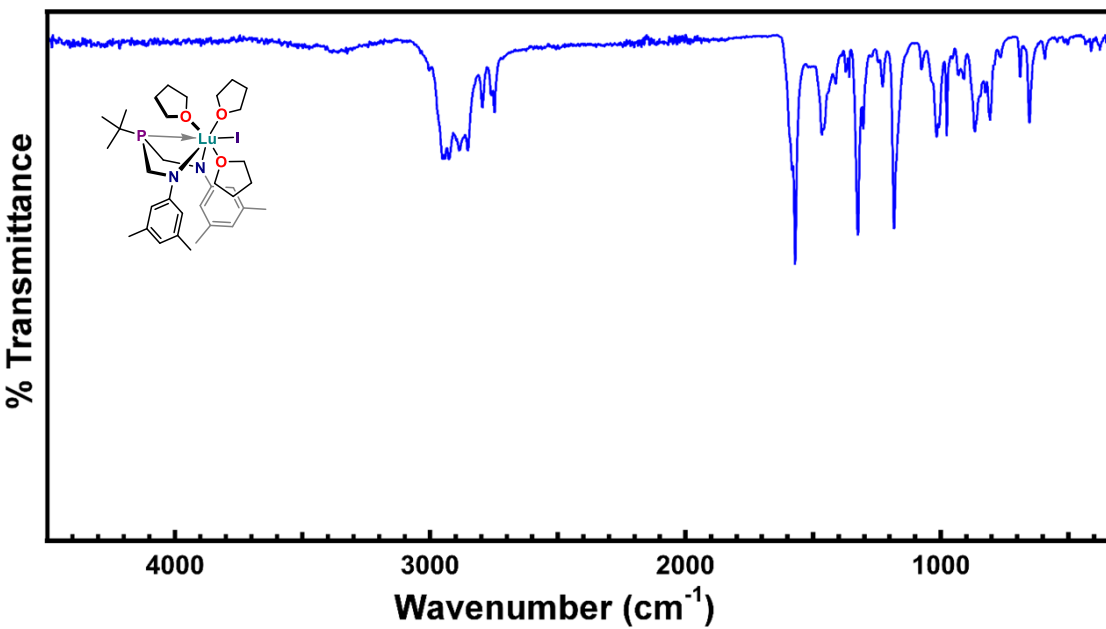


**Figure S47.** FT-IR (ATR) spectrum of  $\text{LuI}(\text{⁴⁹BiAMP}^{\text{⁶Bu}})(\text{THF})_3$  (3).  $\nu$  ( $\text{cm}^{-1}$ ): 377 (w), 410 (w), 591 (m), 652 (s), 659 (m), 765 (w), 807 (s), 866 (s), 883 (m), 929 (m), 977 (s), 1016 (s), 1075 (w), 1183 (s), 1227 (m), 1303 (s), 1324 (s), 1359 (m), 1411 (m), 1465 (s), 1570 (s), 2747 (m), 2795 (m), 2852 (s), 2882 (s), 2925 (s), 2951 (s).

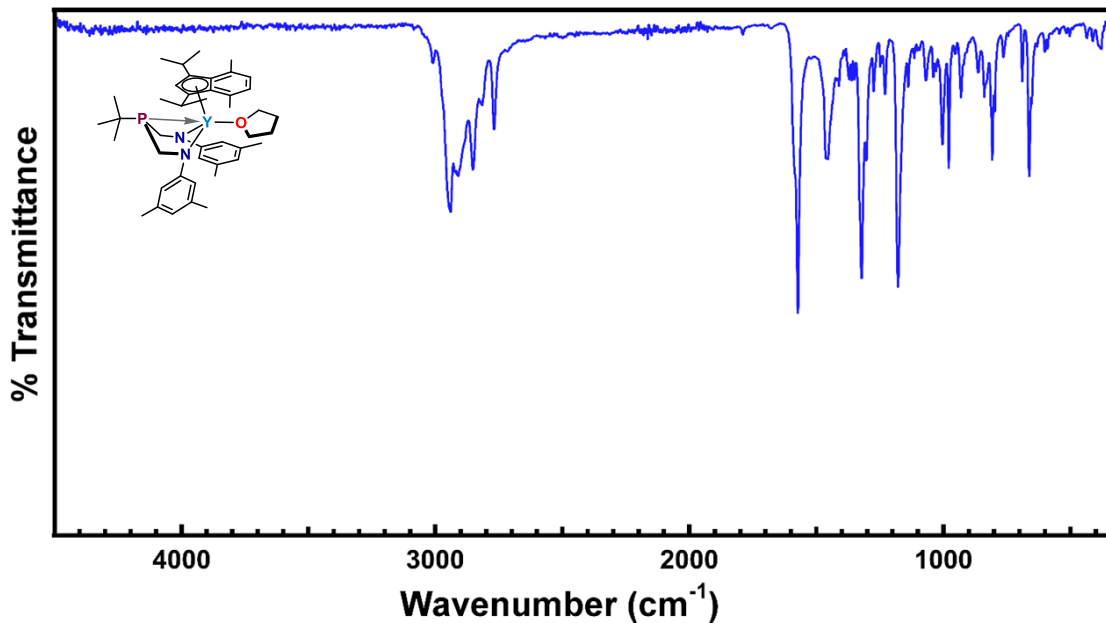


**Figure S48.** FT-IR (ATR) spectrum of  $\text{Y}(\eta^5\text{-}(1,3\text{-diisopropyl-4,7-dimethylindenyl})^{(\text{Ar})}\text{BiAMP}^{t\text{Bu}})(\text{THF})$  (**4**).  $\nu$  ( $\text{cm}^{-1}$ ): 378 (w), 391 (w), 435 (w), 589 (w), 662 (s), 689 (m), 763 (w), 807 (s), 838 (m), 864 (m), 930 (m), 979 (s), 1003 (s), 1040 (w), 1068 (m), 1138 (m), 1178 (s), 1229 (m), 1275 (m), 1322 (s), 1455 (s), 1572 (s), 2768 (s), 2851 (s), 2910 (s), 2940 (s), 3009 (m).

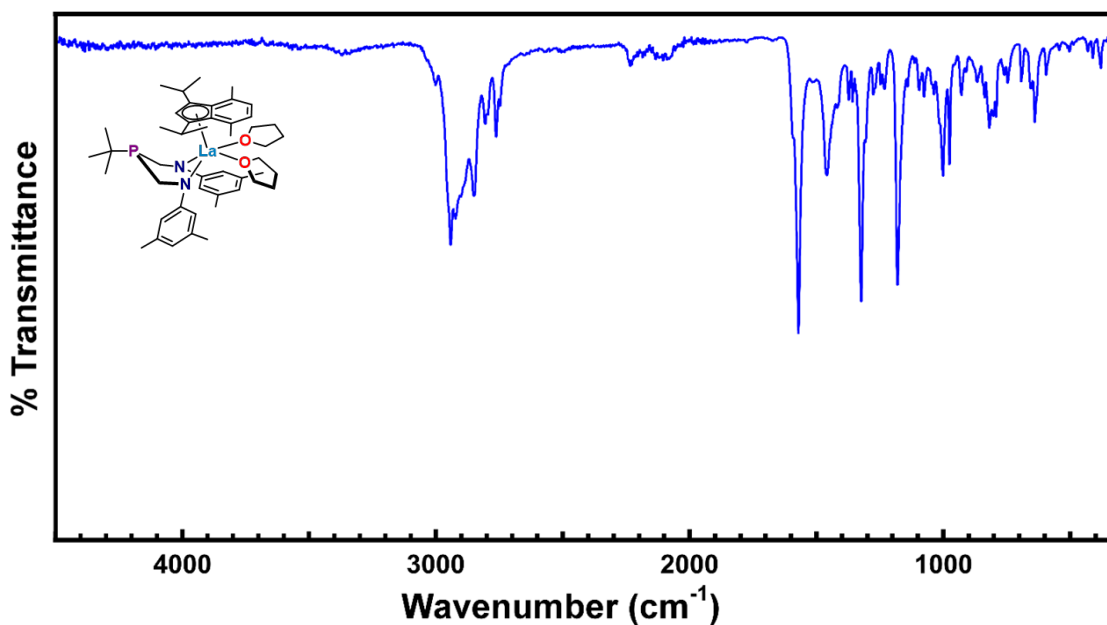


**Figure S49.** FT-IR (ATR) spectrum of  $\text{La}(\eta^5\text{-}(1,3\text{-diisopropyl-4,7-dimethylindenyl})^{(\text{Ar})}\text{BiAMP}^{t\text{Bu}})_2(\text{THF})_2$  (**5**).  $\nu$  ( $\text{cm}^{-1}$ ): 379 (w), 383 (w), 594 (m), 639 (s), 693 (m), 745 (m), 791 (s), 818 (s), 867 (m), 927 (m), 976 (s), 1001 (s), 1076 (m), 1078 (m), 1180 (s), 1230 (m), 1275 (m), 1323 (s), 1456 (s), 1570 (s), 2081 (m), 2234 (m), 2762 (s), 2805 (s), 2850 (s), 2923 (s), 2942 (s), 3368 (w).

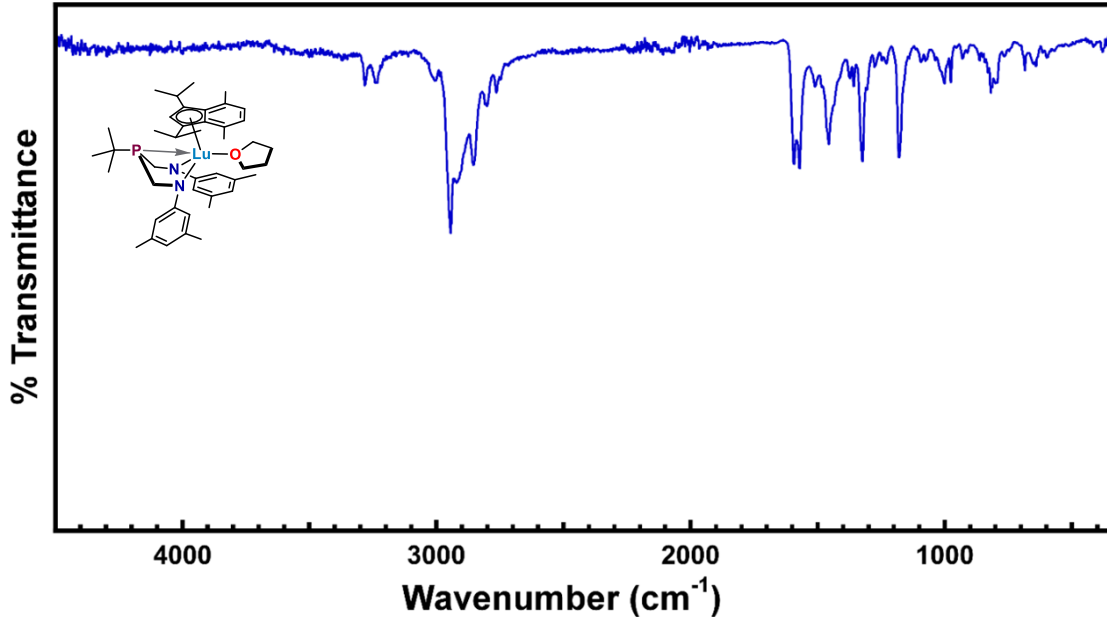
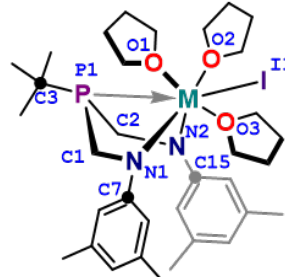


**Figure S50.** FT-IR (ATR) spectrum of  $\text{Lu}(\eta^5\text{-}(1,3\text{-diisopropyl-4,7-dimethylindenyl})(^{47}\text{BiAMP}^{68_9})(\text{THF})$  (**6**).  $\nu$  ( $\text{cm}^{-1}$ ): 379 (w), 595 (w), 640 (w), 685 (m), 793 (m), 819 (m), 929 (w), 976 (m), 1001 (m), 1037 (w), 1093 (w), 1179 (s), 1193 (w), 1276 (w), 1324 (s), 1337 (m), 1356 (m), 1456 (s), 1510 (m), 1571 (s), 1594 (s), 2764 (m), 2800 (m), 2853 (s), 2919 (s), 2944 (s), 3003 (m), 3233 (m), 3282 (m).

### 2.3. Supplemental Tables and Graphs

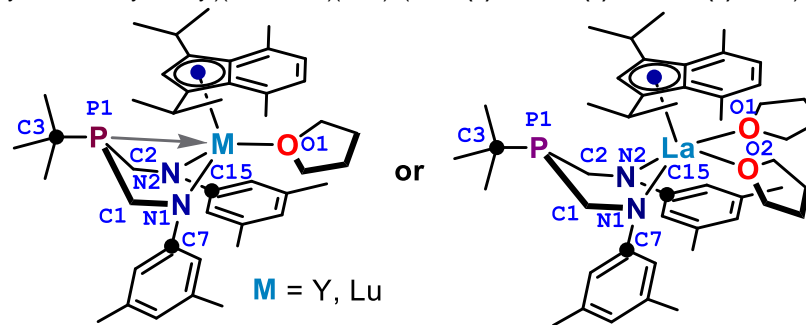
**Table S1a.** Comparative bond lengths and angles for complexes  $\text{MI}^{(\text{ArBiAMP}^{\text{tBu}})}(\text{THF})_3$  ( $\text{M} = \text{Y(1)}, \text{La(2)}, \text{Lu(3)}$ )



Compound / Atom <sup>1</sup> -Atom <sup>2</sup> *	$\text{YI}^{(\text{ArBiAMP}^{\text{tBu}})}(\text{THF})_3$ (1)	$\text{LaI}^{(\text{ArBiAMP}^{\text{tBu}})}(\text{THF})_3$ (2)	$\text{LuI}^{(\text{ArBiAMP}^{\text{tBu}})}(\text{THF})_3$ (3)
Selected bond lengths, Å			
Metal-P1	3.124(2)	3.192(1)	3.077(1)
Metal-I1	3.119(2)	3.226(6)	3.046(4)
Metal-N1	2.296(4)	2.405(3)	2.244(3)
Metal-N2	2.330(5)	2.402(4)	2.239(4)
Metal-O1	2.456(4)	2.552(3)	2.330(3)
Metal-O2	2.427(4)	2.537(3)	2.377(3)
Metal-O3	2.395(4)	2.571(3)	2.374(3)
P1-C1	1.863(5)	1.858(4)	1.842(5)
P1-C2	1.874(5)	1.848(4)	1.841(5)
P1-C3	1.883(5)	1.869(5)	1.868(5)
N1-C1	1.485(6)	1.453(5)	1.465(6)
N1-C7	1.397(6)	1.378(5)	1.377(6)
N2-C2	1.476(6)	1.460(5)	1.465(6)
N2-C15	1.402(6)	1.385(5)	1.387(6)
Atom <sup>1</sup> -Atom <sup>2</sup> -Atom <sup>3</sup> * Selected angles, °			
I1-Metal-P1	160.4(4)	163.2(2)	159.2(2)
N1-Metal-N2	91.7(1)	88.8(1)	92.2(1)
I1-Metal-N1	139.6(1)	139.9(8)	140.1(1)
I1-Metal-N2	121.0(1)	122.7(8)	120.2(9)
I1-Metal-O1	81.7(1)	80.6(7)	81.3(8)
I1-Metal-O2	80.9(8)	83.7(9)	82.4(9)
I1-Metal-O3	81.5(9)	83.0(7)	80.2(8)
N1-Metal-P1	57.4(1)	55.2(9)	57.6(9)
N2-Metal-P1	56.2(9)	54.2(9)	57.1(9)
O1-Metal-P1	93.1(1)	113.9(7)	117.3(8)
O2-Metal-P1	79.5(8)	92.2(9)	91.8(9)
O3-Metal-P1	115.8(9)	80.2(7)	79.0(8)
O1-Metal-O2	76.6(1)	130.1(1)	127.9(1)
O1-Metal-O3	128.2(1)	146.0(1)	146.7(1)
O2-Metal-O3	146.6(1)	76.7(1)	76.4(1)
C3-P1-Metal	175.2(2)	173.9(1)	176.2(2)
C1-N1-Metal	115.0(3)	115.0(2)	115.8(3)
C2-N2-Metal	120.1(3)	120.7(3)	119.5(3)
C7-N1-Metal	127.9(3)	126.5(3)	127.7(3)
C15-N2-Metal	125.6(3)	122.5(3)	125.7(3)
N1-C1-P1	107.0(3)	107.7(3)	106.9(3)
N2-C2-P1	104.5(3)	105.4(3)	105.8(3)
C1-N1-C7	115.0(4)	115.5(3)	115.1(3)
C2-N2-C15	114.3(4)	116.8(3)	114.8(4)
C1-P1-C2	100.5(2)	101.0(2)	100.2(2)
C1-P1-C3	104.0(2)	103.9(2)	103.7(2)
C2-P1-C3	105.6(2)	106.1(2)	106.3(2)

\* Atom labeling in the table refers to the graphic representation of the corresponding molecular structures elucidated from XRD analysis data. Please refer to corresponding figures (S42-S44) and tables in section 3 of the S.I. for the exact atom labeling, complete listing of bond distances and angles.

**Table S1b.** Comparative interatomic distances<sup>\*</sup> and angles for complexes  $M(\eta^5\text{-}(1,3\text{-diisopropyl-4,7-dimethylindenyl})^{Ar}\text{BiAMP}^{t\text{Bu}})(\text{THF})_n$  ( $M = Y(4)$ ,  $n = 1$ ,  $La(5)$ ,  $n = 2$ ,  $Lu(6)$ ,  $n = 1$ )

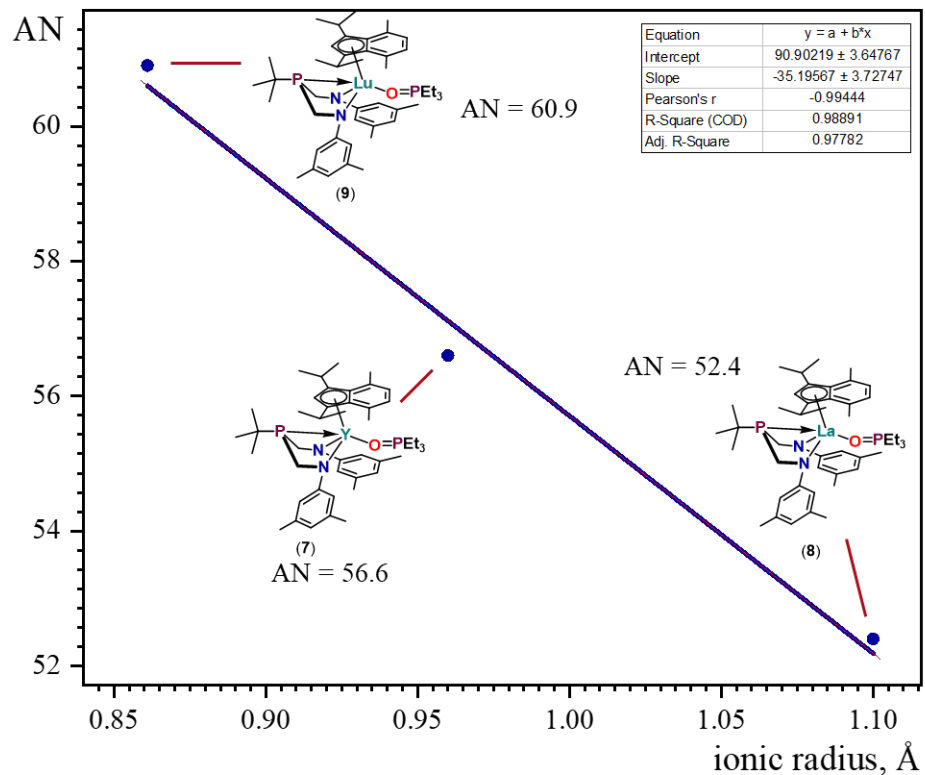


Compound / Atom <sup>1</sup> -Atom <sup>2</sup> <sup>**</sup>	$Y(\text{Ind})^{Ar}\text{BiAMP}^{t\text{Bu}}(\text{THF})$ (4)	$La(\text{Ind})^{Ar}\text{BiAMP}^{t\text{Bu}}(\text{THF})_2$ (5)	$Lu(\text{Ind})^{Ar}\text{BiAMP}^{t\text{Bu}}(\text{THF})$ (6)
Selected distances, Å			
Metal-P1	2.886(6)	3.658(1)	2.858(8)
Metal-( $\eta^5$ -Ind) centroid	2.389(1)	2.645(2)	2.343(1)
Metal-N1	2.267(2)	2.388(2)	2.203(3)
Metal-N2	2.238(2)	2.388(2)	2.225(3)
Metal-O1	2.319(1)	2.610(4)	2.264(2)
Metal-O2	N/A	2.674(3)	N/A
P1-C1	1.851(2)	1.857(3)	1.851(3)
P1-C2	1.855(2)	1.857(3)	1.850(3)
P1-C3	1.858(2)	1.878(5)	1.859(3)
N1-C1	1.463(3)	1.459(4)	1.473(4)
N1-C7	1.387(3)	1.374(4)	1.380(4)
N2-C2	1.465(3)	1.459(4)	1.467(4)
N2-C15	1.377(3)	1.374(4)	1.371(4)
Atom <sup>1</sup> -Atom <sup>2</sup> -Atom <sup>3</sup> <sup>**</sup>			
Selected angles, °			
( $\eta^5$ -Ind) centroid -Metal-P1	111.0(3)	N/A	111.3(4)
( $\eta^5$ -Ind) centroid -Metal-N1	124.2(6)	108.7(7)	127.3(8)
( $\eta^5$ -Ind) centroid -Metal-N2	127.5(6)	108.7(7)	124.2(8)
( $\eta^5$ -Ind) centroid -Metal-O1	119.2(5)	99.3(8)	118.5(6)
( $\eta^5$ -Ind) centroid -Metal-O2	N/A	167.4(7)	N/A
N1-Metal-P1	60.4(5)	N/A	60.9(7)
N2-Metal-P1	60.1(5)	N/A	61.3(7)
O1-Metal-P1	129.8(4)	N/A	130.1(6)
O2-Metal-P1	N/A	N/A	N/A
C3-P1-Metal	169.5(7)	N/A	170.5(1)
C1-N1-Metal	113.5(1)	127.8(2)	113.0(2)
C2-N2-Metal	113.4(1)	127.8(2)	113.3(2)
C7-N1-Metal	131.1(1)	112.7(2)	128.1(2)
C15-N2-Metal	127.4(1)	112.7(2)	131.3(2)
N1-C1-P1	105.5(1)	109.2(2)	103.8(2)
N2-C2-P1	103.9(1)	109.2(2)	105.4(2)
C1-N1-C7	115.4(2)	115.7(3)	117.3(3)
C2-N2-C15	117.3(2)	115.7(3)	115.4(3)
C1-P1-C2	103.5(1)	98.8(2)	103.5(1)
C1-P1-C3	105.6(1)	102.8(1)	107.0(1)
C2-P1-C3	107.4(1)	102.8(1)	105.6(2)

\* We used term 'interatomic distances' rather than 'bond lengths' in the table to compare directly the complexes of **Y(4)** and **Lu(6)** to the complex of **La(5)** where no coordination of the phosphorus atom to La was observed.

\*\* Atom labeling in the table refers to the graphic representation of the corresponding molecular structures elucidated from XRD analysis data. Please refer to corresponding figures (S45, S46, S47) and tables in section 3 of the S.I. for the exact atom labeling, complete listing of bond distances and angles.

N/A – not applicable.



**Graph S1.** A correlation between the experimentally derived Gutmann-Beckett acceptor numbers (AN) and the effective ionic radii of the corresponding  $M^{3+}$  TEPO adducts (7-9).

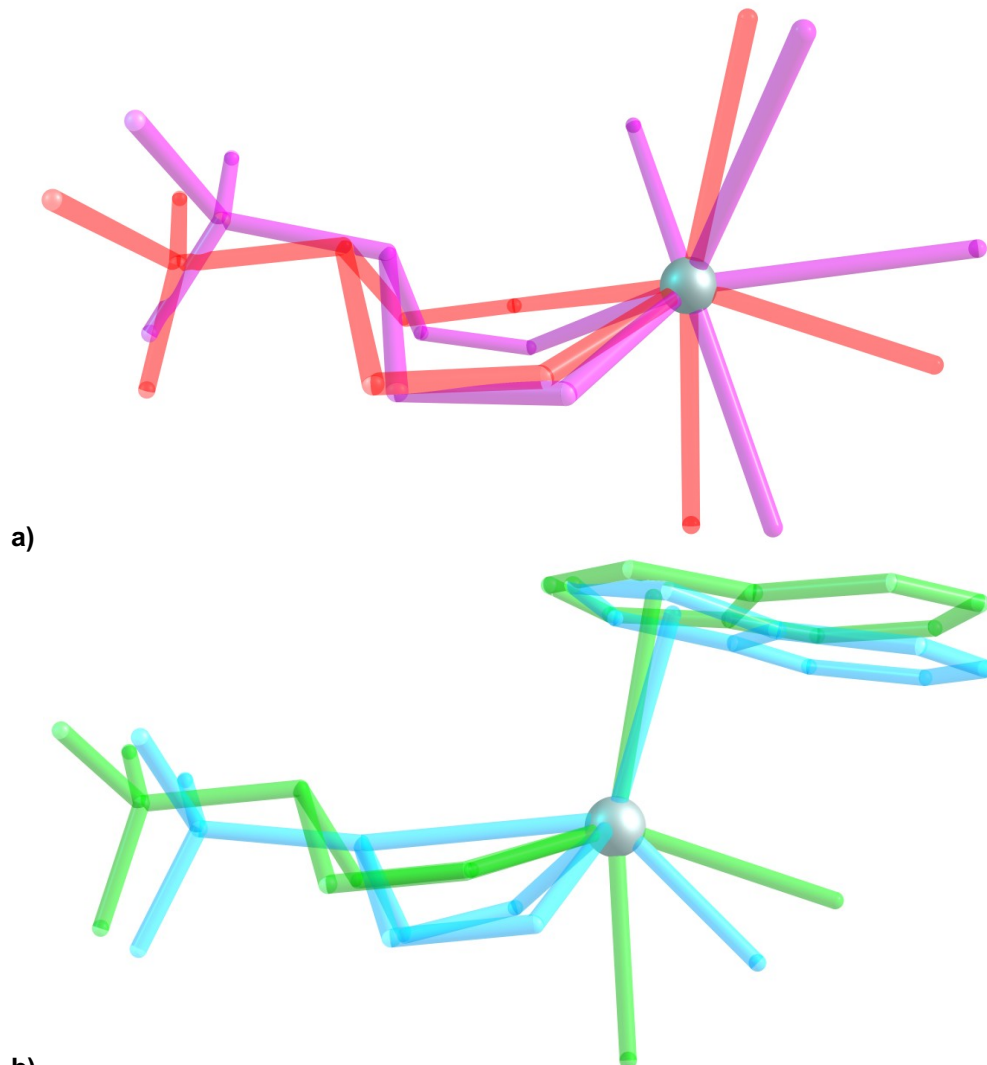


**Figure S51.** a) Solid state structural overlays of **2** (purple) and **5** (red) highlighting the differences observed at the La-center upon substitution of the I- ligand with  $\eta^5\text{-}i\text{PrMeInd}$ ; b) Solid state structural overlays of **4** (blue) and **5** (green) highlighting the geometric difference of the La-based complex.

### 3. Single Crystal X-ray Diffraction Data

#### 3.1. CCDC deposition numbers 2328028-2328036

$^{Ar}BiAMP^{tBu}$  : **2328028**

$(^{Ar}BiAMP^{tBu})CH_2$  : **2328029**

$YI(^{Ar}BiAMP^{tBu})(thf)_3$  (**1**) : **2328030**

$Lal(^{Ar}BiAMP^{tBu})(thf)_3$  (**2**) : **2328031**

$LuI(^{Ar}BiAMP^{tBu})(thf)_3$  (**3**) : **2328032**

$Y(\eta^5-(1,3-diisopropyl-4,7-dimethylindenyl)(^{Ar}BiAMP^{tBu})(thf)$  (**4**) : **2328033**

$Y(\eta^5-(1,3-diisopropyl-4,7-dimethylindenyl)(^{Ar}BiAMP^{tBu})(thf)(Et_2O)$  (**4a**) : **2328034**

$La(\eta^5-(1,3-diisopropyl-4,7-dimethylindenyl)(^{Ar}BiAMP^{tBu})(thf)_2$  (**5**) : **2328035**

$Lu(\eta^5-(1,3-diisopropyl-4,7-dimethylindenyl)(^{Ar}BiAMP^{tBu})(thf)$  (**6**) : **2328036**

### 3.2. $^{Ar}\text{BiAMP}^{\text{tBu}}$

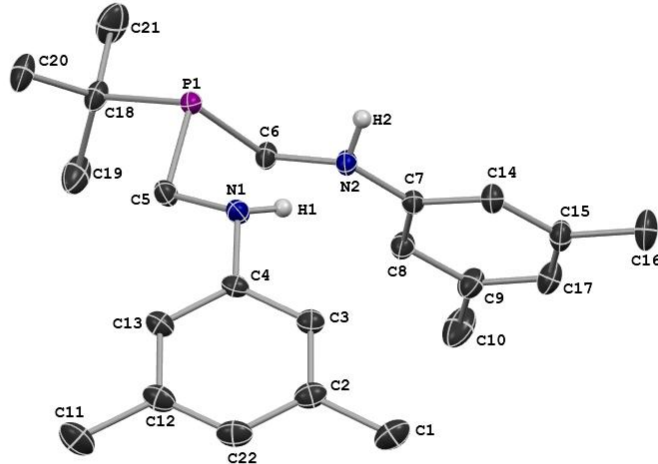


**Figure S52.** Solid state molecular structure of  $^{Ar}\text{BiAMP}^{\text{tBu}}$  (recrystallized from *n*-pentane) shown with non-relevant hydrogen atoms omitted for clarity and the thermal ellipsoids set at 50% probability.

**Table S2.** Crystal data and structure refinement for  $^{Ar}\text{BiAMP}^{\text{tBu}}$ .

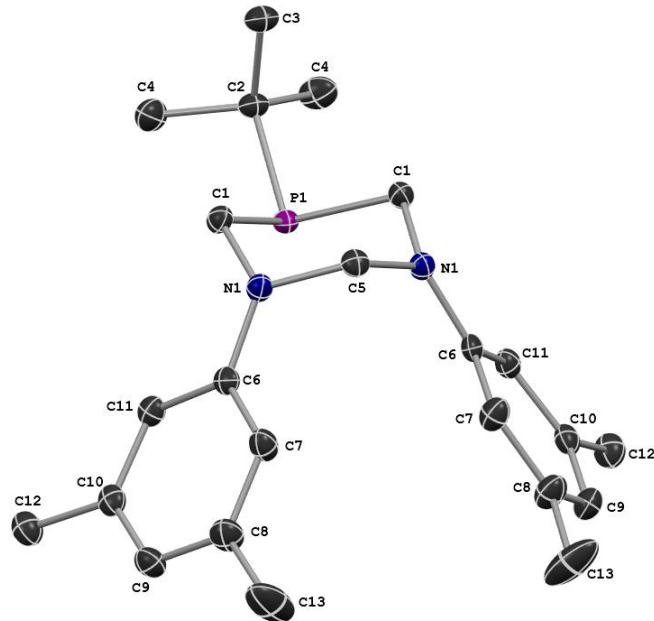
Empirical formula	C <sub>22</sub> H <sub>33</sub> N <sub>2</sub> P
Formula weight	356.47
Temperature/K	109.0
Crystal system	triclinic
Space group	P-1
a/Å	8.9968(3)
b/Å	11.2118(4)
c/Å	11.8000(5)
$\alpha/^\circ$	97.9300(10)
$\beta/^\circ$	103.0220(10)
$\gamma/^\circ$	108.0500(10)
Volume/Å <sup>3</sup>	1074.49(7)
Z	2
$\rho_{\text{calc}}/\text{g/cm}^3$	1.102
$\mu/\text{mm}^{-1}$	0.135
F(000)	388.0
Crystal size/mm <sup>3</sup>	0.35 × 0.35 × 0.3
Radiation	MoK $\alpha$ ( $\lambda = 0.71073$ )
2 $\Theta$ range for data collection/ $^\circ$	5.128 to 62.74
Index ranges	-13 ≤ h ≤ 13, -16 ≤ k ≤ 16, -17 ≤ l ≤ 17
Reflections collected	23544
Independent reflections	6992 [ $R_{\text{int}} = 0.0183$ , $R_{\text{sigma}} = 0.0175$ ]
Data/restraints/parameters	6992/0/241
Goodness-of-fit on $F^2$	1.061
Final R indexes [ $ I  \geq 2\sigma (I)$ ]	$R_1 = 0.0374$ , $wR_2 = 0.1031$
Final R indexes [all data]	$R_1 = 0.0402$ , $wR_2 = 0.1052$
Largest diff. peak/hole / e Å <sup>-3</sup>	0.49/-0.32

**Table S3.** Bond Lengths for  ${}^{\text{Ar}}\text{BiAMP}^{\text{tBu}}$ .

<b>Atom</b>	<b>Atom</b>	<b>Length/<math>\text{\AA}</math></b>	<b>Atom</b>	<b>Atom</b>	<b>Length/<math>\text{\AA}</math></b>
P1	C5	1.8526(9)	C7	C14	1.4025(12)
P1	C6	1.8556(9)	C8	C9	1.3972(13)
P1	C18	1.8708(9)	C9	C10	1.5054(15)
N1	C4	1.4079(11)	C9	C17	1.3895(14)
N1	C5	1.4631(11)	C11	C12	1.5074(14)
N2	C6	1.4569(11)	C12	C13	1.3947(13)
N2	C7	1.3999(11)	C12	C22	1.3906(15)
C1	C2	1.5089(15)	C14	C15	1.3864(13)
C2	C3	1.3902(13)	C15	C16	1.5083(14)
C2	C22	1.3974(15)	C15	C17	1.3963(14)
C3	C4	1.4006(12)	C18	C19	1.5247(14)
C4	C13	1.3956(12)	C18	C20	1.5345(14)
C7	C8	1.3956(12)	C18	C21	1.5399(16)

**Table S4.** Bond Angles for  ${}^{\text{Ar}}\text{BiAMP}^{\text{tBu}}$ .

<b>Atom</b>	<b>Atom</b>	<b>Atom</b>	<b>Angle/<math>^{\circ}</math></b>	<b>Atom</b>	<b>Atom</b>	<b>Atom</b>	<b>Angle/<math>^{\circ}</math></b>
C5	P1	C6	98.13(4)	C17	C9	C8	119.38(9)
C5	P1	C18	102.10(4)	C17	C9	C10	120.88(9)
C6	P1	C18	101.56(4)	C13	C12	C11	119.40(10)
C4	N1	C5	117.51(7)	C22	C12	C11	121.27(9)
C7	N2	C6	119.15(7)	C22	C12	C13	119.33(9)
C3	C2	C1	119.85(9)	C12	C13	C4	120.58(9)
C3	C2	C22	119.33(9)	C15	C14	C7	120.98(9)
C22	C2	C1	120.79(9)	C14	C15	C16	120.44(9)
C2	C3	C4	120.52(9)	C14	C15	C17	119.23(9)
C3	C4	N1	118.94(8)	C17	C15	C16	120.33(9)
C13	C4	N1	121.71(8)	C9	C17	C15	120.85(9)
C13	C4	C3	119.35(8)	C19	C18	P1	115.11(7)
N1	C5	P1	109.23(6)	C19	C18	C20	109.92(9)
N2	C6	P1	108.91(6)	C19	C18	C21	109.22(10)
N2	C7	C14	118.52(8)	C20	C18	P1	107.35(7)
C8	C7	N2	122.56(8)	C20	C18	C21	108.79(9)
C8	C7	C14	118.91(8)	C21	C18	P1	106.25(7)
C7	C8	C9	120.64(8)	C12	C22	C2	120.87(9)
C8	C9	C10	119.72(9)				

3.3 (<sup>Ar</sup>**iAMP<sup>tBu</sup>**)CH<sub>2</sub>

**Figure S53.** Solid state molecular structure of (<sup>Ar</sup>**iAMP<sup>tBu</sup>**)CH<sub>2</sub> (recrystallized from *n*-pentane) shown with hydrogen atoms omitted for clarity and the thermal ellipsoids set at 50% probability.

**Table S5.** Crystal data and structure refinement for (<sup>Ar</sup>**iAMP<sup>tBu</sup>**)CH<sub>2</sub>.

Empirical formula	C <sub>23</sub> H <sub>33</sub> N <sub>2</sub> P
Formula weight	368.48
Temperature/K	108.0
Crystal system	orthorhombic
Space group	Pnma
a/Å	9.9418(8)
b/Å	16.3863(10)
c/Å	13.0368(9)
α/°	90
β/°	90
γ/°	90
Volume/Å <sup>3</sup>	2123.8(3)
Z	4
ρ <sub>calc</sub> g/cm <sup>3</sup>	1.152
μ/mm <sup>-1</sup>	0.138
F(000)	800.0
Crystal size/mm <sup>3</sup>	0.42 × 0.12 × 0.09
Radiation	MoK $\alpha$ ( $\lambda$ = 0.71073)
2θ range for data collection/°	4.972 to 56.04
Index ranges	-12 ≤ h ≤ 13, -21 ≤ k ≤ 21, -12 ≤ l ≤ 17
Reflections collected	11477
Independent reflections	2630 [R <sub>int</sub> = 0.0409, R <sub>sigma</sub> = 0.0342]
Data/restraints/parameters	2630/0/128
Goodness-of-fit on F <sup>2</sup>	1.080
Final R indexes [I>=2σ (I)]	R <sub>1</sub> = 0.0521, wR <sub>2</sub> = 0.1163
Final R indexes [all data]	R <sub>1</sub> = 0.0622, wR <sub>2</sub> = 0.1209
Largest diff. peak/hole / e Å <sup>-3</sup>	0.41/-0.37

**Table S6.** Bond Lengths for (<sup>Ar</sup>BiAMP<sup>tBu</sup>)CH<sub>2</sub>.

<b>Atom</b>	<b>Atom</b>	<b>Length/Å</b>	<b>Atom</b>	<b>Atom</b>	<b>Length/Å</b>
P1	C2	1.879(2)	C2	C3	1.529(3)
P1	C1 <sup>1</sup>	1.8748(17)	C2	C4	1.537(2)
P1	C1	1.8749(17)	C2	C4 <sup>1</sup>	1.537(2)
N1	C5	1.4576(19)	C7	C8	1.387(2)
N1	C6	1.398(2)	C10	C9	1.392(2)
N1	C1	1.456(2)	C10	C12	1.507(2)
C6	C11	1.403(2)	C9	C8	1.392(3)
C6	C7	1.406(2)	C8	C13	1.513(3)
C11	C10	1.395(2)			

**Table S7.** Bond Angles for (<sup>Ar</sup>BiAMP<sup>tBu</sup>)CH<sub>2</sub>.

<b>Atom</b>	<b>Atom</b>	<b>Atom</b>	<b>Angle/°</b>	<b>Atom</b>	<b>Atom</b>	<b>Atom</b>	<b>Angle/°</b>
C1 <sup>1</sup>	P1	C2	102.97(8)	C3	C2	C4 <sup>1</sup>	109.22(14)
C1	P1	C2	102.97(8)	C4	C2	P1	106.48(12)
C1 <sup>1</sup>	P1	C1	92.88(11)	C4 <sup>1</sup>	C2	P1	106.48(12)
C6	N1	C5	121.93(15)	C4 <sup>1</sup>	C2	C4	109.2(2)
C6	N1	C1	121.28(14)	N1	C1	P1	110.36(11)
C1	N1	C5	111.90(15)	C8	C7	C6	121.24(17)
N1 <sup>1</sup>	C5	N1	113.26(19)	C11	C10	C12	120.06(16)
N1	C6	C11	121.61(15)	C9	C10	C11	119.46(16)
N1	C6	C7	120.46(15)	C9	C10	C12	120.47(16)
C11	C6	C7	117.76(16)	C8	C9	C10	120.28(17)
C10	C11	C6	121.31(16)	C7	C8	C9	119.86(17)
C3	C2	P1	116.07(17)	C7	C8	C13	119.56(18)
C3	C2	C4	109.22(13)	C9	C8	C13	120.58(17)

### 3.4 $\text{YI}(\text{ArBiAMP}^{\text{tBu}})(\text{THF})_3$ (1)

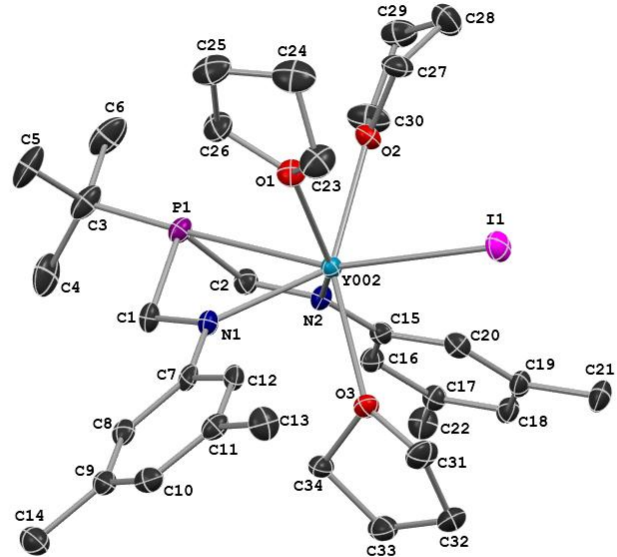


**Figure S54.** Solid state molecular structure of  $\text{YI}(\text{ArBiAMP}^{\text{tBu}})(\text{THF})_3$  (1) (recrystallized from THF/n-pentane) shown with hydrogen atoms omitted for clarity and the thermal ellipsoids set at 50% probability.

**Table S8.** Crystal data and structure refinement for  $\text{YI}(\text{ArBiAMP}^{\text{tBu}})(\text{THF})_3$  (1).

Empirical formula	$\text{C}_{34}\text{H}_{55}\text{IN}_2\text{O}_3\text{PY}$
Formula weight	786.58
Temperature/K	100.0
Crystal system	orthorhombic
Space group	$\text{P}2_1\text{2}_1\text{2}_1$
a/ $\text{\AA}$	13.453(9)
b/ $\text{\AA}$	14.372(15)
c/ $\text{\AA}$	19.53(3)
$\alpha/^\circ$	90
$\beta/^\circ$	90
$\gamma/^\circ$	90
Volume/ $\text{\AA}^3$	3776(7)
Z	4
$\rho_{\text{calc}}$ /g/ $\text{cm}^{-3}$	1.384
$\mu/\text{mm}^{-1}$	2.437
F(000)	1616.0
Crystal size/ $\text{mm}^3$	0.34 $\times$ 0.28 $\times$ 0.22
Radiation	$\text{MoK}\alpha$ ( $\lambda = 0.71073$ )
2 $\Theta$ range for data collection/°	4.642 to 56.858
Index ranges	-18 $\leq$ h $\leq$ 16, -19 $\leq$ k $\leq$ 19, -23 $\leq$ l $\leq$ 25
Reflections collected	32996
Independent reflections	9281 [ $R_{\text{int}} = 0.0518$ , $R_{\text{sigma}} = 0.0509$ ]
Data/restraints/parameters	9281/0/387
Goodness-of-fit on $F^2$	1.052
Final R indexes [ $ I  >= 2\sigma (I)$ ]	$R_1 = 0.0340$ , $wR_2 = 0.0761$
Final R indexes [all data]	$R_1 = 0.0407$ , $wR_2 = 0.0780$
Largest diff. peak/hole / e $\text{\AA}^{-3}$	1.80/-0.53
Flack parameter	0.426(6)

**Table S9.** Bond Lengths for  $\text{YI}^{(\text{Ar})}\text{BiAMP}^{(\text{Bu})}(\text{THF})_3$  (1).

Atom	Atom	Length/ $\text{\AA}$	Atom	Atom	Length/ $\text{\AA}$
I1	Y002	3.1192(18)	C17	C18	1.392(6)
Y002	P1	3.124(2)	C27	C28	1.523(7)
Y002	O1	2.456(4)	C26	C25	1.567(7)
Y002	O2	2.427(4)	C15	C16	1.434(7)
Y002	O3	2.395(4)	C15	C20	1.424(6)
Y002	N1	2.296(4)	C18	C19	1.434(7)
Y002	N2	2.330(5)	C34	C33	1.525(7)
P1	C1	1.863(5)	C14	C9	1.526(7)
P1	C2	1.874(5)	C9	C10	1.398(7)
P1	C3	1.883(5)	C9	C8	1.394(7)
O1	C26	1.459(6)	C28	C29	1.549(8)
O1	C23	1.472(6)	C7	C8	1.413(7)
O2	C27	1.483(6)	C21	C19	1.514(6)
O2	C30	1.477(7)	C30	C29	1.510(8)
O3	C34	1.477(6)	C10	C11	1.418(7)
O3	C31	1.455(6)	C11	C13	1.539(7)
N1	C1	1.485(6)	C20	C19	1.409(7)
N1	C7	1.397(6)	C3	C6	1.540(8)
N2	C2	1.476(6)	C3	C5	1.546(7)
N2	C15	1.402(6)	C3	C4	1.552(8)
C12	C7	1.436(7)	C23	C24	1.507(8)
C12	C11	1.386(7)	C33	C32	1.548(8)
C17	C22	1.529(7)	C31	C32	1.545(8)
C17	C16	1.413(6)	C25	C24	1.520(9)

**Table S10.** Bond Angles for  $\text{YI}^{(\text{ArBiAMPtBu})}(\text{THF})_3$  (1).

Atom	Atom	Atom	Angle/ $^{\circ}$	Atom	Atom	Atom	Angle/ $^{\circ}$
I1	Y002	P1	160.44(4)	C16	C17	C22	120.9(4)
O1	Y002	I1	81.75(10)	C18	C17	C22	120.0(4)
O1	Y002	P1	93.15(11)	C18	C17	C16	119.0(4)
O2	Y002	I1	80.93(8)	O2	C27	C28	103.9(4)
O2	Y002	P1	79.51(8)	N1	C1	P1	107.0(3)
O2	Y002	O1	76.60(12)	N2	C2	P1	104.5(3)
O3	Y002	I1	81.48(9)	O1	C26	C25	106.2(4)
O3	Y002	P1	115.79(9)	N2	C15	C16	125.5(4)
O3	Y002	O1	128.22(11)	N2	C15	C20	117.4(4)
O3	Y002	O2	146.63(12)	C20	C15	C16	117.1(4)
N1	Y002	I1	139.56(10)	C17	C16	C15	122.5(4)
N1	Y002	P1	57.36(10)	C17	C18	C19	120.4(4)
N1	Y002	O1	83.04(13)	O3	C34	C33	105.7(4)
N1	Y002	O2	130.90(13)	C10	C9	C14	120.6(4)
N1	Y002	O3	79.06(14)	C8	C9	C14	118.7(5)
N1	Y002	N2	91.67(14)	C8	C9	C10	120.7(4)
N2	Y002	I1	121.05(10)	C27	C28	C29	102.8(4)
N2	Y002	P1	56.16(9)	N1	C7	C12	118.8(4)
N2	Y002	O1	145.12(13)	N1	C7	C8	124.2(4)
N2	Y002	O2	81.29(13)	C8	C7	C12	117.0(4)
N2	Y002	O3	83.85(13)	O2	C30	C29	107.0(5)
C1	P1	Y002	75.71(15)	C9	C10	C11	120.0(4)
C1	P1	C2	100.5(2)	C12	C11	C10	118.8(5)
C1	P1	C3	104.0(2)	C12	C11	C13	121.2(5)
C2	P1	Y002	79.07(17)	C10	C11	C13	120.0(4)
C2	P1	C3	105.6(2)	C9	C8	C7	121.1(5)
C3	P1	Y002	175.21(17)	C19	C20	C15	121.0(4)
C26	O1	Y002	118.8(3)	C18	C19	C21	120.6(4)
C26	O1	C23	106.8(4)	C20	C19	C18	120.0(4)
C23	O1	Y002	133.2(3)	C20	C19	C21	119.4(4)
C27	O2	Y002	127.1(3)	C6	C3	P1	107.6(4)
C30	O2	Y002	123.7(3)	C6	C3	C5	108.9(5)
C30	O2	C27	109.0(4)	C6	C3	C4	110.6(5)
C34	O3	Y002	119.0(3)	C5	C3	P1	106.1(4)
C31	O3	Y002	137.4(3)	C5	C3	C4	110.3(5)
C31	O3	C34	103.5(3)	C4	C3	P1	113.2(4)
C1	N1	Y002	115.0(3)	O1	C23	C24	105.0(4)
C7	N1	Y002	127.9(3)	C30	C29	C28	103.3(4)
C7	N1	C1	115.0(4)	C34	C33	C32	103.8(4)
C2	N2	Y002	120.1(3)	O3	C31	C32	104.4(4)
C15	N2	Y002	125.6(3)	C24	C25	C26	104.1(4)
C15	N2	C2	114.3(4)	C23	C24	C25	101.9(5)
C11	C12	C7	122.3(4)	C31	C32	C33	104.7(4)

### 3.5 $\text{LaI}(\text{ArBiAMP}^{\text{tBu}})(\text{THF})_3$ (2)

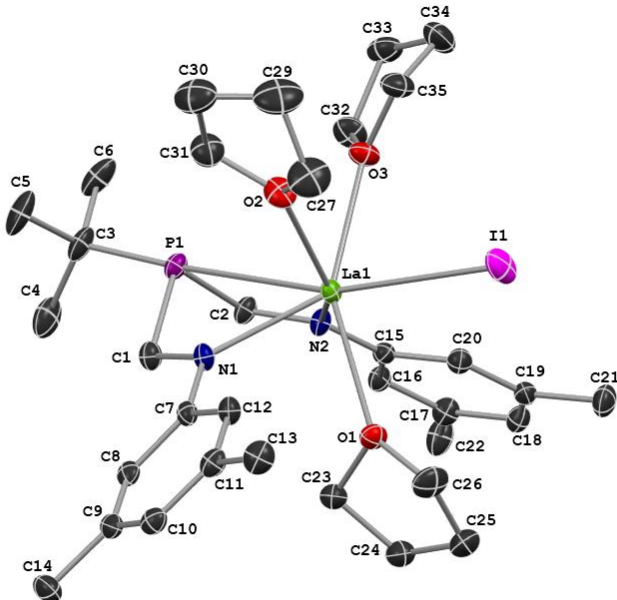


**Figure S55.** Solid state molecular structure of  $\text{LaI}(\text{ArBiAMP}^{\text{tBu}})(\text{THF})_3$  (2) (recrystallized from THF/n-pentane) shown with hydrogen atoms omitted for clarity and the thermal ellipsoids set at 50% probability.

**Table S11.** Crystal data and structure refinement for  $\text{LaI}(\text{ArBiAMP}^{\text{tBu}})(\text{THF})_3$  (2).

Empirical formula	$\text{C}_{34}\text{H}_{55}\text{ILaN}_2\text{O}_3\text{P}$
Formula weight	836.58
Temperature/K	100.0
Crystal system	orthorhombic
Space group	$\text{P}2_1\text{2}_1\text{2}_1$
$a/\text{\AA}$	13.352(2)
$b/\text{\AA}$	14.546(3)
$c/\text{\AA}$	19.171(4)
$\alpha/^\circ$	90
$\beta/^\circ$	90
$\gamma/^\circ$	90
Volume/ $\text{\AA}^3$	3723.2(12)
Z	4
$\rho_{\text{calc}}/\text{g/cm}^3$	1.492
$\mu/\text{mm}^{-1}$	2.052
F(000)	1688.0
Crystal size/ $\text{mm}^3$	0.24 × 0.18 × 0.16
Radiation	MoK $\alpha$ ( $\lambda = 0.71073$ )
2 $\Theta$ range for data collection/ $^\circ$	5.602 to 56.746
Index ranges	-17 ≤ h ≤ 17, -19 ≤ k ≤ 19, -25 ≤ l ≤ 25
Reflections collected	63378
Independent reflections	9274 [ $R_{\text{int}} = 0.0310$ , $R_{\text{sigma}} = 0.0202$ ]
Data/restraints/parameters	9274/0/387
Goodness-of-fit on $F^2$	1.060
Final R indexes [ $I >= 2\sigma (I)$ ]	$R_1 = 0.0262$ , $wR_2 = 0.0617$
Final R indexes [all data]	$R_1 = 0.0264$ , $wR_2 = 0.0619$
Largest diff. peak/hole / e $\text{\AA}^{-3}$	3.47/-2.01
Flack parameter	0.020(16)

**Table S12.** Bond Lengths for  $\text{La}(\text{ArBiAMP}^{\text{tBu}})(\text{THF})_3$  (2).

Atom	Atom	Length/ $\text{\AA}$	Atom	Atom	Length/ $\text{\AA}$
La1	I1	3.2263(6)	C17	C16	1.395(6)
La1	P1	3.1918(11)	C24	C25	1.533(8)
La1	O2	2.552(3)	C24	C23	1.521(6)
La1	O1	2.537(3)	C11	C12	1.381(6)
La1	O3	2.571(3)	N1	C1	1.453(5)
La1	N1	2.405(3)	N1	C7	1.378(5)
La1	N2	2.402(4)	C19	C18	1.401(6)
P1	C3	1.869(5)	C19	C21	1.507(6)
P1	C1	1.858(4)	C19	C20	1.377(6)
P1	C2	1.848(4)	C25	C26	1.512(8)
O2	C31	1.427(7)	C8	C9	1.389(6)
O2	C27	1.451(6)	C8	C7	1.407(6)
O1	C23	1.448(5)	C14	C9	1.506(6)
O1	C26	1.453(5)	C12	C7	1.415(6)
O3	C32	1.459(6)	C33	C34	1.517(8)
O3	C35	1.453(5)	C33	C32	1.505(7)
C13	C11	1.513(6)	C34	C35	1.518(7)
C3	C6	1.532(8)	C2	N2	1.460(5)
C3	C4	1.531(8)	C16	C15	1.413(6)
C3	C5	1.531(7)	C31	C30	1.550(7)
C10	C11	1.397(6)	C20	C15	1.417(6)
C10	C9	1.394(6)	C30	C29	1.512(10)
C17	C22	1.503(6)	C29	C27	1.481(9)
C17	C18	1.387(6)	N2	C15	1.385(5)

**Table S13.** Bond Angles for  $\text{La}(\text{ArBiAMP}^{\text{tBu}})(\text{THF})_3$  (2).

Atom	Atom	Atom	Angle/ $^\circ$	Atom	Atom	Atom	Angle/ $^\circ$
P1	La1	I1	163.20(2)	C18	C17	C22	119.6(4)
O2	La1	I1	83.70(9)	C18	C17	C16	120.2(4)
O2	La1	P1	92.20(9)	C16	C17	C22	120.2(4)
O2	La1	O3	76.74(11)	C23	C24	C25	104.2(4)
O1	La1	I1	80.65(7)	C10	C11	C13	119.7(4)
O1	La1	P1	113.88(7)	C12	C11	C13	120.6(4)
O1	La1	O2	130.13(11)	C12	C11	C10	119.7(4)
O1	La1	O3	146.05(11)	C1	N1	La1	115.0(2)
O3	La1	I1	82.96(7)	C7	N1	La1	126.5(3)
O3	La1	P1	80.24(7)	C7	N1	C1	115.5(3)
N1	La1	I1	139.91(8)	C18	C19	C21	120.1(4)
N1	La1	P1	55.18(9)	C20	C19	C18	119.2(4)
N1	La1	O2	84.41(12)	C20	C19	C21	120.7(4)
N1	La1	O1	78.26(11)	C26	C25	C24	104.7(4)
N1	La1	O3	130.71(11)	C9	C8	C7	121.4(4)
N2	La1	I1	122.66(8)	O1	C23	C24	104.7(4)
N2	La1	P1	54.16(9)	C17	C18	C19	120.2(4)
N2	La1	O2	141.70(13)	C11	C12	C7	122.1(4)
N2	La1	O1	84.63(11)	C32	C33	C34	104.5(4)
N2	La1	O3	79.55(12)	N1	C1	P1	107.7(3)
N2	La1	N1	88.82(12)	C10	C9	C14	120.5(4)
C3	P1	La1	173.93(15)	C8	C9	C10	120.3(4)
C1	P1	La1	76.38(14)	C8	C9	C14	119.1(4)
C1	P1	C3	103.9(2)	C33	C34	C35	102.8(4)
C2	P1	La1	79.67(13)	N2	C2	P1	105.4(3)
C2	P1	C3	106.1(2)	C17	C16	C15	121.2(4)
C2	P1	C1	101.0(2)	O2	C31	C30	105.6(5)
C31	O2	La1	119.9(3)	C19	C20	C15	122.7(4)
C31	O2	C27	109.8(4)	O3	C32	C33	106.9(4)
C27	O2	La1	129.8(3)	C29	C30	C31	103.0(5)
C23	O1	La1	118.7(2)	C27	C29	C30	103.2(5)
C23	O1	C26	104.2(3)	N1	C7	C8	124.5(4)
C26	O1	La1	137.0(3)	N1	C7	C12	118.6(4)
C32	O3	La1	124.6(3)	C8	C7	C12	116.8(4)

**Table S13 (Continued).** Bond Angles for  $\text{La}(\text{ArBiAMP}^{\text{Bu}})(\text{THF})_3$  (2).

<b>Atom</b>	<b>Atom</b>	<b>Atom</b>	<b>Angle/°</b>	<b>Atom</b>	<b>Atom</b>	<b>Atom</b>	<b>Angle/°</b>
C35	O3	La1	126.6(3)	C2	N2	La1	120.7(3)
C35	O3	C32	108.8(3)	C15	N2	La1	122.5(3)
C6	C3	P1	107.8(4)	C15	N2	C2	116.8(3)
C4	C3	P1	112.9(3)	O3	C35	C34	104.2(4)
C4	C3	C6	110.4(4)	O1	C26	C25	104.6(4)
C5	C3	P1	107.2(3)	O2	C27	C29	104.0(5)
C5	C3	C6	108.5(4)	C16	C15	C20	116.5(4)
C5	C3	C4	109.9(5)	N2	C15	C16	124.9(4)
C9	C10	C11	119.6(4)	N2	C15	C20	118.6(4)

### 3.6 Lu(<sup>Ar</sup>BiAMP<sup>tBu</sup>)(THF)<sub>3</sub> (3)

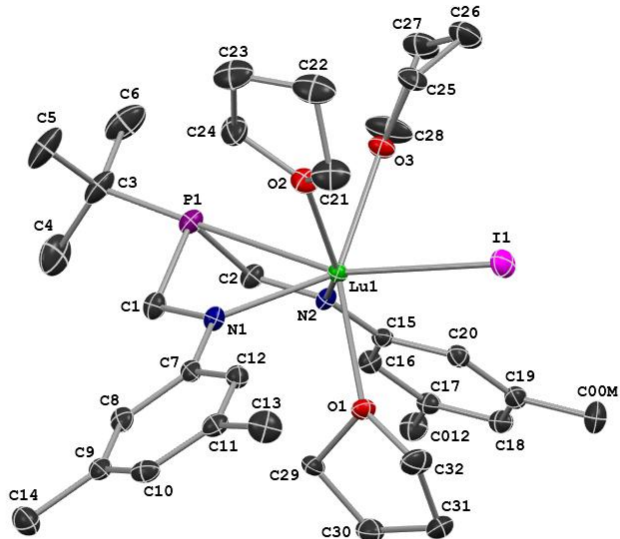


**Figure S56.** Solid state molecular structure of Lu(<sup>Ar</sup>BiAMP<sup>tBu</sup>)(THF)<sub>3</sub> (3) (recrystallized from THF/n-pentane) shown with hydrogen atoms omitted for clarity and the thermal ellipsoids set at 50% probability.

**Table S14.** Crystal data and structure refinement for Lu(<sup>Ar</sup>BiAMP<sup>tBu</sup>)(THF)<sub>3</sub> (3).

Empirical formula	C <sub>34</sub> H <sub>55</sub> LuN <sub>2</sub> O <sub>3</sub> P
Formula weight	872.64
Temperature/K	100.0
Crystal system	orthorhombic
Space group	P2 <sub>1</sub> 2 <sub>1</sub> 2 <sub>1</sub>
a/Å	13.4115(9)
b/Å	14.1878(10)
c/Å	19.0912(14)
α/°	90
β/°	90
γ/°	90
Volume/Å <sup>3</sup>	3632.7(4)
Z	4
ρ <sub>calc</sub> g/cm <sup>3</sup>	1.596
μ/mm <sup>-1</sup>	3.645
F(000)	1744.0
Crystal size/mm <sup>3</sup>	0.22 × 0.12 × 0.03
Radiation	MoK $\alpha$ ( $\lambda$ = 0.71073)
2θ range for data collection/°	6.126 to 56.67
Index ranges	-17 ≤ h ≤ 17, -17 ≤ k ≤ 18, -25 ≤ l ≤ 25
Reflections collected	35210
Independent reflections	9000 [ $R_{\text{int}} = 0.0318$ , $R_{\text{sigma}} = 0.0295$ ]
Data/restraints/parameters	9000/0/388
Goodness-of-fit on $F^2$	1.126
Final R indexes [ $I \geq 2\sigma(I)$ ]	$R_1 = 0.0215$ , $wR_2 = 0.0443$
Final R indexes [all data]	$R_1 = 0.0232$ , $wR_2 = 0.0447$
Largest diff. peak/hole / e Å <sup>-3</sup>	0.96/-0.87
Flack parameter	0.290(6)

**Table S15.** Bond Lengths for  $\text{LuI}(\text{ArBiAMP}^{\text{tBu}})(\text{THF})_3$  (3).

Atom	Atom	Length/ $\text{\AA}$	Atom	Atom	Length/ $\text{\AA}$
Lu1	I1	3.0456(4)	C28	C27	1.499(7)
Lu1	P1	3.0766(12)	C19	C00M	1.509(6)
Lu1	O1	2.330(3)	C19	C18	1.409(6)
Lu1	O2	2.377(3)	C30	C31	1.526(7)
Lu1	N2	2.239(4)	C12	C7	1.405(6)
Lu1	O3	2.374(3)	C12	C11	1.389(6)
Lu1	N1	2.244(3)	C15	C16	1.416(6)
P1	C1	1.842(5)	C7	C8	1.410(6)
P1	C2	1.841(5)	C3	C6	1.530(8)
P1	C3	1.868(5)	C3	C4	1.522(8)
O1	C29	1.470(5)	C3	C5	1.542(7)
O1	C32	1.453(6)	C25	C26	1.510(7)
O2	C24	1.450(6)	C24	C23	1.533(7)
O2	C21	1.449(6)	C8	C9	1.384(7)
N2	C2	1.465(6)	C17	C16	1.395(6)
N2	C15	1.387(6)	C17	C18	1.377(6)
O3	C28	1.447(6)	C17	C012	1.507(6)
O3	C25	1.461(6)	C27	C26	1.518(8)
N1	C1	1.465(6)	C21	C22	1.503(8)
N1	C7	1.377(6)	C14	C9	1.517(6)
C20	C19	1.373(6)	C13	C11	1.507(7)
C20	C15	1.418(6)	C9	C10	1.377(7)
C29	C30	1.511(6)	C11	C10	1.402(7)
C32	C31	1.525(7)	C23	C22	1.516(9)

**Table S16.** Bond Angles for  $\text{LuI}(\text{ArBiAMP}^{\text{tBu}})(\text{THF})_3$  (3).

Atom	Atom	Atom	Angle/ $^\circ$	Atom	Atom	Atom	Angle/ $^\circ$
I1	Lu1	P1	159.25(2)	N1	C1	P1	106.9(3)
O1	Lu1	I1	81.27(8)	N2	C2	P1	105.8(3)
O1	Lu1	P1	117.29(8)	O1	C29	C30	105.0(4)
O1	Lu1	O2	127.95(11)	O1	C32	C31	104.8(4)
O1	Lu1	O3	146.73(11)	O3	C28	C27	107.3(4)
O2	Lu1	I1	82.42(9)	C20	C19	C00M	120.6(4)
O2	Lu1	P1	91.83(9)	C20	C19	C18	120.3(4)
N2	Lu1	I1	120.20(9)	C18	C19	C00M	119.1(4)
N2	Lu1	P1	57.13(9)	C29	C30	C31	104.8(4)
N2	Lu1	O1	84.48(12)	C11	C12	C7	122.6(4)
N2	Lu1	O2	144.84(13)	N2	C15	C20	118.9(4)
N2	Lu1	O3	81.30(13)	N2	C15	C16	124.7(4)
N2	Lu1	N1	92.25(14)	C16	C15	C20	116.4(4)
O3	Lu1	I1	80.24(8)	N1	C7	C12	119.5(4)
O3	Lu1	P1	79.03(8)	N1	C7	C8	124.2(4)
O3	Lu1	O2	76.37(11)	C12	C7	C8	116.3(4)
N1	Lu1	I1	140.14(10)	C6	C3	P1	107.7(4)
N1	Lu1	P1	57.63(9)	C6	C3	C5	108.2(5)
N1	Lu1	O1	79.48(12)	C4	C3	P1	113.3(4)
N1	Lu1	O2	82.48(13)	C4	C3	C6	111.1(5)
N1	Lu1	O3	130.80(12)	C4	C3	C5	110.2(5)
C1	P1	Lu1	75.60(16)	C5	C3	P1	106.1(4)
C1	P1	C3	103.7(2)	O3	C25	C26	104.4(4)
C2	P1	Lu1	77.42(15)	O2	C24	C23	106.4(4)
C2	P1	C1	100.2(2)	C9	C8	C7	121.7(5)
C2	P1	C3	106.3(2)	C16	C17	C012	120.0(4)
C3	P1	Lu1	176.24(17)	C18	C17	C16	120.4(4)
C29	O1	Lu1	118.8(3)	C18	C17	C012	119.6(4)
C32	O1	Lu1	138.1(3)	C32	C31	C30	104.3(4)
C32	O1	C29	103.1(3)	C17	C16	C15	121.6(4)
C24	O2	Lu1	119.3(3)	C28	C27	C26	102.5(4)
C21	O2	Lu1	132.0(3)	O2	C21	C22	103.5(4)
C21	O2	C24	107.2(4)	C25	C26	C27	102.5(4)
C2	N2	Lu1	119.5(3)	C8	C9	C14	119.0(4)

**Table S16 (Continued).** Bond Angles for  $\text{LuI}(\text{ArBiAMP}^{\text{tBu}})(\text{THF})_3$  (3).

C15	N2	Lu1	125.7(3)	C10	C9	C8	120.5(4)
C15	N2	C2	114.8(4)	C10	C9	C14	120.5(4)
C28	O3	Lu1	123.6(3)	C17	C18	C19	119.5(4)
C28	O3	C25	108.6(3)	C12	C11	C13	120.8(4)
C25	O3	Lu1	127.5(3)	C12	C11	C10	118.9(4)
C1	N1	Lu1	115.8(3)	C10	C11	C13	120.4(4)
C7	N1	Lu1	127.7(3)	C22	C23	C24	103.9(5)
C7	N1	C1	115.1(3)	C9	C10	C11	120.0(4)
C19	C20	C15	121.9(4)	C21	C22	C23	102.2(5)

### 3.7 $\text{Y}(\eta^5\text{-}(1,3\text{-diisopropyl-4,7-dimethylindenyl})(^{Ar}\text{BiAMP}^{t\text{Bu}})(\text{THF})$ (4)

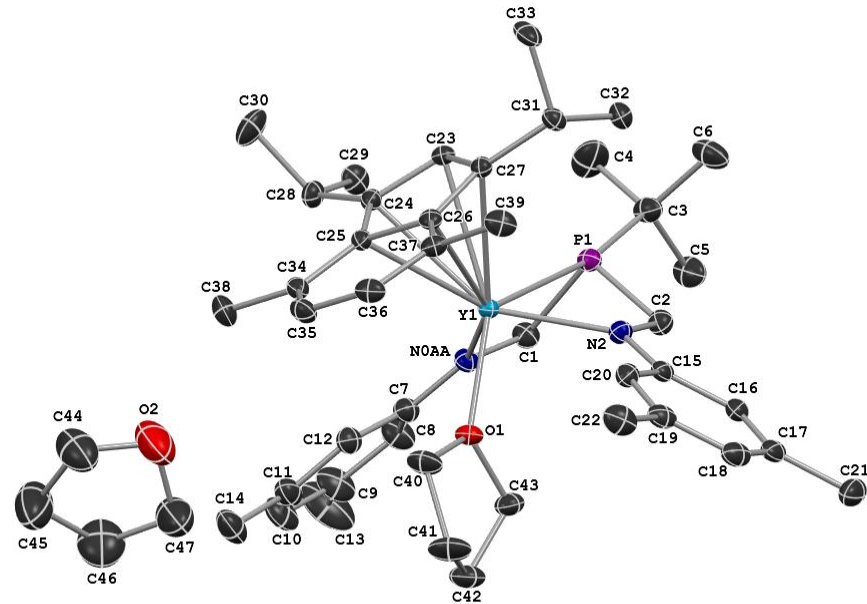


**Figure S57.** Solid state molecular structure of  $\text{Y}(\eta^5\text{-}(1,3\text{-diisopropyl-4,7-dimethylindenyl})(^{Ar}\text{BiAMP}^{t\text{Bu}})(\text{THF})$  (4) (recrystallized from THF/n-pentane) shown with hydrogen atoms omitted for clarity and the thermal ellipsoids set at 50% probability.

**Table S17.** Crystal data and structure refinement for  $\text{Y}(\eta^5\text{-}(1,3\text{-diisopropyl-4,7-dimethylindenyl})(^{Ar}\text{BiAMP}^{t\text{Bu}})(\text{THF})$  (4).

Empirical formula	$\text{C}_{47}\text{H}_{70}\text{N}_2\text{O}_2\text{PY}$
Formula weight	814.93
Temperature/K	100.0
Crystal system	monoclinic
Space group	$\text{P}2_1/\text{c}$
a/ $\text{\AA}$	10.0823(13)
b/ $\text{\AA}$	28.934(4)
c/ $\text{\AA}$	15.635(2)
$\alpha/^\circ$	90
$\beta/^\circ$	99.158(4)
$\gamma/^\circ$	90
Volume/ $\text{\AA}^3$	4503.1(10)
Z	4
$\rho_{\text{calc}}$ g/cm <sup>3</sup>	1.202
$\mu/\text{mm}^{-1}$	1.368
F(000)	1744.0
Crystal size/mm <sup>3</sup>	0.38 $\times$ 0.24 $\times$ 0.032
Radiation	MoK $\alpha$ ( $\lambda = 0.71073$ )
2 $\Theta$ range for data collection/ $^\circ$	4.328 to 56.592
Index ranges	-13 $\leq$ h $\leq$ 13, -38 $\leq$ k $\leq$ 35, -20 $\leq$ l $\leq$ 20
Reflections collected	38274
Independent reflections	11171 [ $R_{\text{int}} = 0.0650$ , $R_{\text{sigma}} = 0.0637$ ]
Data/restraints/parameters	11171/0/491
Goodness-of-fit on $F^2$	1.046
Final R indexes [ $I \geq 2\sigma (I)$ ]	$R_1 = 0.0428$ , $wR_2 = 0.1043$
Final R indexes [all data]	$R_1 = 0.0608$ , $wR_2 = 0.1109$
Largest diff. peak/hole / e $\text{\AA}^{-3}$	0.83/-0.51

**Table S18.** Bond Lengths for Y( $\eta^5$ -1,3-diisopropyl-4,7-dimethylindenyl)( $^{Ar}$ BiAMP $tBu$ )(THF) (4).

Atom	Atom	Length/ $\text{\AA}$	Atom	Atom	Length/ $\text{\AA}$
Y1	P1	2.8856(6)	C37	C39	1.509(3)
Y1	O1	2.3193(14)	C36	C35	1.415(3)
Y1	N0AA	2.2667(17)	C35	C34	1.369(3)
Y1	N2	2.2383(18)	C34	C38	1.504(3)
Y1	C27	2.686(2)	C31	C33	1.536(3)
Y1	C23	2.656(2)	C31	C32	1.526(3)
Y1	C24	2.663(2)	C15	C20	1.412(3)
Y1	C25	2.690(2)	C15	C16	1.408(3)
Y1	C26	2.709(2)	C20	C19	1.382(3)
P1	C1	1.851(2)	C19	C22	1.506(3)
P1	C2	1.855(2)	C19	C18	1.397(3)
P1	C3	1.858(2)	C18	C17	1.393(4)
O1	C40	1.461(3)	C17	C21	1.507(3)
O1	C43	1.473(3)	C17	C16	1.390(3)
O2	C44	1.382(4)	C3	C4	1.523(4)
O2	C47	1.409(4)	C3	C5	1.521(3)
N0AA	C1	1.463(3)	C3	C6	1.535(3)
N0AA	C7	1.387(3)	C7	C12	1.412(3)
N2	C2	1.465(3)	C7	C8	1.401(3)
N2	C15	1.377(3)	C12	C11	1.384(3)
C27	C23	1.410(3)	C11	C14	1.513(3)
C27	C26	1.435(3)	C11	C10	1.391(3)
C27	C31	1.518(3)	C10	C9	1.381(4)
C23	C24	1.410(3)	C9	C8	1.396(3)
C24	C28	1.525(3)	C9	C13	1.517(4)
C24	C25	1.432(3)	C40	C41	1.512(3)
C28	C29	1.526(3)	C41	C42	1.520(4)
C28	C30	1.533(3)	C42	C43	1.505(3)
C25	C26	1.467(3)	C46	C45	1.534(5)
C25	C34	1.439(3)	C46	C47	1.478(5)
C26	C37	1.437(3)	C45	C44	1.486(5)
C37	C36	1.372(3)			

**Table S18.** Bond Angles for Y( $\eta^5$ -1,3-diisopropyl-4,7-dimethylindenyl)( $^{Ar}$ BiAMP $tBu$ )(THF) (4).

Atom	Atom	Atom	Angle/ $^{\circ}$	Atom	Atom	Atom	Angle/ $^{\circ}$
O1	Y1	P1	129.81(4)	C24	C28	C29	112.95(18)
O1	Y1	C27	126.61(6)	C24	C28	C30	110.40(18)
O1	Y1	C23	145.34(6)	C29	C28	C30	109.38(19)
O1	Y1	C24	121.40(6)	C24	C25	Y1	73.44(12)
O1	Y1	C25	95.48(6)	C24	C25	C26	107.78(17)
O1	Y1	C26	98.28(6)	C24	C25	C34	132.69(19)
N0AA	Y1	P1	60.45(5)	C26	C25	Y1	74.94(11)
N0AA	Y1	O1	89.96(6)	C34	C25	Y1	121.15(13)
N0AA	Y1	C27	139.60(6)	C34	C25	C26	119.35(19)
N0AA	Y1	C23	109.40(6)	C27	C26	Y1	73.69(11)
N0AA	Y1	C24	97.03(6)	C27	C26	C25	107.45(18)
N0AA	Y1	C25	116.27(6)	C27	C26	C37	132.17(19)
N0AA	Y1	C26	147.10(6)	C25	C26	Y1	73.53(11)
N2	Y1	P1	60.08(5)	C37	C26	Y1	122.30(14)
N2	Y1	O1	87.96(6)	C37	C26	C25	120.16(18)
N2	Y1	N0AA	97.21(7)	C26	C37	C39	123.07(19)
N2	Y1	C27	100.29(6)	C36	C37	C26	117.31(19)
N2	Y1	C23	116.47(6)	C36	C37	C39	119.5(2)
N2	Y1	C24	147.22(6)	C37	C36	C35	122.8(2)
N2	Y1	C25	146.29(6)	C34	C35	C36	122.5(2)
N2	Y1	C26	114.78(6)	C25	C34	C38	122.7(2)
C27	Y1	P1	98.28(5)	C35	C34	C25	117.86(19)
C27	Y1	C25	51.60(6)	C35	C34	C38	119.36(19)
C27	Y1	C26	30.86(6)	C27	C31	C33	109.52(17)
C23	Y1	P1	84.78(5)	C27	C31	C32	113.09(17)

**Table S18 (Continued).** Bond Angles for Y( $\eta^5$ -1,3-diisopropyl-4,7-dimethylindenyl)( $^{Ar}$ BiAMP<sup>tBu</sup>)(THF) (4).

C23	Y1	C27	30.60(6)	C32	C31	C33	110.29(18)
C23	Y1	C24	30.76(6)	N0AA	C1	P1	105.50(14)
C23	Y1	C25	50.41(6)	N2	C2	P1	103.90(14)
C23	Y1	C26	50.29(6)	N2	C15	C20	117.84(19)
C24	Y1	P1	102.94(5)	N2	C15	C16	125.6(2)
C24	Y1	C27	51.75(6)	C16	C15	C20	116.5(2)
C24	Y1	C25	31.02(6)	C19	C20	C15	123.0(2)
C24	Y1	C26	51.68(6)	C20	C19	C22	120.0(2)
C25	Y1	P1	133.01(5)	C20	C19	C18	118.6(2)
C25	Y1	C26	31.52(6)	C18	C19	C22	121.4(2)
C26	Y1	P1	129.10(5)	C17	C18	C19	120.4(2)
C1	P1	Y1	80.15(7)	C18	C17	C21	120.8(2)
C1	P1	C2	103.49(10)	C16	C17	C18	119.9(2)
C1	P1	C3	105.60(11)	C16	C17	C21	119.3(2)
C2	P1	Y1	79.17(7)	C17	C16	C15	121.5(2)
C2	P1	C3	107.44(10)	C4	C3	P1	107.85(17)
C3	P1	Y1	169.50(7)	C4	C3	C6	108.8(2)
C40	O1	Y1	132.56(13)	C5	C3	P1	110.54(16)
C40	O1	C43	109.09(16)	C5	C3	C4	110.9(2)
C43	O1	Y1	118.31(12)	C5	C3	C6	109.9(2)
C44	O2	C47	106.3(2)	C6	C3	P1	108.85(17)
C1	N0AA	Y1	113.54(13)	N0AA	C7	C12	118.7(2)
C7	N0AA	Y1	131.06(15)	N0AA	C7	C8	124.6(2)
C7	N0AA	C1	115.40(18)	C8	C7	C12	116.7(2)
C2	N2	Y1	113.39(13)	C11	C12	C7	122.4(2)
C15	N2	Y1	127.39(14)	C12	C11	C14	120.1(2)
C15	N2	C2	117.29(17)	C12	C11	C10	119.1(2)
C23	C27	Y1	73.52(11)	C10	C11	C14	120.8(2)
C23	C27	C26	106.52(17)	C9	C10	C11	120.4(2)
C23	C27	C31	123.96(18)	C10	C9	C8	120.1(2)
C26	C27	Y1	75.45(11)	C10	C9	C13	120.7(2)
C26	C27	C31	128.62(18)	C8	C9	C13	119.2(3)
C31	C27	Y1	124.79(13)	C9	C8	C7	121.3(2)
C27	C23	Y1	75.89(12)	O1	C40	C41	105.2(2)
C27	C23	C24	111.74(18)	C40	C41	C42	102.6(2)
C24	C23	Y1	74.89(11)	C43	C42	C41	101.93(19)
C23	C24	Y1	74.35(11)	O1	C43	C42	104.45(19)
C23	C24	C28	124.02(19)	C47	C46	C45	102.8(3)
C23	C24	C25	106.47(17)	C44	C45	C46	103.9(3)
C28	C24	Y1	121.45(13)	O2	C44	C45	107.7(3)
C25	C24	Y1	75.54(12)	O2	C47	C46	105.7(3)
C25	C24	C28	129.07(18)				

### 3.7.1. $\text{Y}(\eta^5\text{-}(1,3\text{-diisopropyl-4,7-dimethylindenyl})(^\text{Ar}\text{BiAMP}^\text{tBu})(\text{THF})(\text{Et}_2\text{O})$ (4a)

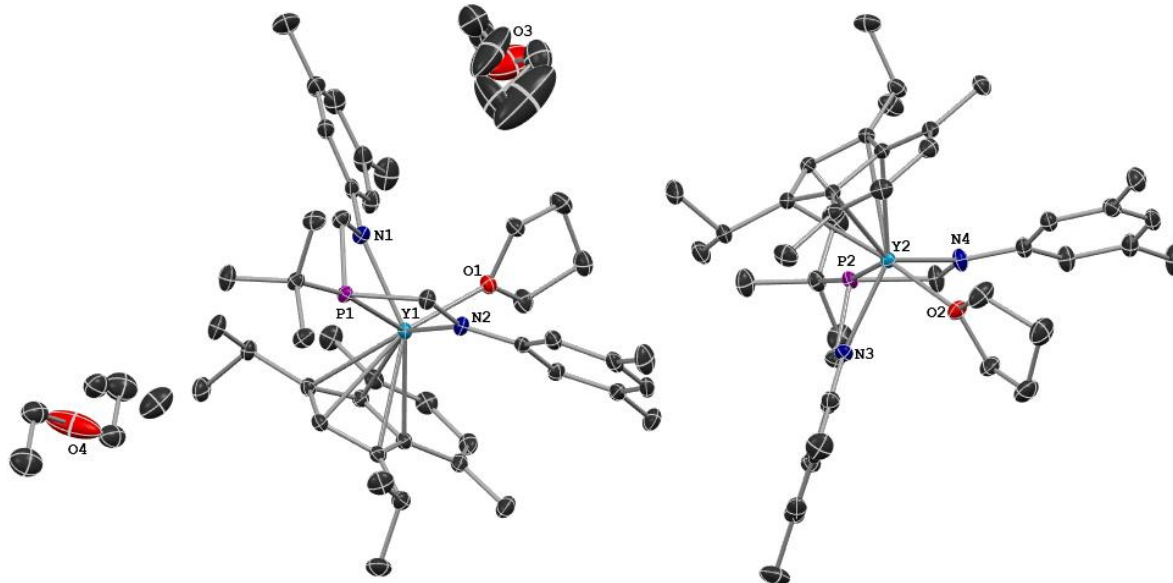


**Figure S57a.** Solid state molecular structure of  $\text{Y}(\eta^5\text{-}(1,3\text{-diisopropyl-4,7-dimethylindenyl})(^\text{Ar}\text{BiAMP}^\text{tBu})(\text{THF})(\text{Et}_2\text{O})$  (4a) (recrystallized from THF / Et<sub>2</sub>O) shown with hydrogen atoms omitted for clarity and the thermal ellipsoids set at 50% probability.

**Table S17a.** Crystal data and structure refinement for  $\text{Y}(\eta^5\text{-}(1,3\text{-diisopropyl-4,7-dimethylindenyl})(^\text{Ar}\text{BiAMP}^\text{tBu})(\text{THF})(\text{Et}_2\text{O})$  (4a)..

Identification code	BiAMPYInd_Ether (1)
Empirical formula	C <sub>92</sub> H <sub>139</sub> N <sub>4</sub> O <sub>3.5</sub> P <sub>2</sub> Y <sub>2</sub>
Formula weight	1596.82
Temperature/K	100.0
Crystal system	triclinic
Space group	P-1
a/Å	12.7857(14)
b/Å	18.839(2)
c/Å	19.534(2)
α°	98.801(3)
β°	105.570(3)
γ°	99.416(3)
Volume/Å <sup>3</sup>	4374.2(9)
Z	2
ρ <sub>calcd</sub> /g/cm <sup>3</sup>	1.212
μ/mm <sup>-1</sup>	1.406
F(000)	1710.0
Crystal size/mm <sup>3</sup>	0.15 × 0.09 × 0.09
Radiation	MoKα (λ = 0.71073)
2θ range for data collection/°	4.568 to 56.564
Index ranges	-17 ≤ h ≤ 17, -25 ≤ k ≤ 25, -26 ≤ l ≤ 26
Reflections collected	74818
Independent reflections	21611 [R <sub>int</sub> = 0.0282, R <sub>sigma</sub> = 0.0267]
Data/restraints/parameters	21611/0/1002
Goodness-of-fit on F <sup>2</sup>	1.023
Final R indexes [ >=2σ (I) ]	R <sub>1</sub> = 0.0279, wR <sub>2</sub> = 0.0659
Final R indexes [all data]	R <sub>1</sub> = 0.0342, wR <sub>2</sub> = 0.0683
Largest diff. peak/hole / e Å <sup>-3</sup>	0.63/-0.53

### 3.8 $\text{La}(\eta^5\text{-}(1,3\text{-diisopropyl-4,7-dimethylindenyl})(^{Ar}\text{BiAMP}^{tBu})\text{(THF)}_2$ (5)

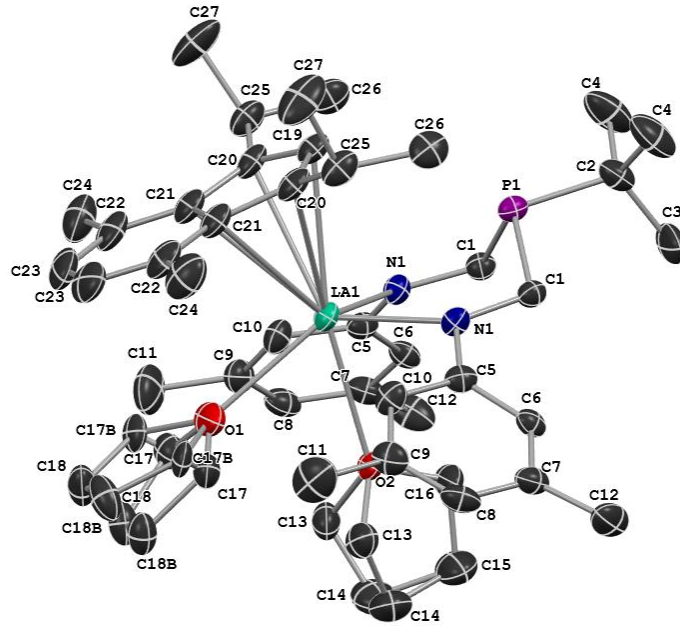


**Figure S58.** Solid state molecular structure of  $\text{La}(\eta^5\text{-}(1,3\text{-diisopropyl-4,7-dimethylindenyl})(^{Ar}\text{BiAMP}^{tBu})\text{(THF)}_2$  (5) (recrystallized from THF/n-pentane) shown with hydrogen atoms omitted for clarity and the thermal ellipsoids set at 50% probability. The disorder arising from the symmetry generation is shown on the coordinated THF molecules. Two solvent molecules that are present in the unit cell, pentane and THF, are not well-resolved, and the carbon atoms remain isotropic; these molecules are omitted for clarity.

**Table S19.** Crystal data and structure refinement for  $\text{La}(\eta^5\text{-}(1,3\text{-diisopropyl-4,7-dimethylindenyl})(^{Ar}\text{BiAMP}^{tBu})\text{(THF)}_2$  (5).

Empirical formula	$\text{C}_{51}\text{H}_{69}\text{LaN}_2\text{O}_2\text{P}$
Formula weight	911.96
Temperature/K	100.0
Crystal system	tetragonal
Space group	P-42 <sub>1</sub> m
a/Å	21.1393(6)
b/Å	21.1393(6)
c/Å	10.8270(4)
$\alpha/^\circ$	90
$\beta/^\circ$	90
$\gamma/^\circ$	90
Volume/Å <sup>3</sup>	4838.3(3)
Z	4
$\rho_{\text{calc}}/\text{g/cm}^3$	1.252
$\mu/\text{mm}^{-1}$	0.954
F(000)	1908.0
Crystal size/mm <sup>3</sup>	0.22 × 0.15 × 0.15
Radiation	MoKα ( $\lambda = 0.71073$ )
2θ range for data collection/°	4.226 to 56.658
Index ranges	-25 ≤ h ≤ 28, -28 ≤ k ≤ 28, -14 ≤ l ≤ 14
Reflections collected	87253
Independent reflections	6246 [ $R_{\text{int}} = 0.0804$ , $R_{\text{sigma}} = 0.0361$ ]
Data/restraints/parameters	6246/9/317
Goodness-of-fit on F <sup>2</sup>	1.062
Final R indexes [ >=2σ (I)]	$R_1 = 0.0333$ , $wR_2 = 0.0867$
Final R indexes [all data]	$R_1 = 0.0372$ , $wR_2 = 0.0880$
Largest diff. peak/hole / e Å <sup>-3</sup>	0.78/-0.68
Flack parameter	0.02(2)

**Table S20.** Bond Lengths for La( $\eta^5$ -(1,3-diisopropyl-4,7-dimethylindenyl)( $^{Ar}$ BiAMP<sup>tBu</sup>)(THF)<sub>2</sub> (5).

Atom	Atom	Length/ $\text{\AA}$	Atom	Atom	Length/ $\text{\AA}$
La1	O1	2.573(5)	C2	C3	1.517(6)
La1	N11	2.386(3)	C2	C31	1.517(6)
La1	N1	2.386(3)	C2	C4	1.542(11)
La1	O2	2.668(4)	C25	C26	1.530(7)
La1	C19	2.872(6)	C25	C27	1.543(6)
La1	C20	2.894(4)	C6	C5	1.409(7)
La1	C201	2.894(4)	C13	C14	1.513(9)
La1	C21	2.956(4)	C14	C15	1.450(15)
La1	C211	2.956(4)	C23	C231	1.387(13)
P1	C11	1.858(4)	C23	C22	1.379(8)
P1	C1	1.858(4)	C24	C22	1.508(9)
P1	C2	1.876(7)	C17	C18	1.80(2)
O1	C171	1.296(16)	C18A	C18A1	1.148(18)
O1	C17	1.296(16)	C18A	C17A	1.578(15)
O1	C17A	1.564(12)	C18	C181	1.18(2)
O1	C17A1	1.564(12)	C36	C352	1.48(3)
N1	C1	1.472(5)	C36	C35	1.48(3)
N1	C5	1.377(5)	C29	C293	1.94(4)
O2	C16	1.532(10)	C29	C294	1.94(4)
O2	C13	1.419(7)	C29	C283	1.13(5)
C19	C20	1.415(6)	C29	C28	0.95(5)
C19	C201	1.415(6)	C35	C34	1.09(6)
C20	C21	1.431(7)	C28	C284	1.66(6)
C20	C25	1.517(6)	C28	C283	1.66(6)
C9	C10	1.377(6)	C30	C302	1.41(6)
C9	C8	1.391(7)	C30	C31	1.55(2)
C9	C12	1.519(7)	C30	C311	1.55(2)
C16	C15	1.50(2)	C31	C312	1.52(6)
C10	C5	1.423(7)	C31	C315	1.30(6)
C21	C211	1.484(9)	C31	C311	0.79(6)
C21	C22	1.426(7)	C31	C322	1.95(4)
C7	C6	1.397(6)	C31	C32	1.55(3)
C7	C8	1.379(7)	C32	C322	1.08(11)
C7	C11	1.501(8)	C34	C33	1.38(6)

**Table S21.** Bond Angles for La( $\eta^5$ -(1,3-diisopropyl-4,7-dimethylindenyl)( $^{Ar}$ BiAMP<sup>tBu</sup>)(THF)<sub>2</sub> (5).

Atom	Atom	Atom	Angle/ $^\circ$	Atom	Atom	Atom	Angle/ $^\circ$
O1	La1	O2	68.28(13)	C20	C21	La1	73.5(2)
O1	La1	C19	123.36(18)	C20	C21	C211	107.3(3)
O1	La1	C201	105.84(14)	C211	C21	La1	75.46(9)
O1	La1	C20	105.84(14)	C22	C21	La1	119.0(3)
O1	La1	C211	79.32(14)	C22	C21	C20	133.2(5)
O1	La1	C21	79.32(14)	C22	C21	C211	119.4(3)
N11	La1	O1	126.26(10)	C6	C7	C11	118.9(5)
N1	La1	O1	126.26(10)	C8	C7	C6	119.9(5)
N1	La1	N11	86.40(16)	C8	C7	C11	121.2(4)
N11	La1	O2	79.81(11)	C3	C2	P1	107.5(4)
N1	La1	O2	79.81(11)	C31	C2	P1	107.5(4)
N11	La1	C19	91.76(13)	C31	C2	C3	109.8(6)
N1	La1	C19	91.76(13)	C3	C2	C4	108.9(4)
N11	La1	C201	119.13(13)	C31	C2	C4	108.9(4)
N1	La1	C20	119.13(13)	C4	C2	P1	114.1(4)
N11	La1	C20	86.25(13)	C20	C25	C26	113.6(4)
N1	La1	C201	86.25(13)	C20	C25	C27	109.5(4)
N1	La1	C21	133.34(13)	C26	C25	C27	107.9(4)
N1	La1	C211	110.03(12)	C7	C6	C5	121.2(5)
N11	La1	C21	110.03(12)	O2	C13	C14	109.1(6)
N11	La1	C211	133.34(13)	C15	C14	C13	102.4(7)
O2	La1	C19	168.37(16)	N1	C5	C10	118.3(4)
O2	La1	C20	155.84(9)	N1	C5	C6	125.1(4)

O2	La1	C201	155.84(9)	C6	C5	C10	116.6(4)
O2	La1	C21	144.49(12)	C7	C8	C9	120.6(4)
O2	La1	C211	144.49(13)	C22	C23	C231	122.9(3)
C19	La1	C201	28.41(12)	C21	C22	C24	122.9(5)
C19	La1	C20	28.41(12)	C23	C22	C21	117.7(5)
C19	La1	C21	46.24(17)	C23	C22	C24	119.4(5)
C19	La1	C211	46.24(17)	O1	C17	C18	99.4(11)
C20	La1	C201	47.58(18)	C18A1	C18A	C17A	115.4(5)
C201	La1	C21	47.32(13)	C181	C18	C17	104.3(6)
C20	La1	C211	47.32(13)	O1	C17A	C18A	94.2(9)
C201	La1	C211	28.30(13)	C14	C15	C16	107.4(10)
C20	La1	C21	28.30(13)	C35	C36	C352	97(5)
C21	La1	C211	29.09(18)	C293	C29	C294	81.6(11)
C11	P1	C1	99.5(2)	C28	C29	C293	86(3)
C1	P1	C2	102.30(18)	C28	C29	C294	24(3)
C11	P1	C2	102.30(18)	C283	C29	C293	20(3)
C17	O1	La1	122.3(7)	C283	C29	C294	97(3)
C171	O1	La1	122.3(7)	C28	C29	C283	105(5)
C171	O1	C17	106.2(14)	C34	C35	C36	130(5)
C171	O1	C17A1	22.2(6)	C29	C28	C294	137(5)
C17	O1	C17A1	110.7(7)	C294	C28	C284	34(3)
C17A	O1	La1	126.2(4)	C29	C28	C283	41(3)
C17A1	O1	La1	126.2(4)	C29	C28	C284	104(5)
C17A	O1	C17A1	106.2(9)	C294	C28	C283	114(3)
C1	N1	La1	127.3(2)	C283	C28	C284	84(2)
C5	N1	La1	113.1(3)	C302	C30	C31	88.1(17)
C5	N1	C1	115.6(4)	C302	C30	C311	88.1(17)
C16	O2	La1	126.3(4)	C31	C30	C311	30(2)
C13	O2	La1	118.9(4)	C315	C31	C30	91.9(17)
C13	O2	C16	99.5(5)	C312	C31	C30	84.0(17)
C20	C19	La1	76.7(3)	C311	C31	C30	75.2(12)
C201	C19	La1	76.7(3)	C311	C31	C312	59(2)
C20	C19	C201	111.2(6)	C315	C31	C312	31(2)
C19	C20	La1	74.9(3)	C312	C31	C32	79(2)
C19	C20	C21	107.1(4)	C315	C31	C32	86(2)
C19	C20	C25	123.9(5)	C311	C31	C32	75.2(12)
C21	C20	La1	78.2(2)	C32	C31	C30	150(2)
C21	C20	C25	127.5(4)	C31	C32	C312	50(2)
C25	C20	La1	123.7(3)	C311	C32	C312	42(2)
N1	C1	P1	108.7(2)	C311	C32	C31	30(2)
C10	C9	C8	119.5(4)	C322	C32	C311	94(2)
C10	C9	C12	121.8(5)	C322	C32	C31	94(2)
C8	C9	C12	118.6(4)	C322	C32	C312	52.4(15)
C15	C16	O2	99.9(11)	C35	C34	C33	131(5)
C9	C10	C5	122.0(5)	C342	C33	C34	102(5)

### 3.9 Lu( $\eta^5$ -(1,3-diisopropyl-4,7-dimethylindenyl)( $^{Ar}$ BiAMP<sup>tBu</sup>)(THF) (6)

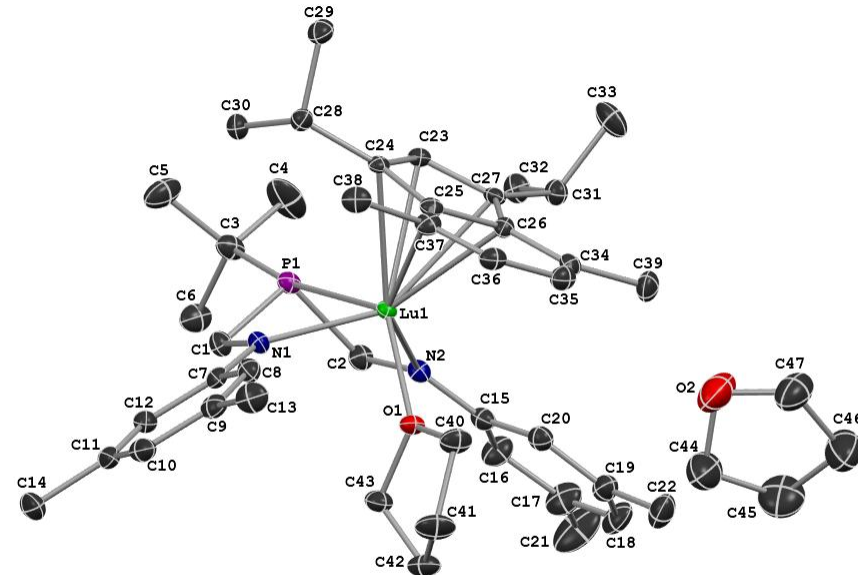


**Figure S59.** Solid state molecular structure of Lu( $\eta^5$ -(1,3-diisopropyl-4,7-dimethylindenyl)( $^{Ar}$ BiAMP<sup>tBu</sup>)(THF) (6) (recrystallized from THF/n-pentane) shown with hydrogen atoms omitted for clarity and the thermal ellipsoids set at 50% probability.

**Table S22.** Crystal data and structure refinement for Lu( $\eta^5$ -(1,3-diisopropyl-4,7-dimethylindenyl)( $^{Ar}$ BiAMP<sup>tBu</sup>)(THF) (6).

Identification code	LuBiAMPInd (2)
Empirical formula	C <sub>47</sub> H <sub>70</sub> LuN <sub>2</sub> O <sub>2</sub> P
Formula weight	900.99
Temperature/K	100.0
Crystal system	monoclinic
Space group	P2 <sub>1</sub> /c
a/ $\text{\AA}$	10.0585(4)
b/ $\text{\AA}$	28.9336(10)
c/ $\text{\AA}$	15.5726(6)
$\alpha/^\circ$	90
$\beta/^\circ$	99.117(2)
$\gamma/^\circ$	90
Volume/ $\text{\AA}^3$	4474.8(3)
Z	4
$\rho_{\text{calc}}$ g/cm <sup>3</sup>	1.337
$\mu/\text{mm}^{-1}$	2.279
F(000)	1872.0
Crystal size/mm <sup>3</sup>	0.17 × 0.12 × 0.03
Radiation	MoK $\alpha$ ( $\lambda = 0.71073$ )
2 $\Theta$ range for data collection/°	3.866 to 56.566
Index ranges	-13 ≤ h ≤ 13, -38 ≤ k ≤ 38, -20 ≤ l ≤ 19
Reflections collected	99041
Independent reflections	11121 [ $R_{\text{int}} = 0.0538$ , $R_{\text{sigma}} = 0.0258$ ]
Data/restraints/parameters	11121/0/492
Goodness-of-fit on F <sup>2</sup>	1.237
Final R indexes [ $ I  \geq 2\sigma(I)$ ]	$R_1 = 0.0350$ , $wR_2 = 0.0736$
Final R indexes [all data]	$R_1 = 0.0397$ , $wR_2 = 0.0747$
Largest diff. peak/hole / e $\text{\AA}^{-3}$	1.71/-2.60

**Table S23.** Bond Lengths for Lu( $\eta^5$ -(1,3-diisopropyl-4,7-dimethylindenyl)( $^{Ar}$ BiAMP $tBu$ )(THF) (6).

Atom	Atom	Length/ $\text{\AA}$	Atom	Atom	Length/ $\text{\AA}$
Lu1	P1	2.8578(8)	C28	C30	1.533(4)
Lu1	O1	2.264(2)	C34	C39	1.508(5)
Lu1	C23	2.607(3)	C34	C35	1.377(5)
Lu1	N2	2.225(3)	C35	C36	1.411(5)
Lu1	N1	2.203(3)	C36	C37	1.356(4)
Lu1	C25	2.676(3)	C37	C38	1.524(5)
Lu1	C26	2.663(3)	C15	C16	1.413(4)
Lu1	C27	2.616(3)	C15	C20	1.414(5)
Lu1	C24	2.638(3)	C16	C17	1.390(5)
P1	C2	1.850(3)	C17	C21	1.512(5)
P1	C1	1.851(3)	C17	C18	1.385(6)
P1	C3	1.859(3)	C18	C19	1.399(5)
O1	C43	1.477(4)	C19	C22	1.513(5)
O1	C40	1.462(4)	C19	C20	1.378(5)
O2	C44	1.409(6)	C7	C8	1.407(5)
O2	C47	1.392(6)	C7	C12	1.407(4)
C23	C27	1.413(4)	C8	C9	1.385(5)
C23	C24	1.413(4)	C9	C13	1.508(5)
N2	C2	1.467(4)	C9	C10	1.402(5)
N2	C15	1.371(4)	C10	C11	1.384(5)
N1	C1	1.473(4)	C11	C14	1.518(5)
N1	C7	1.380(4)	C11	C12	1.395(5)
C25	C26	1.455(4)	C3	C6	1.521(5)
C25	C24	1.432(4)	C3	C5	1.531(5)
C25	C37	1.441(4)	C3	C4	1.526(5)
C26	C27	1.444(4)	C43	C42	1.511(5)
C26	C34	1.434(4)	C42	C41	1.525(5)
C27	C31	1.524(4)	C41	C40	1.513(5)
C31	C32	1.531(5)	C46	C45	1.527(8)
C31	C33	1.532(5)	C46	C47	1.505(7)
C24	C28	1.519(4)	C45	C44	1.484(7)
C28	C29	1.531(4)			

**Table S24.** Bond Angles for Lu( $\eta^5$ -(1,3-diisopropyl-4,7-dimethylindenyl)( $^{Ar}$ BiAMP $tBu$ )(THF) (6).

Atom	Atom	Atom	Angle/ $^{\circ}$	Atom	Atom	Atom	Angle/ $^{\circ}$
O1	Lu1	P1	130.12(6)	C23	C27	Lu1	73.92(17)
O1	Lu1	C23	145.38(9)	C23	C27	C26	106.4(3)
O1	Lu1	C25	97.43(9)	C23	C27	C31	124.1(3)
O1	Lu1	C26	94.48(8)	C26	C27	Lu1	75.89(16)
O1	Lu1	C27	120.98(9)	C26	C27	C31	128.8(3)
O1	Lu1	C24	125.99(9)	C31	C27	Lu1	122.7(2)
C23	Lu1	P1	84.45(7)	C27	C31	C32	112.4(3)
C23	Lu1	C25	51.11(9)	C27	C31	C33	110.5(3)
C23	Lu1	C26	51.46(9)	C32	C31	C33	109.2(3)
C23	Lu1	C27	31.39(9)	C23	C24	Lu1	73.14(16)
C23	Lu1	C24	31.25(9)	C23	C24	C25	106.5(3)
N2	Lu1	P1	61.34(7)	C23	C24	C28	123.7(3)
N2	Lu1	O1	89.79(9)	C25	C24	Lu1	75.82(17)
N2	Lu1	C23	109.38(9)	C25	C24	C28	128.8(3)
N2	Lu1	C25	146.89(9)	C28	C24	Lu1	125.3(2)
N2	Lu1	C26	115.85(9)	C24	C28	C29	109.6(3)
N2	Lu1	C27	96.40(9)	C24	C28	C30	113.3(3)
N2	Lu1	C24	140.30(9)	C29	C28	C30	110.3(3)
N1	Lu1	P1	60.89(7)	C26	C34	C39	123.2(3)
N1	Lu1	O1	87.46(9)	C35	C34	C26	117.3(3)
N1	Lu1	C23	116.46(10)	C35	C34	C39	119.5(3)
N1	Lu1	N2	98.52(10)	C34	C35	C36	122.5(3)
N1	Lu1	C25	114.00(10)	C37	C36	C35	122.5(3)
N1	Lu1	C26	145.56(9)	C25	C37	C38	122.3(3)
N1	Lu1	C27	147.85(10)	C36	C37	C25	118.3(3)

**Table S24 (Continued).** Bond Angles for  
**Lu( $\eta^5$ -(1,3-diisopropyl-4,7-dimethylindenyl)( $^{Ar}$ BiAMP $tBu$ )(THF) (6).**

N1	Lu1	C24	99.56(9)	C36	C37	C38	119.3(3)
C25	Lu1	P1	129.48(7)	N2	C2	P1	105.4(2)
C26	Lu1	P1	133.79(7)	N2	C15	C16	124.8(3)
C26	Lu1	C25	31.63(9)	N2	C15	C20	119.6(3)
C27	Lu1	P1	103.06(7)	C16	C15	C20	115.7(3)
C27	Lu1	C25	52.39(9)	C17	C16	C15	121.9(3)
C27	Lu1	C26	31.74(9)	C16	C17	C21	119.5(4)
C27	Lu1	C24	52.77(9)	C18	C17	C16	120.2(3)
C24	Lu1	P1	98.27(7)	C18	C17	C21	120.3(4)
C24	Lu1	C25	31.26(9)	C17	C18	C19	119.8(3)
C24	Lu1	C26	52.36(9)	C18	C19	C22	120.2(3)
C2	P1	Lu1	79.59(10)	C20	C19	C18	119.3(3)
C2	P1	C1	103.51(15)	C20	C19	C22	120.5(3)
C2	P1	C3	105.58(16)	C19	C20	C15	123.0(3)
C1	P1	Lu1	78.92(10)	N1	C1	P1	103.8(2)
C1	P1	C3	107.04(15)	N1	C7	C8	117.7(3)
C3	P1	Lu1	170.54(11)	N1	C7	C12	125.0(3)
C43	O1	Lu1	118.69(18)	C12	C7	C8	117.3(3)
C40	O1	Lu1	132.38(19)	C9	C8	C7	122.4(3)
C40	O1	C43	108.9(2)	C8	C9	C13	119.9(3)
C47	O2	C44	105.8(4)	C8	C9	C10	118.7(3)
C27	C23	Lu1	74.69(17)	C10	C9	C13	121.4(3)
C27	C23	C24	111.4(3)	C11	C10	C9	120.5(3)
C24	C23	Lu1	75.60(17)	C10	C11	C14	120.8(3)
C2	N2	Lu1	113.27(19)	C10	C11	C12	120.1(3)
C15	N2	Lu1	131.3(2)	C12	C11	C14	119.0(3)
C15	N2	C2	115.4(3)	C11	C12	C7	121.0(3)
C1	N1	Lu1	113.03(19)	C6	C3	P1	110.8(2)
C7	N1	Lu1	128.1(2)	C6	C3	C5	109.7(3)
C7	N1	C1	117.3(3)	C6	C3	C4	110.5(3)
C26	C25	Lu1	73.68(16)	C5	C3	P1	109.0(2)
C24	C25	Lu1	72.91(16)	C4	C3	P1	107.7(3)
C24	C25	C26	108.2(3)	C4	C3	C5	109.2(3)
C24	C25	C37	132.2(3)	O1	C43	C42	104.5(3)
C37	C25	Lu1	124.4(2)	C43	C42	C41	101.7(3)
C37	C25	C26	119.2(3)	C40	C41	C42	102.3(3)
C25	C26	Lu1	74.69(16)	O1	C40	C41	105.3(3)
C27	C26	Lu1	72.37(16)	C47	C46	C45	104.0(4)
C27	C26	C25	107.4(3)	C44	C45	C46	102.8(4)
C34	C26	Lu1	123.4(2)	O2	C44	C45	106.4(4)
C34	C26	C25	120.1(3)	O2	C47	C46	107.6(4)
C34	C26	C27	132.1(3)				

### 3.10 $[\text{La}(\eta^5\text{-}(1,3\text{-diisopropyl-4,7-dimethylindenyl})(^{Ar}\text{BiAMP}^{t\text{Bu}})]_2$ connectivity structure

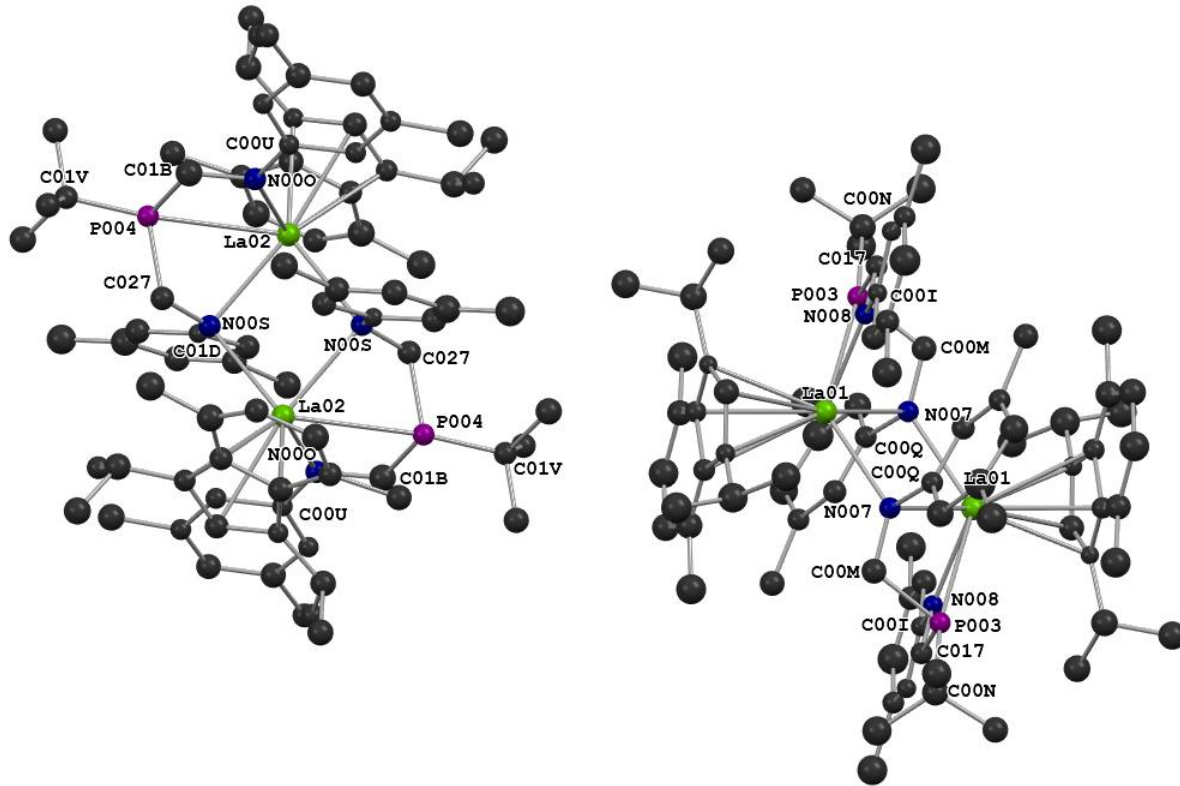


**Figure S60.** Solid state connectivity structure of  $[\text{La}(\eta^5\text{-}(1,3\text{-diisopropyl-4,7-dimethylindenyl})(^{Ar}\text{BiAMP}^{t\text{Bu}})]_2$  (recrystallized from diethyl ether) shown with hydrogen atoms omitted for clarity. The

**Table S25.** Crystal data and structure refinement for  $[\text{La}(\eta^5\text{-}(1,3\text{-diisopropyl-4,7-dimethylindenyl})(^{Ar}\text{BiAMP}^{t\text{Bu}})]_2$ .

Empirical formula	$\text{C}_{88}\text{H}_{100}\text{La}_2\text{N}_4\text{O}_4\text{P}_2$
Formula weight	1617.47
Temperature/K	108.0
Crystal system	triclinic
Space group	P-1
a/Å	13.5052(14)
b/Å	14.2084(14)
c/Å	21.380(2)
$\alpha/^\circ$	75.505(6)
$\beta/^\circ$	77.674(6)
$\gamma/^\circ$	75.599(6)
Volume/Å³	3796.8(7)
Z	2
$\rho_{\text{calc}}/\text{g/cm}^3$	1.415
$\mu/\text{mm}^{-1}$	1.206
F(000)	1664.0
Crystal size/mm³	? × ? × ?
Radiation	$\text{MoK}\alpha (\lambda = 0.71073)$
2θ range for data collection/°	3.956 to 50.694
Index ranges	-16 ≤ h ≤ 16, -16 ≤ k ≤ 17, -20 ≤ l ≤ 25
Reflections collected	39437
Independent reflections	13842 [ $R_{\text{int}} = 0.1120$ , $R_{\text{sigma}} = 0.1427$ ]
Data/restraints/parameters	13842/0/372
Goodness-of-fit on $F^2$	1.248
Final R indexes [ $ I  \geq 2\sigma (I)$ ]	$R_1 = 0.2350$ , $wR_2 = 0.5269$
Final R indexes [all data]	$R_1 = 0.2601$ , $wR_2 = 0.5371$
Largest diff. peak/hole / e Å⁻³	9.53/-3.07

### 3.11 References

1. Conway, B.; Graham, D. V.; Hevia, E.; Kennedy, A. R.; Klett, J.; Mulvey, R. E. *Chem. Commun.* **2008**, *23*, 2638–2640.
2. G. P. McGovern, F. Hung-Low, J. W. Tye and C. A. Bradley, *Organometallics*, 2012, **31**, 3865-3879
3. Bruker Instrument Service, Version 2010.1.0.0; Bruker AXS Inc.: Madison, WI, USA, **2010**.
4. SAINT Plus, Data Reduction Software, Version 7.68A; Bruker AXS Inc.: Madison, WI, USA, 2009.
5. G. M. Sheldrick, *Acta Crystallogr., Sect. A: Found. Crystallogr.* **A64**, 2008, 112–122.
6. G.M. Sheldrick, SADABS, University of Göttingen, Germany: 2005.
7. G. M. Sheldrick, *Acta Crystallogr., Sect. A: Found. Adv.* **C71**, 2015, 3–8;
8. APEX2, Data Refinement Software, Version 2010.1-2; Bruker AXS Inc.: Madison, WI, USA, 2010.
9. Olex2 1.2 (compiled 2014.06.27) svn.r2953 for OlexSys, GUI svn.r4855.
10. O. V. Dolomanov, L. J. Bourhis, R. J. Gildea, J. A. K. Howard and H. Puschmann, *J. Appl. Cryst.*, 2009, **42**, 339-341.